UNIVERSITY OF GLASGOW

CHEMISTRY DEPARTMENT

RADIO AND MICROWAVE SPECTROSCOPY OF SOME COMPLEXES OF VANADIUM, NIOBIUM AND TANTALUM

being

A thesis submitted in part fulfilment of the requirement for the

DEGREE OF DOCTOR OF PHILOSOPHY

by

CHARLES P. STEWART

October 1973.

ProQuest LLC.
789 East Eisenhower Parkway
P.O. Box 1346
Ann Arbor, MI 48106 – 1346

ACKNOWLEDGEMENTS

I would like to express my sincere gratitude to Dr A. L. Porte for his constant assistance and encouragement in the course of this work.

I thank Professor G. Sim for the gift of a sample of $(\pi\text{-}C_5H_5)_2\ V(OCN)_2$ and for the use of his x-ray data on bis-(π-cyclopentadienyl) complexes which were of great help in the studies described in part III of this thesis.

I would also like to thank the many people in the Chemistry Department of the University of Glasgow whom it would be impossible to mention by name here, whose assistance and advice were of value to me in the course of this work.

Finally I would like to acknowledge with gratitude the award of a Carnegie Research Scholarship, during the tenure of which this work was carried out.

Preface

This thesis deals with the information which can be obtained from e.p.r. and n.q.r. spectroscopic studies of transition metal ions, in this case specifically ions of vanadium, niobium, and tantalum.

In the first section of the thesis the principles of e.p.r. and n.q.r. spectroscopy are outlined and the subsequent chapters describe several systems to which these principles have been applied.

In the second chapter, it is shown how e.p.r. studies can be used to obtain information about the electron distribution and the ordering of the energy levels in several vanadyl chelates, and about the effect on these properties of adduct formation between the chelates and molecules of pyridine and ethanol.

In the third and fourth chapter, the electron distribution and the ordering of the energy levels in some bis - (π-cyclopentadienyl) compounds of vanadium, niobium and tantalum are elucidated by e.p.r. studies together with molecular orbital calculations. It is shown that solution e.p.r. linewidths can be analysed to obtain information about the electron distribution in these complexes.

In the final part of the thesis it is shown how it should be possible to use ^{93}Nb n.q.r. coupling constants to obtain information about the geometry of niobium-containing complexes of unknown structure.

The work described in this thesis is original and was carried out in partial fulfilment of the requirements for the degree of Ph.D. in the University of Glasgow.

October 1973. C.P. Stewart.

Charles P. Stewart, Ph.D. Thesis, 1973.

RADIO AND MICROWAVE SPECTROSCOPY OF SOME COMPLEXES OF VANADIUM, NIOBIUM AND TANTALUM

Summary

The thesis is subdivided into five main parts, which are summarised separately below.

Part I

This first part of the thesis is introductory in nature. The basic magnetic and electrostatic interactions which are of importance in understanding the form of electron paramagnetic resonance and nuclear quadrupole resonance spectra are discussed with particular reference to transition metal complexes of the type studied in this work. The way in which these spectra can be interpreted to obtain information about various aspects of the electronic structures of transition metal complexes is also discussed, and finally the spectrometers used in carrying out this work are described briefly.

Part II

This section describes a study of some oxovanadium (IV) chelates and their adducts with ethanol and pyridine.

The X-band e.p.r. spectra of some five- and six-membered ring chelates of the VO^{2+} ion have been recorded in solution at room temperature and in magnetically dilute glasses at 77K. This study indicates that the chelates form adducts with pyridine and with ethanol, and that they are readily oxidised, especially in hydroxylic solvents, to oxovanadium (V) complexes. The oxidation may be reversible in some cases. A method is described for deriving very accurate values of the spin Hamiltonian parameters from glassy spectra of these complexes, which have effective C_{2v} symmetry, and the parameters which were derived in this way are listed, together with the band maxima in the visible-u.v. spectra of the complexes. The spin Hamiltonian parameters are equated to the atomic orbital coefficients in some of the molecular orbitals involved in the bonding in the complexes, and it is thereby shown that whereas the

in-plane σ-bonding in the complexes is fairly covalent, the delocalisation of the unpaired electron onto the ligands via in-plane π-bonding is very slight. The weak C_{2v} component of the ligand field in these complexes mixes a small amount of $3d_{z^2}$ and 4s orbital character into the $3d_{x^2-y^2}$ orbital which contains the unpaired electron, and the magnetic resonance data is used to estimate the extent of this mixing. Mixing $3d_{z^2}$ character into the orbital containing the unpaired electron accounts for the in-plane anisotropy of the g- and hyperfine tensor components. Mixing in 4s character accounts for characteristic differences between the hyperfine tensor components observed for the five- and six-membered ring chelates, and for the differences in the changes which occur in these when additional complexing with solvent molecules takes place. The principal values of the hyperfine tensor components and the isotropic contribution to hyperfine coupling can be used to distinguish between five- and six-membered ring chelates.

Part III

This section describes a study of the complexes $(\pi\text{-}C_5H_5)_2\,MX_2$ where M = vanadium (IV), niobium (IV) or tantalum (IV) and X = Cl^-, SCN^-, OCN^-, CN^- or $\sigma\text{-}C_5H_5^-$.

The e.p.r. spectra of these compounds have been recorded at room temperature and in magnetically dilute glasses at 77K, and these spectra have been analysed in detail.

From Huckel L.C.A.O. molecular orbital calculations carried out on the complex $(\pi\text{-}C_5H_5)_2\,VCl_2$, the metal ion spin-orbit coupling constants ζ_V and ζ_{Nb} in these complexes are estimated to be 133 cm^{-1} and 490 cm^{-1} respectively. Spin Hamiltonian parameters are listed for each substance, and are equated to the atomic orbital coefficients in some of the molecular orbitals involved in bonding in these complexes, and good agreement is obtained between the values derived in this way and those derived from the molecular orbital calculations. Except for the cyanides, in each case the unpaired electron lies essentially in a non-bonding nd_{z^2} metal ion orbital, mixed with a small amount of the corresponding metal ion $nd_{x^2-y^2}$ orbital, the Z-axis coinciding with the C_2 axis of

the compound; in the cyanides the unpaired electron is delocalised into p_x orbitals on the ligands. The bonding of the metal ion to the cyclopentadienide rings and to the other ligands X is almost completely covalent, the bonding to the cyclopentadienide rings being stronger than that to the ligands X. Several redistribution complexes of the type $(\pi\text{-}C_5H_5)_2$ MXY have also been detected and characterised by their e.p.r. spectra. E.p.r. techniques can be used to distinguish compounds of the type $(\pi\text{-}C_5H_5)_2$ MX_2 from other compounds which contain vanadium (IV) and niobium (IV).

The difference between the e.p.r. spectra arising from complexes containing tantalum (IV) and those containing vanadium (IV) or niobium (IV) may be due to the presence of a large quadrupolar interaction in the tantalum complexes.

Part IV

This section deals with a detailed study of the linewidths in the e.p.r. spectra of solutions of the complexes $(\pi\text{-}C_5H_5)_2$ VCl_2, $(\pi\text{-}C_5H_5)_2$ $NbCl_2$ and $(\pi\text{-}C_5H_5)_2$ $Nb(\sigma\text{-}C_5H_5)_2$ as a function of temperature.

In the case of the complexes $(\pi\text{-}C_5H_5)_2$ VCl_2 and $(\pi\text{-}C_5H_5)_2$ $NbCl_2$ these studies have been used to estimate the size of the proton and chlorine nuclear hyperfine coupling constants in these complexes, and hence to estimate the extent to which the unpaired electron in the complexes is delocalised on to the ligands. In this way it has been shown that the unpaired electrons are delocalised on to the cyclopentadienide groups to a negligible extent, and that they are delocalised on to the chloride ligands to the extent of about 0.7% and 1.4% in the vanadium and niobium complexes respectively.

In the case of the complex $(\pi\text{-}C_5H_5)_2$ $Nb(\sigma\text{-}C_5H_5)_2$ the studies show that the interconversion of the σ and π ring systems in this complex, if it occurs, is likely to be a very slow process, due to the low concentration of any intermediate which might be involved in the interconversion.

Part V

The ^{93}Nb n.q.r. spectra of several complexes of niobium (V) with oxygen donor ligands have been recorded at room temperature and at 77K, and signals have been detected in two of these compounds, niobium penta-methoxide $Nb(OMe)_5$ and niobium tetra-ethoxide acetylacetonate $Nb(OEt)_4$ Acac.

It has been shown that the complexes $Nb(OMe)_5$, $Nb(OEt)_4$ Acac and $NbCl_5$, which are structurally related, have very similar ^{93}Nb n.q.r. coupling constants, and that it is possible to differentiate between complexes of this type and complexes of different structural types on the basis of their n.q.r. coupling constants.

The study suggests that it should be possible to use the characteristic ^{93}Nb n.q.r. coupling constants for complexes of known structures to obtain information about the geometry of niobium-containing complexes whose structures are not known.

TABLE OF CONTENTS

PART I

INTRODUCTION

PART II

AN E.P.R. STUDY OF THE ELECTRONIC STRUCTURE OF SOME OXOVANADIUM (IV) CHELATES, AND THEIR ADDUCTS WITH PYRIDINE AND ETHANOL

PART III

AN ELECTRON PARAMAGNETIC RESONANCE STUDY OF THE BIS-(π-CYCLOPENTADIENYL) VANADIUM (IV), BIS-(π-CYCLOPENTADIENYL)-NIOBIUM (IV) AND BIS-(π-CYCLOPENTADIENYL) TANTALUM (IV) COMPLEXES $(\pi\text{-}C_5H_5)_2\ VX_2$, $(\pi\text{-}C_5H_5)_2\ NbX_2$ AND $(\pi\text{-}C_5H_5)_2\ TaX_2$

PART IV

STUDIES OF THE E.P.R. LINEWIDTHS IN SOLUTION SPECTRA OF THE COMPLEXES $(\pi\text{-}C_5H_5)_2\ VCl_2$, $(\pi\text{-}C_5H_5)_2\ NbCl_2$ AND $(\pi\text{-}C_5H_5)_2\ Nb(\sigma\text{-}C_5H_5)_2$

PART V

NUCLEAR QUADRUPOLE RESONANCE STUDIES OF SOME COMPLEXES OF NIOBIUM (V) WITH OXYGEN DONOR LIGANDS

PART I

INTRODUCTION

1.1 Magnetic properties of charged particles

Charged particles may undergo closed-loop like motions. They possess angular momentum and an associated magnetic moment. For a charged particle which has an angular momentum $\underline{G}$, quantum mechanics yields the following two results.

(a) The square of the total angular momentum is given by

$$\underline{G}^2 = G(G+1)\hbar^2 \qquad 1.1$$

where G, the total angular momentum quantum number, may be an integer or a half-integer.

(b) The component of $\underline{G}$ along one axis, usually chosen as the z-axis, is given by

$$G_z = m_G \hbar \qquad 1.2$$

where $m_G = G, G-1, \ldots . -G.$

Electrons have angular momentum as a result of their intrinsic spin, $\underline{S}$, and their orbital motion $\underline{L}$. Where an electron has both of these, they couple together to give a total angular momentum $\underline{J}$. Nuclei also have angular momentum $\underline{I}$, arising from the combination of the angular momenta of their constituent nucleons. For electrons $S = \frac{1}{2}$, L must be an integer, while J and I may have either integral or half integral values.

The magnetic moment associated with a charged particle having angular momentum $\underline{G}$ is given by

$$\begin{aligned} \underline{\mu} &= \gamma \underline{G} \\ &= \gamma \hbar (G(G+1))^{\frac{1}{2}} \\ &= g \beta (G(G+1))^{\frac{1}{2}} \end{aligned} \qquad 1.3$$

where γ is the magnetogyric ratio for the particle and β is the Bohr magneton for the particle. g is the Landé g-factor, which equals 1 and

2.0023 for the electron orbital and spin angular momenta respectively. Nuclear g-values are found experimentally.

In many cases, the orbital contribution to the electron's magnetic moment is almost completely removed, and in this case the magnetic moment is sometimes written as

$$\mu = -g_{eff}\beta_e(S(S+1))^{\frac{1}{2}} \qquad 1.4$$

where the magnetic moment is assumed to arise from the spin of the electron only, and the orbital contribution is taken into the effective g-factor, which thus deviates slightly from 2.0023.

1.2 The Zeeman interaction

Consider a molecule containing an unpaired electron whose orbital magnetic moment is almost zero, in an applied magnetic field. The energy of interaction of the electron's magnetic moment with the applied field is given by

$$\begin{aligned} E &= -\underline{\mu}.\underline{H} \\ &= -\mu_z H \\ &= g_{eff}\beta_e H m_s \end{aligned} \qquad 1.5$$

where the field is assumed to lie along the z-axis direction, and β_e is the numerical value of the electronic Bohr magneton.

Thus, in an applied magnetic field, the z component of the electron magnetic moment may align itself parallel (β state) or antiparallel (α state) to the direction of the applied field, these states having energies of $-\frac{1}{2}\, g_{eff}\beta_e H$ and $+\frac{1}{2}\, g_{eff}\beta_e H$ respectively and it is now possible to cause transitions between the two states by supplying the system with energy in the form of radiation of the correct frequency. This is the basis of electron paramagnetic resonance (e.p.r.) spectroscopy.

The expression for the Zeeman energy given in equation 1.5 is not quite correct, since the direction of the applied magnetic field can only be chosen as that of the z-axis if the g-factor is isotropic, and this is only true in cases where the electron's orbital magnetic moment is zero. In cases where there is a small orbital contribution to paramagnetism, it is shown later that the e.p.r. spectrum can be accounted for by using a Hamiltonian which contains only spin operators, and by assuming that the electronic states are pure spin states. The Zeeman contribution to this Hamiltonian, which is known as the spin Hamiltonian, is given by

$$\mathcal{H}_z = \beta_e \underline{H} \cdot g \cdot \underline{S} \qquad 1.6$$

where g is a symmetric second rank tensor.

1.3 The hyperfine interaction

If an unpaired electron is in the vicinity of a nucleus which has a magnetic moment, there will be an interaction between the magnetic moment of the electron and that of the nucleus. There are three main contributions to this interaction:

a) An isotropic contribution, called the Fermi contact interaction which arises from the presence of unpaired spin density at the magnetic nucleus, due to the wavefunction of the unpaired electron having a finite value at the nucleus, or due to polarisation of paired S electrons about the nucleus by the unpaired electron.

b) An anisotropic contribution arising from the dipolar coupling between the spin magnetic moments of the electron and the nucleus.

c) A contribution from the interaction of the orbital magnetic moment of the electron with the nuclear magnetic dipole. This is fairly small in many transition metal complexes.

The magnetic hyperfine interaction can be represented by a contribution to the spin Hamiltonian of the form

$$\mathcal{H}_{SI} = \underline{S}.A.\underline{I} \qquad 1.7$$

where A is again a symmetric tensor, the hyperfine coupling tensor.

For a particular orientation of a molecule containing an unpaired electron with respect to an applied magnetic field, it can be shown that to first order the energy of the system is given by

$$E = g_{eff}\beta_e H m_S + A' m_S m_I \qquad 1.8$$

where A' is the effective hyperfine coupling constant for that particular orientation of the molecule. The allowed transitions are those with $\Delta m_S = \pm 1, \Delta m_I = 0$, and the energy of these is given by

$$\Delta E = g_{eff}\beta_e H + A' m_I \qquad 1.9$$

ie. the single transition which would be observed in the absence of hyperfine coupling is split into $2I + 1$ components separated to first order by A'.

Nuclei with $I \geq 1$ also have a quadrupole moment, and although this does not interact directly with the magnetic moment of the unpaired electron, it does interact with the asymmetric electric field gradients produced at the nucleus by the surrounding electrons and nuclei in the molecule containing the nucleus. This interaction has an indirect effect on the e.p.r. spectrum, leading to changes in the position of the lines in the spectrum, and to forbidden transitions with $\Delta m_I = \pm 2$ becoming allowed.

The quadrupolar interaction can be represented by a contribution to the spin Hamiltonian of the form

$$\mathcal{H}_Q = \underline{I}.P.\underline{I} \qquad 1.10$$

where P is the quadrupole coupling tensor.

1.4 The spin Hamiltonian

The complexes whose e.p.r. spectra will be discussed later contain only one unpaired electron, the orbital magnetic moment of which is almost zero, and for such complexes the spin Hamiltonian can be written as the sum of the individual contributions listed above, ie

$$\mathcal{H} = \beta_e \underline{H}.\underline{g}.\underline{S} + \underline{S}.\underline{A}.\underline{I} + \underline{I}.\underline{P}.\underline{I} \qquad 1.11$$

The spin Hamiltonian is an artificial concept, since the true Hamiltonian should contain orbital angular momentum operators as well as spin operators. The spin Hamiltonian simply represents a convenient way of presenting data obtained from e.p.r. spectra, and the true value of the spin Hamiltonian parameters is only realised when these are interpreted in terms of more basic properties of the system. It should also be noted that the form of the spin Hamiltonian depends very much on the nature of the system being studied, so that although the spin Hamiltonian 1.11 was that appropriate to the systems studied in this work, for other systems it may be necessary to use a different form of the spin Hamiltonian to account for the observed e.p.r. spectra.

In many cases it is possible to choose an axis system, the principal axis system, which simultaneously diagonalises the g, A and P tensors, so that the spin Hamiltonian becomes

$$\mathcal{H} = \sum_i (\beta_e g_{ii} H_i S_i + A_{ii} S_i I_i + P_{ii} I_i^2) \qquad 1.12$$

where the summation is over the principal axis coordinates, X, Y, and Z, say.

In cases where the orientation of the system with respect to the applied magnetic field is not fixed, eg in solution, the rotation of the system averages out anisotropic contributions to the various tensors, giving a Hamiltonian of the form

$$\mathcal{H} = A_o \underline{S}.\underline{I} + g_o \beta_e \underline{H}.\underline{S} \qquad 1.13$$

where

$$A_o = \tfrac{1}{3}\sum_i A_{ii} \quad \text{and} \quad g_o = \tfrac{1}{3}\sum_i g_{ii} \qquad 1.14$$

Since the quadrupole tensor is traceless, there is no contribution from this in this case.

1.5 Spin relaxation and lineshapes

The spin Hamiltonian deals with the energy levels in magnetic resonance, and would predict infinitely sharp transitions between levels. In practice this is not observed to be the case, and the width of the spectral lines observed can be accounted for by considering the dynamics of the system.

Consider a collection of spins with a bulk magnetisation $\underline{M}$ having components M_x, M_y and M_z along three axis directions, in a magnetic field applied along the z-axis.

At equilibrium M_z has some value, M_o say, and M_x and M_y are zero. If the system is removed from equilibrium, it will relax back to equilibrium at a rate defined by

$$\frac{dM_z}{dt} = \frac{-(M_z - M_o)}{T_1}$$

$$\frac{dM_x}{dt} = \frac{-M_x}{T_2}$$

$$\frac{dM_y}{dt} = \frac{-M_y}{T_2} \qquad 1.15$$

The constant T_1 is called the spin-lattice relaxation time, because for M_z to relax back to its equilibrium value the spins have to exchange energy with the lattice, ie the medium in which they find themselves. The constant T_2 is called the spin-spin relaxation time. The relaxation of M_x and M_y does not involve exchange of energy with the lattice, but is concerned with a redistribution of the total energy of the system

among the various spins.

The applied field H_o exerts a torque on M, causing it to precess about H_o according to the equation.

$$\frac{d\underline{M}}{dt} = \gamma_e(\underline{M} \times \underline{H}_o) \qquad 1.16$$

Combining 1.15 and 1.16 yields

$$\frac{d\underline{M}}{dt} = \gamma_e(\underline{M} \times \underline{H}_o) - \frac{(\underline{i}\, M_x + \underline{j}\, M_y)}{T_2} - \underline{k}\,\frac{(M_z - M_o)}{T_1} \qquad 1.17$$

where $\underline{i}$, $\underline{j}$ and $\underline{k}$ are unit vectors directed along the X, Y and Z axes. 1.17 are the Bloch equations.

If a circularly polarised magnetic field H_1, rotating in the XY plane with angular velocity ω in the same direction as the Larmor precession, is applied to the system, the Bloch equations become

$$\frac{d\underline{M}}{dt} = \gamma_e(\underline{M} \times \underline{H}_o) + \gamma_e(\underline{M} \times \underline{H}_1) - \frac{(\underline{i}\, M_x + \underline{j}\, M_y)}{T_2} - \underline{k}\,\frac{(M_z - M_o)}{T_1} \qquad 1.18$$

This equation can be solved to yield expressions for the equilibrium values of the components, u and v, of the magnetisation M which lie parallel to and at right angles to H_1 in the XY plane, and for M_z.

The v mode for a particular transition then reflects the absorption of energy from the field H_1, ie the work which H_1 does on the system. This is given by $\underline{M} \times \underline{H}.\omega$, which in this case reduces to $\omega v H_1$.

From the solution of 1.18,

$$v = \frac{M_o\, \gamma_e\, H_1\, T_2}{1 + T_2^2(\omega_o - \omega)^2 + \gamma_e^2\, H_1^2\, T_1\, T_2} \qquad 1.19$$

Thus, the rate of work of H_1, and the lineshape $g(\omega)$, are given by

$$g(\omega) = \chi_o \omega_o \omega H_1^2 \frac{T_2}{1 + T_2^2 (\omega_o - \omega)^2 + \gamma_e^2 H_1^2 T_1 T_2} \quad 1.20$$

where M_o is written as $\chi_o H_o$ in recognition of the fact that M_o will depend on H_o. If $\gamma_e^2 H_1^2 T_1 T_2$ is small, as is often the case, the line is Lorentzian in shape, the classical normalised form for this being

$$g(\omega) = \frac{T_2}{\pi} \frac{1}{1 + T_2^2 (\omega_o - \omega)^2} \quad 1.21$$

If H_1 or T_1 is large, the term $\gamma_e^2 H_1^2 T_1 T_2$ may become important, and the lineshape is no longer Lorentzian. This effect is called saturation and it arises because the system cannot relax fast enough to maintain the population difference between the upper and lower spin states. Saturation relatively weakens the centre of the absorption line, and causes apparent broadening.

1.6 Sources of line broadening

The linewidth is thus governed in most cases by T_2, and there are various effects which may contribute to this, their relative importance depending on the particular system being studied.

In magnetically concentrated systems, where neighbouring paramagnetic species are very close to one another, the unpaired electron can jump rapidly from one molecule to another. This has the effect of averaging out the hyperfine interactions in the species, and, depending on the rate of jumping, this may produce a very broad line where hyperfine coupling is present. For this reason e.p.r. studies are usually carried out on magnetically dilute systems, eg in solution, or using crystals of a diamagnetic host into which the paramagnetic species are doped.

The main contributions to the linewidths in solutions of transition metal complexes where there is little orbital contribution to paramagnetism are outlined below:

a) The rate of rotation of the complex in solution is not fast enough to completely average out the anisotropic contributions to the g and hyperfine tensors, and the fluctuating magnetic fields which this produces causes broadening.

b) When a molecule rotates in solution, the motions of the elctrons and nuclei produce magnetic fields which interact with the magnetic moment of the unpaired electron. The magnitude and direction of these fields fluctuates with time and this also results in broadening.

c) There may exist in the complex hyperfine interactions which are not large enough to cause splitting of the spectral lines, but are large enough to contribute to the linewidth.

These are the main effects in complexes where there is only one unpaired electron and little orbital paramagnetism. In other systems, however, other types of effect may be dominant, and each system must be considered individually.

1.7 E.p.r. studies and electronic structure

The complexes to be discussed in this work will have their electronic structures discussed in terms of the L.C.A.O. - M.O. (linear combination of atomic orbitals - molecular orbital) approach. This theory suggests that the electronic states of a molecule may be described in terms of products of one-electron wave-functions, these being formed from a linear combination of the atomic orbitals of the individual atoms making up the complex, ie the molecular orbitals ψ_j are of the form

$$\psi_j = \sum_i c_{ji} \phi_i$$

where ϕ_i are the atomic orbitals. In the case of many transition metal

complexes, and also in the case of the complexes studied here, the atomic orbitals used in forming the molecular orbitals are the nd, (n + 1)p and (n + 1)s orbitals of the metal ion and the s and p orbitals of the ligands.

In many cases the form of the molecular orbitals can be simplified by using the symmetry properties of the system and by noting that

a) Metal ion orbitals which belong to different irreducible representations of the point group of the molecule do not contribute to the same molecular orbital.

b) Although single ligand orbitals cannot be assigned to any irreducible representation of the point group of the molecule, the squares of the coefficients of ligand orbitals which transform into each other under any of the symmetry operations of the molecule must be identical, and therefore such atomic orbitals may be combined to form a linear combination of ligand orbitals which transform according to a particular irreducible representation of the molecular point group. Such linear combinations of ligand orbitals are known as symmetry orbitals, or ligand group orbitals.

Thus, a particular molecular orbital will contain contributions only from metal and ligand group orbitals of the same symmetry type, and can often be written in the form

$$\Psi = c_1\phi_M + c_2\phi_L$$

where ϕ_M is a metal ion orbital and ϕ_L is a ligand group orbital. An electron in such a molecular orbital will thus be located partly on the metal ion, and partly on the ligands.

The effect of forming these molecular orbitals can be shown schematically by the use of molecular orbital diagrams of the type below.

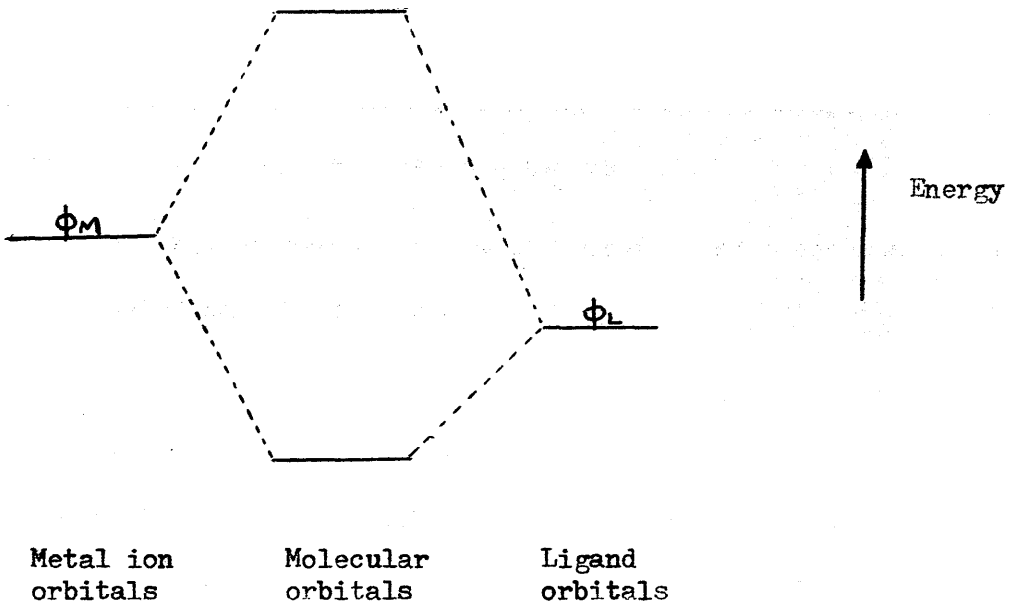

The combination of the metal ion and ligand orbitals produces molecular orbitals at energies above and below those of the atomic orbitals. The upper orbitals are usually called antibonding orbitals, and often contain no electrons in the ground state of the molecule. The lower orbitals are the bonding orbitals and are usually occupied in the ground state. The antibonding molecular orbitals are usually mainly metal ion orbital in character, while the bonding orbitals are mainly ligand.

Electronic transitions which involve the transfer of an electron between orbitals which have mainly metal ion orbital character are called d-d transitions or ligand field transitions. These give rise to the low energy, low intensity bands often observed in the u.v.-visible spectra of transition metal complexes. Transitions which involve the transfer of an electron from one of the filled bonding orbitals which have mainly ligand orbital character, to one of the mainly metal antibonding orbitals are called ligand-to-metal charge transfer transitions. These usually occur at higher energies than the ligand field transitions and are much more intense. It should be stressed, however, that the metal or ligand character of the various molecular orbitals and hence the

nature of the various transitions varies very much from complex to complex, so that each case must be considered individually, although the generalisations mentioned above often hold.

Information can be derived about the distribution of electrons in the complexes studied here in two ways.

First, the size of the hyperfine coupling between an unpaired electron and a magnetic nucleus decreases rapidly with the distance of the electron from the nucleus. Thus, it is possible to estimate the degree of localisation of an unpaired electron on a particular nucleus from the size of the hyperfine coupling constant obtained from the e.p.r. spectrum. This approach yields information about the distribution of the unpaired electron in the molecular orbital it occupies in the ground state of the complex. In cases where the hyperfine coupling is not large enough to cause splitting of the lines in the e.p.r. spectrum, but large enough to cause line broadening, the size of the coupling can be estimated from the linewidths if the other contributions to the linewidths in the spectrum can be calculated.

Information about the electron distribution can also be derived from the size of the orbital contribution to paramagnetism, as reflected in the deviation of the g-tensor values from the spin-only value.

In free transition-metal ions, the unpaired electron occupies an orbital which has both spin and orbital contributions to its magnetic moment. In a complex, the electric fields due to the surrounding ligands force the unpaired electron to occupy an orbital which has no associated orbital magnetic moment. A small amount of orbital paramagnetism may, however, be reinstated by spin-orbit coupling. This is the interaction between the spin magnetic moment of an electron and the magnetic field which it experiences by virtue of its motion in the

electric field of the nucleus. The effect of this is to mix some excited state character into the orbital containing the unpaired electron, so producing a small orbital magnetic moment. The size of the coupling increases with increasing atomic number of the nucleus involved, and in many cases the only effective spin-orbit interaction in a complex is with the heavy transition metal nucleus. The importance of this effect is that the coupling decreases rapidly with the distance of the electron from the nucleus, the result being that the degree of orbital paramagnetism produced depends in many cases on the degree of localisation of the unpaired electron on the metal ion, both in the ground and excited states. Thus, if the degree of localisation of the electron on the metal ion in the ground state is known, from the hyperfine coupling for instance, this effect can be used to study the electron distribution in the excited states, in this case in the empty antibonding molecular orbitals.

If the electron distribution in the antibonding orbitals is known, it is usually possible to deduce the distribution in the filled bonding orbitals of the complex. Consider, for example, the simplest possible situation, where a metal and a ligand orbital are combined to form two molecular orbitals.

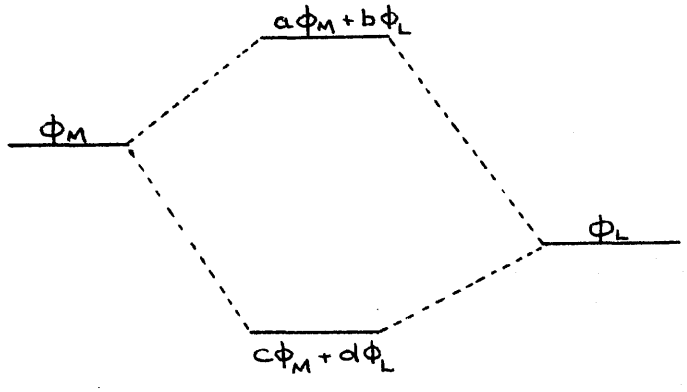

It is possible to define the following quantities

$$P_M^* = a^2 + abS \qquad P_L^* = b^2 + abS$$

$$P_M = c^2 + cdS \qquad P_L = d^2 + cdS \qquad 1.22$$

where $S = \langle \phi_M | \phi_L \rangle$. These are orbital populations. P_M^* for instance is the fraction of one electron which would be localised on the metal ion in the antibonding molecular orbital. From the normalisation and orthogonality properties of the wavefunctions, it is possible to show that

$$P_M + P_M^* = 1 \qquad P_L + P_L^* = 1$$

$$P_M + P_L = 1 \qquad P_L^* + P_M^* = 1 \qquad 1.23$$

Thus, knowing the orbital populations in the antibonding molecular orbitals, the populations in the bonding orbitals can be deduced using these relationships.

E.p.r. spectroscopy is thus a very powerful tool for the study of electron distributions in transition metal complexes.

1.8 Nuclear quadrupole resonance

As noted in section 1.4, nuclei with $I > 1$ have quadrupole moments. The quadrupole moment may assume certain allowed orientations with respect to the asymmetric electric field gradients generated at the nucleus by the surrounding electrons and nuclei. The various allowed orientations have different energies, due to differences in the energy of interaction of the quadrupole moment of the nucleus with the asymmetric electric field gradients, and it is possible to course transitions between the allowed states by supplying energy to the system in the form of radiation of the correct frequency. This is the basis of nuclear quadrupole resonance (n.q.r.) spectroscopy. The frequency at which transitions occur depends very much on the size both of the nuclear quadrupole moment and the electric field gradients, but in many cases it lies in the range 1-200 MHZ.

Since the size of the electric field gradients depends on the distribution of electric charge around the nucleus and in many cases particularly on

the distribution of the valence electrons around the nucleus, the resonance frequency can be used to obtain information about the distribution of electrons in molecules, and in many cases the n.q.r. frequency can be a sensitive indicator of the geometry of the molecule containing the nucleus.

1.9 Experimental aspects

The apparatus used in recording e.p.r. spectra is now fairly standard, and is discussed in numerous texts. The e.p.r. spectra reported in this work were recorded on a Decca X-3 spectrometer, operating in the X-band region of the microwave spectrum at 9270 MHZ, in conjunction with a Newport 11-inch magnet system. The detection system employed 100 KHZ audiomodulation together with a phase sensitive detector, and the e.p.r. spectrum was measured as a first derivative. The e.p.r. spectrum was calibrated using proton magnetic resonance methods, and the calibration system itself was checked using a finely powdered sample of diphenylpicrylhydrazyl, whose g-factor is known accurately to be 2.0036.

Samples studied at room temperature were contained in spectrosil quartz tubes. Spectra recorded at 77K were obtained by placing some of the sample in a long-tailed dewar, the spectrosil quartz tail of which was inserted into the sample cavity, and pouring liquid nitrogen on top of it. For temperatures intermediate between 77K and room temperature, a gas flow system was used. This involved passing gaseous nitrogen through a coil immersed in a bath of liquid nitrogen, and passing the resultant cooled gas into the sample cavity. The temperature of the sample between about 80K and room temperature could be controlled by means of a heating element over which the cooled gaseous nitrogen was passed after leaving the liquid nitrogen bath. Temperatures above

room temperature could be obtained by using the same heating element without the liquid nitrogen bath. For studies in which the temperature had to be known accurately, the temperature of the sample was monitored using a copper-constantan thermocouple together with a digital voltmeter. Using the gas flow system the temperature of the sample could be held within $\pm 1^{\circ}K$ for a period of hours.

The type of spectrometers used in n.q.r. studies are summarised in reference 5. The spectra reported in this work were obtained using a Decca n.q.r. spectrometer which could operate in the range 5.5-55 MHZ, using a super-regenerative oscillator. The samples to be studied were sealed in thin walled glass tubes and held in the coil of the oscillator. They could be studied both at room temperature and, by immersing the sample and coil in liquid nitrogen, at 77K.

PART II

AN E.P.R. STUDY OF THE ELECTRONIC STRUCTURE OF SOME OXOVANADIUM (IV) CHELATES AND THEIR ADDUCTS WITH PYRIDINE AND ETHANOL

2.1 Introduction

Along with systems containing the copper (II) and manganese (II) ions, systems which contain vanadium in its various oxidation states are amongst those most studied by electron paramagnetic resonance methods. High isotopic purity, (^{51}V is almost 100% abundant) and a large magnetic moment both help to simplify vanadium ion spectra. Systems containing to vanadium (IV) ion in particular have been extensively studied, since this ion has a d^1 configuration, and has none of the complications which arise when more than one electron is present. The vanadium (IV) ion has been studied as an impurity substituted into various ionic lattices, and one or two reports have been published on tetrahedral complexes of vanadium (IV), but most of the work published has been concerned with oxovanadium (IV) complexes.[1]

The chemistry of the vanadium (IV) ion is mainly that of the oxovanadium (IV) species and its derivatives, and this is probably the most stable molecule-ion known.[2,3] Oxovanadium (IV) complexes are often fairly stable; they are easily prepared and they are soluble in organic solvents. The strong vanadium-oxygen bond in vanadyl complexes produces a strong axial field, which practically eliminates orbital contributions to paramagnetism. As a result e.p.r. spectra are easily observed for these complexes in solution at room temperature, and they all show eight well resolved sharp signals due to one unpaired electron interacting with the ^{51}V nucleus, with spin quantum number $I = {}^7/_2$.

Ballhausen and Grey[4] carried out an extended Huckel L.C.A.O. molecular orbital calculation on the complex $VO(H_2O)_5^{2+}$, from which they were able to predict the relative energies of the molecular orbitals in the

complex, and the charge distribution. They were then able to use the results of this calculation as a basis for interpreting the visible-u.v. spectrum of the complex, and the magnetic properties of the complex, including its e.p.r. spectrum. In this calculation, they assumed that the unpaired electron in the complex was situated in a non-bonding molecular orbital localised completely on the vanadium ion, an assumption subsequently vindicated by the studies of Kivelson and Lee[5] on the e.p.r. spectra of some vanadyl chelates, including vanadyl acetylacetonate. Since then several reports have been published on studies of oxovanadium complexes containing various ligand atoms, for instance complexes with chloride, oxygen, nitrogen, mixed oxygen and nitrogen, sulphur, and phosphorous - containing ligands have been studied with a view to examining the nature of the bonding in these complexes.[6]

Most of the above reports used the Ballhausen and Grey scheme as a basis for their discussion of the electronic structures of the various complexes, but this scheme was questioned to some extent by Selbin et al[7,3], who proposed an alternative assignment for the bands observed in the u.v.-visible spectra of vanadyl complexes. Subsequently a large number of reports of u.v.-visible spectra of vanadyl complexes appeared supporting one view or the other, but at the date of the studies reported here the controversy had still not been satisfactorily resolved.

Prior to the studies described here, work had mainly centred on unchelated complexes and on six-membered ring chelates, the only five-membered ring chelate studied previously was the oxalate complex.[8]

It was thus decided

a) to study a selection of six- and five-membered ring chelates and to examine the differences, if any, in the magnetic parameters and electronic structures of these chelates.

b) to study a series of adducts of these chelates with suitable bases in the hope of being able to derive further information from the changes occurring on adduct formation. Adduct formation is generally accompanied by large changes in the u.v.-visible spectra, and rather smaller changes in the spin Hamiltonian parameters, of the complexes.

The complexes studied have the general formula I of figure 2.1 below. The ligands used were acetylacetone and benzoylacetone for the six-membered ring chelates, and maltol, kojic acid, tropolone and bromotropolone for the five-membered ring chelates. These had the structures II-VII of figure 2.1 below.

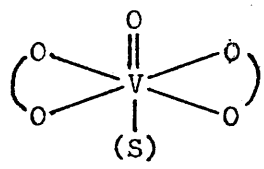

S = co-ordinated base in the adducts.

I Vanadyl Chelates - general structure

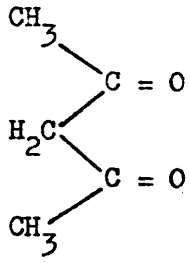

II Acetylacetone

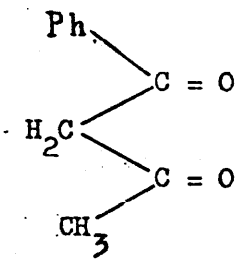

III Benzoylacetone

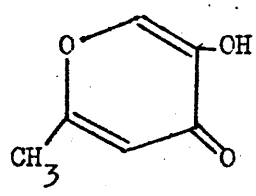

IV Maltol

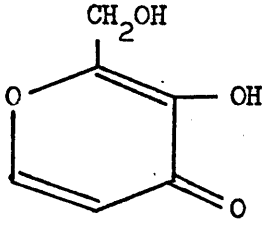

V Kojic Acid

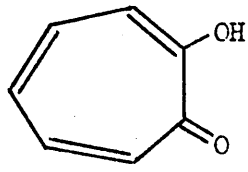

VI Tropolone

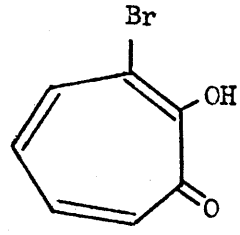

VII α-Bromotropolone

Figure 2.1

The e.p.r. spectrum of vanadyl acetylacetonate had previously been studied in solution[9] and in glasses of toluene[10] and of various organic solvents[5]. The e.p.r. spectrum of the benzoylacetonate had previously been studied substituted in single crystals of palladium benzoylacetonate and zinc benzoylacetonate ethanolate[11]. None of the five-membered ring chelates had been studied previously, and none of the adducts of any of the chelates had previously been studied by the e.p.r. method.

2.2 Experimental

The complexes were all prepared by the same general method.

a) Acetylacetone or benzoylacetone was mixed with vanadyl sulphate in 2:1 mole ratio in aqueous solution. The pH of the solution was adjusted to about 5, and the product precipitated out, and was filtered off. The acetylacetonate is blue, the benzoylacetonate is green.

b) Kojic acid and vanadyl sulphate were mixed in 2:1 mole ratio in aqueous solution and the pH was adjusted to about 5. The resulting green solution was concentrated down until the green crystalline product separated out. The solution was then allowed to cool, and the product was filtered off. If the cooled solution was left for any length of time in contact with the air it began to turn red due to oxidation of vanadium (IV) to vanadium (V).

c) Maltol and vanadyl sulphate were mixed in 2:1 mole ratio in aqueous solution and the pH was adjusted to about 5. On boiling the solution for about five minutes the dark green product separated out, and was filtered off.

d) Tropolone or bromotropolone was mixed with vanadyl sulphate in 2:1 mole ratio in aqueous solution. A precipitate formed immediately on mixing, and this was quickly filtered off and suction dried. The product is light green. If the product is not filtered off immediately it

becomes contaminated with a scummy grey substance, although this does not appear to affect the e.p.r. spectrum.

The compounds were analysed for vanadium by ignition to V_2O_5, and all analysed correctly as VOL_2.

The i.r. spectra of the compounds were recorded in Nujol mull, and those of the maltolate, tropolonate and acetylacetonate were also recorded in chloroform solution. The acetylacetonate spectrum showed the characteristic V = O stretching frequency[12,13] at 996 cm^{-1}, and the five-membered ring chelates had similar sharp bands in the mull and in solution at slightly lower frequency, at 990 cm^{-1}. The carbonyl stretching frequencies in the five-membered ring chelates were shifted to lower frequencies, indicating coordination via the carbonyl oxygens. The i.r. spectra were therefore consistent with the proposed formulation for the chelates.

The e.p.r. spectra were recorded using 10^{-3}M solutions at room temperature and in glasses at 77K with concentrations varying between 10^{-2}M and 10^{-3}M depending on the solubility of the complex in the particular solvent. The spectra of the uncomplexed acetylacetonate and benzoylacetonate were recorded in dry toluene glass, those of the five-membered ring chelates in dried chloroform-toluene (60:40). The spectra of the ethanol adducts of the six-membered ring chelates were recorded in chloroform-toluene (60:40) glass, to which was added 2% ethanol. Those of the five-membered ring chelates were recorded in chloroform, to which was added 2% ethanol. The spectra of the pyridine adducts were recorded in toluene glass to which was added 5% of pyridine. Due to solubility difficulties the spectra of the kojate in chloroform-toluene (60:40) and that of the bromotropolonate in chloroform-toluene (60:40) could not be recorded.

2.3 Analysis of the e.p.r. spectra

A typical solution spectrum, in this case for vanadyl tropolonate in chloroform solution at room temperature, is shown in figure 2.2. The solution spectrum consists of eight lines due to the interaction of one unpaired electron with an applied magnetic field and with the vanadium nucleus, with spin $I = {}^{7}/_{2}$. The separations between successive lines in the spectrum are not equal, due to second order terms in the equations describing the resonant field values, and the lines are not all equal in height, although the area under each peak is the same. This is due to differential line broadening effects. Rotation of the complex in solution averages out the anisotropic contributions to the spectrum better for some lines than for others, hence the variation in linewidth.

As shown in appendix A, expressions for the resonant field positions can be obtained[14] by solving a spin Hamiltonian of the form

$$\mathcal{H} = g_o \beta_e \underline{H}.\underline{S} + A_o \underline{S}.\underline{I} \qquad 2.1$$

where g_o and A_o are the isotropic g-factor and hyperfine coupling constant for the complex.

Solution of the spin Hamiltonian yields the following expression for the allowed $\Delta m_S = +1$, $\Delta m_I = 0$ transition.

$$H = h\nu_o (g_o\beta_e)^{-1} - hc (g_o\beta_e)^{-1} A_o m_I - hc^2 (2g_o\beta_e\nu_o)^{-1} A_o{}^2(I(I+1) - m_I{}^2) \qquad 2.2$$

where A_o now has units of cm^{-1}. Thus, from the observed resonant field values, equation 2.2 can be solved to yield values of g_o and A_o for each of the complexes.

The spectrum of vanadyl tropolonate recorded at 77K in a glass of dry chloroform-toluene (60:40) is shown in spectrum A, of figure 2.3. The spectrum of vanadyl tropolonate at 77K dissolved in chloroform-toluene

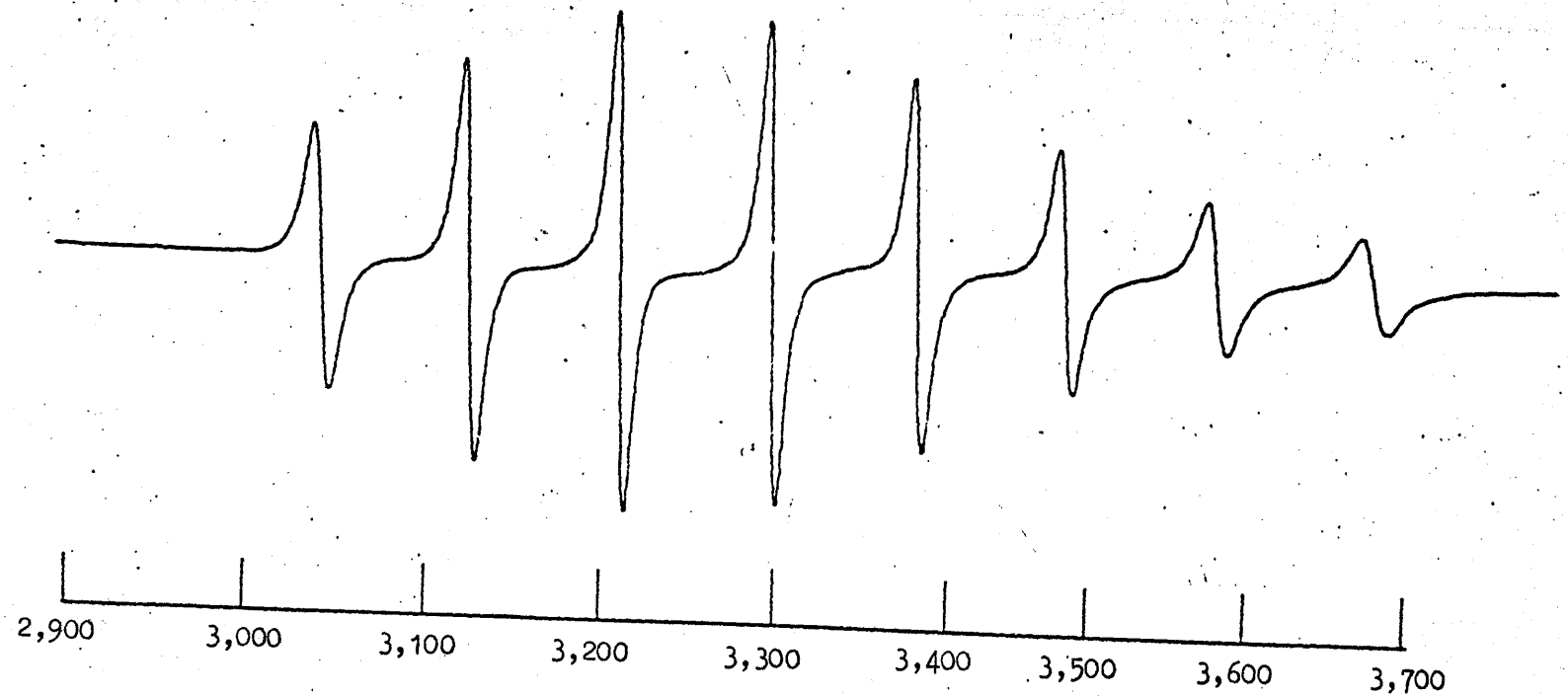

Figure 2.2 E.p.r. spectrum of a 10^{-3}M solution of vanadyl tropolonate in chloroform solution at 293K.

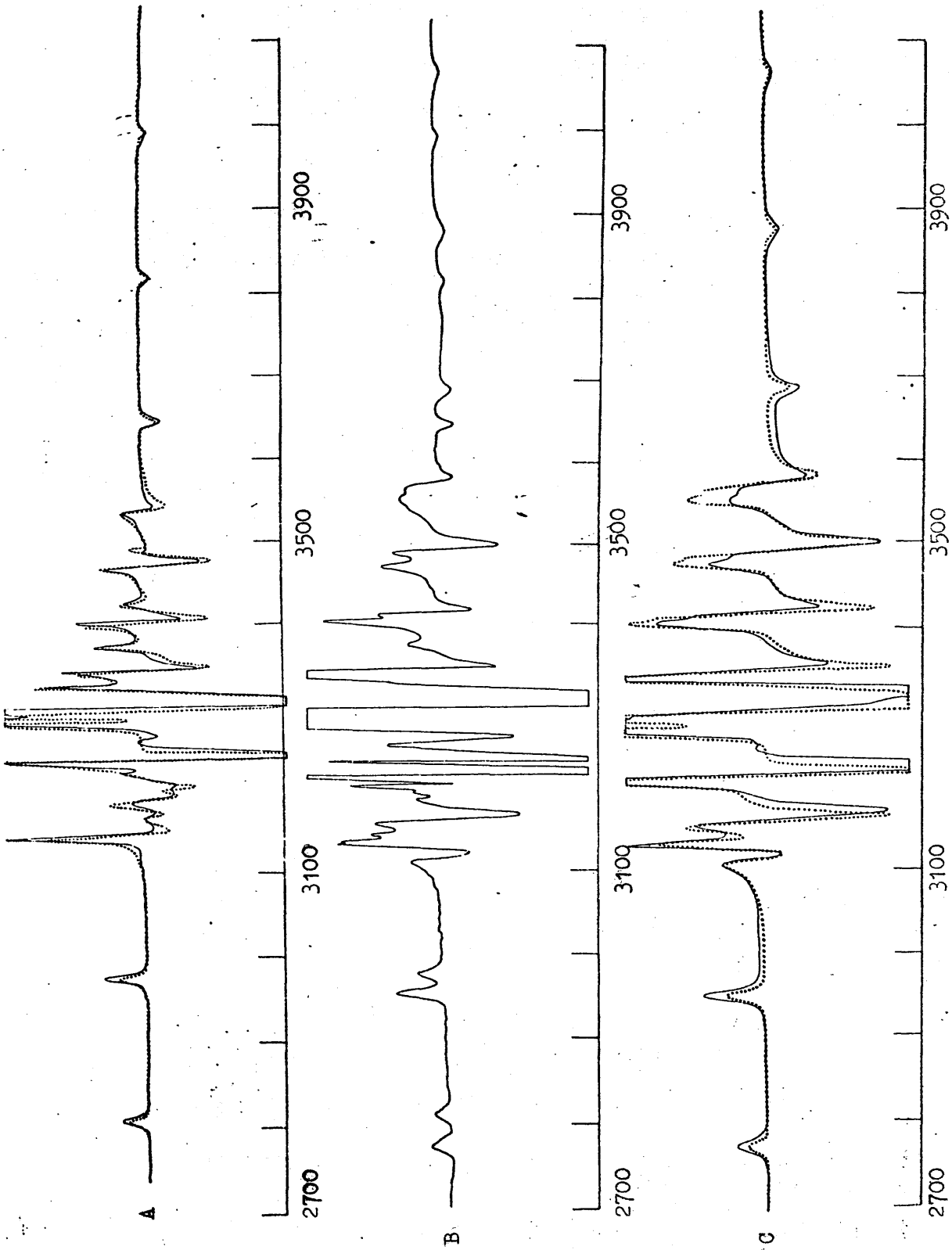

Figure 2.3 Observed (—) and calculated (- -) e.p.r. spectra of 10^{-3}M solutions of vanadyl tropolonate in chloroform-toluene (60:40) glass, A, in chloroform-toluene (60:40) glass containing 1% EtOH, B, and in chloroform glass, containing 2% EtOH, C, all at 77K.

(60:40) using commercial chloroform, which contains a small amount of added ethanol, is shown in spectrum B of figure 2.3. In this spectrum it is possible to distinguish peaks arising from two species, the uncomplexed tropolonate and its ethanol adduct. The complex could be converted entirely to the adduct by annealing the glass at 100K, when the stabler adduct is formed. This occurs more easily in the case of the tropolonate than the maltolate, whereas in the case of the acetylacetonate and the benzoylacetonate only the adduct is formed on freezing the solution. The ease of adduct formation is thus.

acetylacetonate > tropolonate > maltolate.

If a higher concentration of ethanol was used, for instance using pure chloroform, with 2% added ethanol, only the ethanol adduct was formed in the case of the five-membered ring chelates also. The spectrum of the ethanol adduct of the tropolonate is shown in spectrum C of figure 2.3.

Frozen solution spectra of the type shown in figure 2.3 appear formidable at first sight, but the interactions giving rise to such spectra are well understood[15], and are considered in some detail in appendix D.

Essentially it is possible to distinguish peaks in these spectra corresponding to cases where the applied magnetic field lies along the principal axis directions of the system, so that for a nuclear spin of $^7/_2$ there should be eight peaks for the field lying along each principal axis. In a system with rhombic symmetry, it should therefore be possible to detect a maximum of twenty-four peaks, whereas in a system with axial symmetry the maximum number detectable should be sixteen, since two of the sets of eight peaks coincide.

The principal axis system for vanadyl chelates with C_{2v} symmetry is shown in figure 2.4 below.

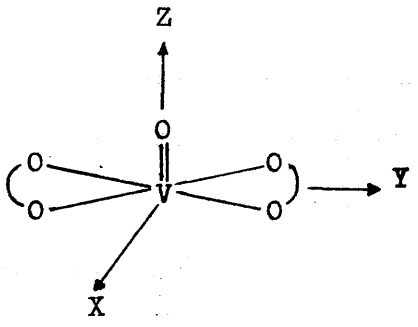

Figure 2.4

In the spectrum of vanadyl tropolonate shown in figure 2.3, the peaks in the wings of the spectrum correspond to cases where the applied field lies along the Z-axis direction of the molecule, whereas the strong peaks in the centre of the spectrum correspond to cases where the applied field lies in the XY plane. The most striking feature about this spectrum, and about the other spectra which were recorded is that in all of them splitting of some of the lines in the centre of the spectra, corresponding to cases where applied field lies in the XY plane, is observed, ie the systems are all totally anisotropic. Although this might be expected for molecules with C_{2v} symmetry, such is not generally the case for oxovanadium derivatives, which usually exhibit effective C_{4v} symmetry in their e.p.r. spectra, and such splitting had only previously been reported for vanadyl acetylacetonate in toluene glass[10].

As shown in appendix A, expressions for the observed resonant fields can be obtained using a Hamiltonian of the form[14]

$$\mathcal{H} = \beta_e \underline{H}.g.\underline{S} + \underline{S}.A.\underline{I} + Q'(I_z^2 - \tfrac{1}{3}I(I+1)). \qquad 2.3$$

where g and A are the anisotropic g and hyperfine tensors for the system, and

$$Q' = \frac{3eqQ}{4I(2I-1)} \qquad 2.4$$

where q is the value of the Z component of the electric field gradient at the nucleus, Q is the quadrupole moment of the nucleus, and eqQ is referred to as the quadrupole coupling constant for systems with axial symmetry. The quadrupole term included in 2.3 is actually that for an axially symmetric system. The value of Q' is small, however, and cannot be very accurately determined from this experiment, and since the deviation from axial symmetry is very slight, it was not felt justifiable to use the more complete expression for the quadrupolar term for rhombic symmetry given in appendix A.

Using equation B10 of appendix B, the general expression for the resonant fields for the cases where the applied field lies along the principal axis directions are given by[16,17]

$$H_z = h\nu_o(g_{zz}\beta_e)^{-1} - hc(g_{zz}\beta_e)^{-1} A_{zz}m_I - hc^2(4g_{zz}\beta_e\nu_o)^{-1} (A_{xx}^2+A_{yy}^2)(I(I+1) - m_I^2) \qquad 2.5$$

$$H_x = h\nu_o(g_{xx}\beta_e)^{-1} - hc(g_{xx}\beta_e)^{-1} A_{xx}m_I - hc^2(4g_{xx}\beta_e\nu_o)^{-1} (A_{yy}^2+A_{zz}^2)(I(I+1) - m_I^2) - hc(2g_{xx}\beta_e A_{xx})^{-1} Q'^2 (2I(I+1) - 2m_I^2 - 1) m_I \qquad 2.6$$

H_y is obtained from 2.6 by interchanging subscripts x and y.

As can be seen from the spectra in figure 2.3, values of the resonant fields H_z can be easily measured since they correspond to the peaks outside the congested central part of the spectrum. Measurement of values of H_x and H_y is more difficult, due to the overlapping of peaks in the central part of the spectrum, and estimation of these was accomplished with the help of a computer programme, whereby it was

possible to simulate the spectrum. The programme involved an iterative procedure, whereby the computer was supplied with a set of resonant fields H_x, H_y and H_z, for each m_I value as estimated from the spectrum. The computer then plotted a set of Kneubuhl curves of the type described in appendix D, added them together, broadened them, and plotted the first derivative of the spectrum. The line shape was assumed to be Gaussian[18,19] and the computer was also supplied with a broadening parameter β. The values of the resonant fields supplied, and the value of β, were then varied until the best fit between the observed and calculated spectra was obtained, and the values of the resonant fields corresponding to the best fit were then used with equations 2.5 and 2.6 to calculate values for the g and hyperfine tensor components, and for Q' for each of the complexes.

The data obtained from the solution and glassy spectra is summarised in tables 2.1 and 2.2. The isotropic parameters obtained from the solution spectra serve as a useful check on the values derived from the glassy spectra, since these are equated by the approximate relationships.

$$\langle A \rangle = \tfrac{1}{3}(A_{xx} + A_{yy} + A_{zz}) \simeq A_o$$

$$\langle g \rangle = \tfrac{1}{3}(g_{xx} + g_{yy} + g_{zz}) \simeq g_o \qquad 2.7$$

and in fact the values of A_o and g_o from the solution spectra agree well with the values estimated from the glassy spectra. The solution values of the ethanol and pyridine adducts, it should be noted, could be obtained by running the spectra in pure ethanol or

Table 2.1

Isotropic spin Hamiltonian parameters for vanadyl chelates in solution at 298K. The A_o values are in units of cm^{-1}. Limits of error are $g_o \pm 0.0005$, $A_o \pm 0.00002$ cm^{-1}. Abbreviations: acac = acetylacetonate, benzac = benzoylacetonate, trop = tropolonate, bromotrop = bromotropolonate.

Complex	Solvent	Ao	go
VO $(acac)_2$	toluene	-0.00999	1.970
VO $(benzac)_2$	"	-0.00994	1.970
VO $(trop)_2$	chloroform	-0.00856	1.972
VO $(maltolate)_2$	"	-0.00913	1.972
VO $(acac)_2$ EtOH	ethanol	-0.00940	1.968
VO $(benzac)_2$ EtOH	"	-0.00940	1.968
VO $(acac)_2$ Py	pyridine	-0.00963	1.972
VO $(benzac)_2$ Py	"	-0.00957	1.970
VO $(trop)_2$ Py	"	-0.00915	1.971
VO $(bromotrop)_2$ Py	"	-0.00916	1.971
VO $(maltolalate)_2$ Py	"	-0.00913	1.972
VO $(kojate)_2$ Py	"	-0.00933	1.970.

Table 2.2

Spin Hamiltonian parameters for vanadyl chelates and their adducts with ethanol and pyridine at 77K. All hyperfine tensor components are in units of cm^{-1}. Limits of error are g_{xx} and $g_{yy} \pm 0.001$ $g_{zz} \pm 0.0005$, A_{xx} and $A_{yy} \pm 0.00005$ cm^{-1}, $A_{zz} \pm 0.00002$ cm^{-1}, $Q' \pm 0.0001$ cm^{-1}. In *, the spectral resolution was insufficient for Q' to be determined.

Complex	g_{xx}	g_{yy}	g_{zz}	A_{xx}	A_{yy}	A_{zz}	$\langle g \rangle$	$\langle A \rangle$	Q'
VO $(acac)_2$	1.984	1.981	1.942	-0.00630	-0.00642	-0.01734	1.969	-0.01007	0.0002
VO $(benzac)_2$	1.984	1.981	1.941	-0.00627	-0.00650	-0.01744	1.969	-0.01011	0.0001
VO $(trop)_2$	1.986	1.979	1.950	-0.00416	-0.00527	-0.01538	1.972	-0.00831	0.0001
VO $(maltolate)_2$	1.986	1.979	1.948	-0.00483	-0.00574	-0.01611	1.971	-0.00895	0.0000
VO $(acac)_2$ EtOH	1.978	1.973	1.947	-0.00543	-0.00594	-0.01670	1.967	-0.00939	0.0003
VO $(benzac)_2$ EtOH	1.978	1.973	1.947	-0.00533	-0.00594	-0.01667	1.967	-0.00936	0.0003
VO $(trop)_2$ EtOH	1.983	1.978	1.941	-0.00562	-0.00599	-0.01679	1.967	-0.00950	0.0003
VO $(bromotrop)_2$ EtOH	1.983	1.978	1.941	-0.00556	-0.00596	-0.01671	1.968	-0.00947	0.0003
VO $(maltolate)_2$ EtOH	1.981	1.978	1.943	-0.00566	-0.00605	-0.01685	1.967	-0.00957	0.0003
VO $(acac)_2$ Py	1.980	1.980	1.945	-0.00618	-0.00618	-0.01674	1.969	-0.00974	*
VO $(benzac)_2$ Py	1.981	1.978	1.944	-0.00590	-0.00617	-0.01672	1.970	-0.00965	0.0002
VO $(trop)_2$ Py	1.984	1.980	1.944	-0.00550	-0.00572	-0.01614	1.969	-0.00917	0.0002
VO $(bromotrop)_2$ Py	1.984	1.980	1.945	-0.00557	-0.00580	-0.01625	1.970	-0.00924	0.0002
VO $(maltolate)_2$ Py	1.982	1.979	1.945	-0.00563	-0.00589	-0.01654	1.969	-0.00943	0.0002
VO $(kojate)_2$ Py	1.980	1.978	1.945	-0.00562	-0.00585	-0.01647	1.969	-0.00935	0.0002

pyridine solution, where the chelates can be safely assumed to exist only in the complexed form. Due to solubility difficulties, however, the ethanol spectra of the five-membered ring chelates could not be recorded. Small differences in the values of g_o and A_o obtained from the solution and glassy spectra are usually observed due to changes in the electron distribution in the complexes due to changes in their environment when the solution freezes, but reasonable agreement between the solution and glassy values serves as a reasonable indication of the accuracy of the parameters derived from the glassy spectra.

The value of the parameter Q'^2 was calculated for each complex, and a small but consistently positive value was obtained, giving values of Q' varying between 0 and 0.0003 cm^{-1}. The large error on this parameter, about ± 0.0001 cm^{-1} makes its use in any calculations limited, but it did appear to contribute very slightly to the observed field values, and its inclusion serves to increase the accuracy of the other parameters.

2.4 U.v.-visible spectra of vanadyl chelates

The interpretation of the e.p.r. data in terms of the electronic structures of the complexes requires that the energy differences between the ground and various excited states of the complexes be known, as will be discussed later. These energy differences can often be equated to the values of the various maxima in the u.v.-visible spectra of the complexes. Since the positions of the maxima depend on the solvent

used[9], due to the formation of adducts between the vanadyl chelates and the solvents, the u.v.-visible spectrum used in interpreting each set of e.p.r. data was that of the appropriate adduct. Thus the u.v.-visible spectra of vanadyl acetylacetonate in toluene and pyridine were used to interpret the e.p.r. data for the uncomplexed acetylacetonate and its pyridine adduct respectively, and so on. The frequencies of the band maxima observed in the u.v.-visible spectra of the various chelates are given in table 2.3. Examples of the spectra for one six-membered ring chelate, vanadyl acetylacetonate, and one five-membered ring chelate, vanadyl maltolate, are given in figures 2.5 and 2.6 respectively.

Due to insolubility problems, the spectra of the five-membered ring chelates could not be recorded in toluene or in ethanol, so that the spectra of the chloroform solutions of these were used in calculations on the uncomplexed chelates, and the spectra of the pyridine solutions were used in the calculations on both the pyridine and ethanol adducts. This is reasonable, considering the similarity between the chloroform and toluene spectra, and the pyridine and ethanol spectra, of the six-membered ring chelates.

Care had to be taken in recording the spectra of the five-membered ring chelates due to the fact that they tended to oxidise in solution, especially in the presence of alcohol or moisture, although they are indefinitely stable as solids. When the maltolate, for instance, is dissolved in commercial chloroform, containing 2% ethanol, within a few minutes the d-d transitions in the spectrum are quickly masked by the development of an intense red colour. At the same time the solution slowly becomes diamagnetic, its e.p.r. spectrum gradually disappears, and the i.r. absorption at 990 cm^{-1} characteristic of the V = O stretching frequency in oxovanadium (IV) compounds is slowly replaced by a new

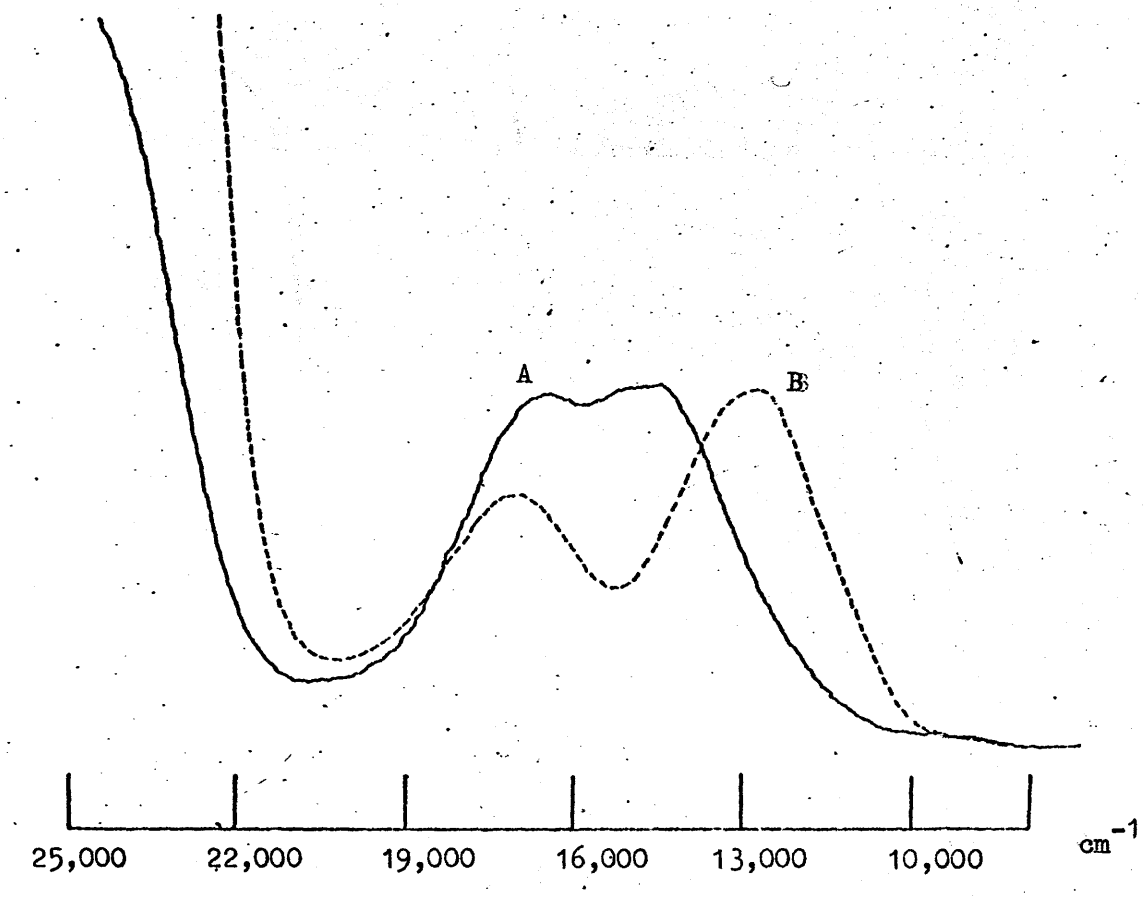

Figure 2.5 U.v.-visible spectrum of vanadyl acetylacetonate in chloroform solution, A, and in pyridine solution, B.

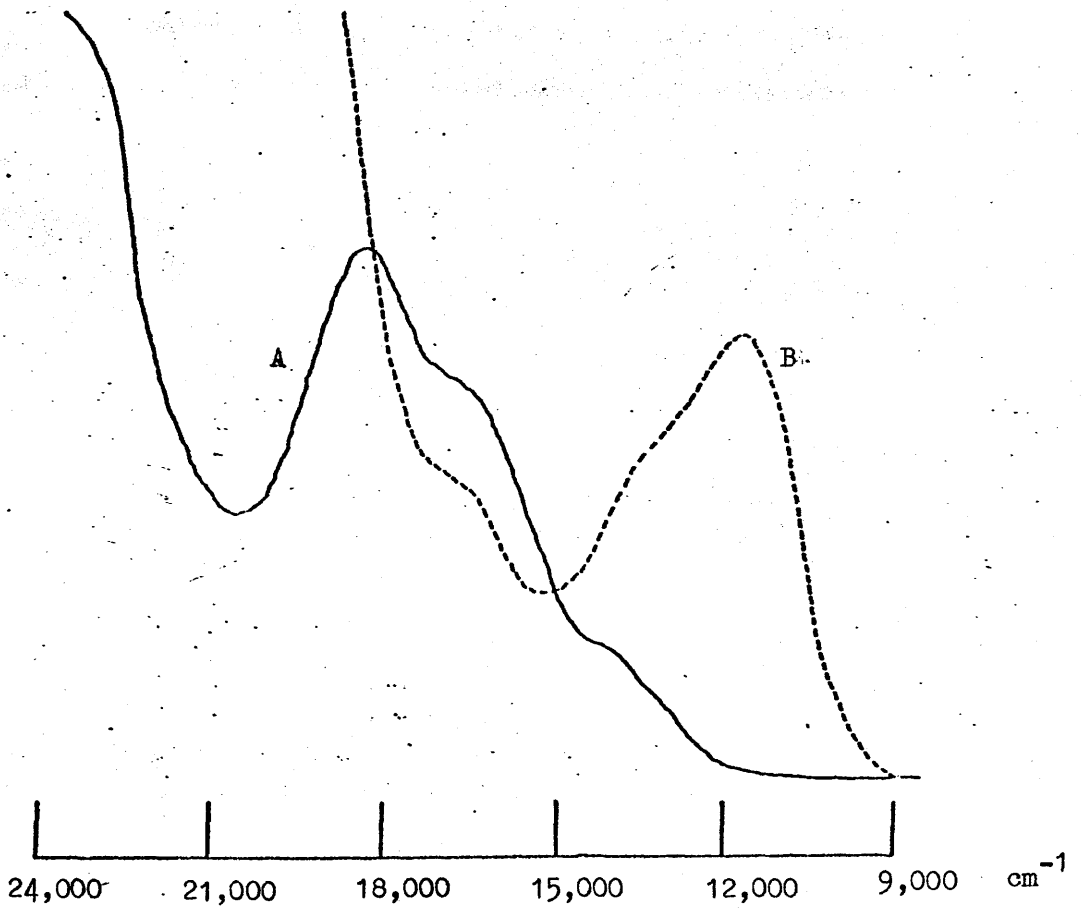

Figure 2.6 U.v.-visible spectrum of vanadyl maltolate in chloroform solution, A, and in pyridine solution, B.

Table 2.3

Band maxima (cm^{-1}) in the visible-u.v. spectra of vanadyl chelates.

Complex	Solvent	ΔE_1	ΔE_2	ΔE_3	ΔE_4
VO $(acac)_2$	toluene	15,100		16,800	25,400
VO $(benzac)_2$	"	14,800		16,800	21,500
VO $(acac)_2$	chloroform	15,000		16,800	25,600
VO $(benzac)_2$	"	14,800		16,900	21,500
VO $(trop)_2$	"	13,300	16,600	18,500	
VO $(bromotrop)_2$	"	13,300	16,600	18,500	
VO $(maltolate)_2$	"	13,300	16,600	18,200	
VO $(kojate)_2$	"	13,300	16,600	18,200	
VO $(acac)_2$	ethanol	12,800		17,200	26,000
VO $(benzac)_2$	"	12,700		17,200	21,500
VO $(acac)_2$	pyridine	13,000		17,200	
VO $(benzac)_2$	"	13,000		17,300	21,500
VO $(trop)_2$	"	11,900	13,000	16,400	
VO $(bromotrop)_2$	"	11,900	13,000	16,400	
VO $(maltolate)_2$	"	11,800	13,000	16,400	21,000
VO $(kojate)_2$	"	11,800	13,000	16,400	21,000

absorption at 960 cm^{-1} which is similar to that reported for oxovanadium (V) complexes[20]. These observations imply that an oxovanadium (V) complex is being formed and that the reaction taking place is

$$VO\ (maltolate)_2 + EtOH + \tfrac{1}{2}O_2 \longrightarrow VO\ (maltolate)_2\ OEt + \tfrac{1}{2}H_2O$$

The corresponding reaction in aqueous solution

$$VO\ (maltolate)_2 + \tfrac{1}{2}H_2O + \tfrac{1}{2}O_2 \rightleftharpoons VO\ (maltolate)_2\ OH$$

is reversible. A freshly prepared, green aqueous solution of vanadyl maltolate turns red when it is allowed to stand in contact with air. When this red solution is boiled, it turns green, the colour change being reversed when the solution is allowed to cool. Furthermore, at pH5, a 2:1 molar aqueous solution of maltol and ammonium metavanadate is red. On boiling this solution, the colour changes to green, and vanadyl maltolate is precipitated.

A similar reaction has been noted by Selbin et al[7], for vanadyl acetylacetonate, but these authors simply noted that the ligand field bands in the spectrum disappeared, without speculating on the nature of the reaction products. The reaction appears to be more rapid in the case of the five-membered ring chelates.

2.5 Molecular orbitals in vanadyl chelates

The data obtained from the e.p.r. and u.v.-visible spectra can now be used to obtain values for the coefficients in the molecular orbitals for the complexes, and hence to obtain information about the bonding. The theory involved in the general case is now fairly well understood[21] and its application to vanadyl chelates is discussed in appendix C.

The nature of the equations relating the spin Hamiltonian parameters and the molecular orbital coefficients depends on the symmetry which is assumed for the complexes. The complexes studied here are assumed to have effective C_{2v} symmetry ie it is assumed that the basal oxygen

ligands are all effectively equivalent, and that the deviation from C_{4v} symmetry arises because the basal O - V - O angles differ from 90^{o}. This is obviously reasonable for all the chelates, except the maltolate and the kojate, which have mixed ketonic and hydroxylic ligands. However in the e.p.r. spectra of vanadyl ketemediimine[22] complexes, which have mixed nitrogen and oxygen basal ligands, no deviation from axial symmetry is observed. This suggests that small differences in the nature of the basal ligands are unimportant in deciding the effective symmetry of the complexes, and that the observed anisotropy in the e.p.r. spectra arises from other factors.

The chelates are all assumed to have the axis system shown in figure 2.7 below.

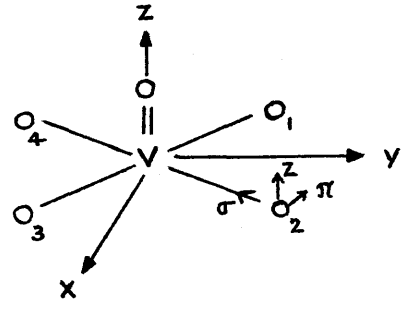

Figure 2.7

The axis systems for the ligands are centred on the ligands, with their σ axes pointing along the O⟶V directions.

The molecular orbitals for the system can now be written as a linear combination of the metal ion orbitals and the corresponding ligand group orbitals, making use of the symmetry properties of the system to decide the form of these.

According to the molecular orbital scheme of Ballhausen and Grey,[4] the unpaired electron in chelates with C_{4v} symmetry occupies the metal ion $3d_{x^2-y^2}$ orbital. In chelates with C_{2v} symmetry, however, the metal $3d_{x^2-y^2}$ orbital belongs to the same representation as the $3d_{z^2}$ and 4s

orbitals so that the ground state molecular orbital A_1^*, is a linear combination of all of these metal ion orbitals, and a ligand group orbital, of the form

$$A_1^* = \alpha_1^*(ad_{x^2-y^2} + bd_{z^2} + CS) + \alpha_1^{*I}(p_\pi^1 - p_\pi^2 + p_\pi^3 - p_\pi^4)$$

In terms of a simple electrostatic model,[23] the mixing of $3d_{z^2}$ and 4s character into the ground state orbital arises because the deviation of the basal O-V-O angle from 90° results in one lobe of the $3d_{x^2-y^2}$ orbital experiencing greater electrostatic repulsion than the other. Mixing $3d_{z^2}$ and 4s character into the ground state results in a redistribution of electron density into regions of lower electrostatic repulsion. Since the mixing arises from the superposition of a small C_{2v} field on a larger C_{4v} ligand field, $a \gg b, c$.

The spin-orbit interaction between the unpaired electron and the vanadium nucleus mixes into the ground state contributions from excited state molecular orbitals, which are then able to contribute to the expressions for the spin Hamiltonian parameters. The only states which are able to contribute effectively are those which are closest to the ground state in energy and which, in the case of the vanadyl chelates studied here, have appreciable metal ion orbital character. In fact in this case the only states which are important are those which are produced by promoting the unpaired electron into a low-lying molecular orbital of mainly metal ion 3d orbital character. The form of the molecular orbitals which contribute to the ground state are

$$B_1^* = \beta_1^* d_{xz} + \frac{\beta_1^{*I}}{2}(p_z^2 + p_z^3 - p_z^1 - p_z^4) + \beta_1^{*II} p_x^5$$

$$B_2^* = \beta_2^* d_{yz} + \frac{\beta_2^{*I}}{2}(p_z^1 + p_z^2 - p_z^3 - p_z^4) + \beta_2^{*II} p_y^5$$

$$A_2^* = \alpha_2^* d_{xy} + \frac{\alpha_2^{*I}}{2}(s^2 + s^4 - s^1 - s^3) + \frac{\alpha_2^{*II}}{2}(p_\sigma^2 + p_\sigma^4 - p_\sigma^3 - p_\sigma^1)$$

The other molecular orbitals of A_1 symmetry, derived mainly from the metal ion $3d_{z^2}$ and 4s orbitals, although they are fairly close to the ground state in energy, are not in fact mixed into the ground state by spin-orbit coupling, and so can be ignored.

The relative energies of the magnetically important molecular orbitals are shown in figure 2.8.

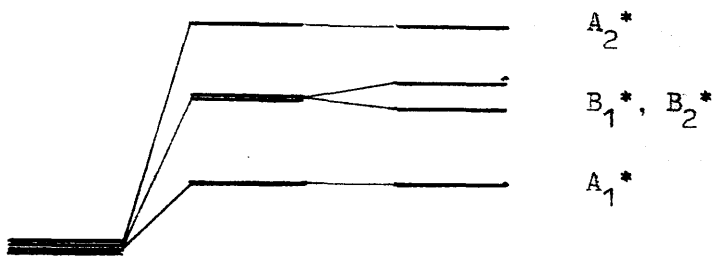

Figure 2.8

The expressions relating the spin Hamiltonian parameters to the molecular orbital coefficients can now be obtained by comparing elements of the true Zeeman and hyperfine Hamiltonians with the corresponding matrix elements of the spin Hamiltonian 2.3. If this is done, the following relationships, derived in appendix C, are obtained for the g-tensor components.

$$g_{xx} = 2.0023 - \frac{2(a + b\sqrt{3})^2 \zeta_v \alpha_1^{*2} \text{ Pmd } (B_2^*)}{\Delta E\ (B_2^*)}$$

$$g_{yy} = 2.0023 - \frac{2(a - b\sqrt{3})^2 \xi_v \alpha_1^{*2} \text{ Pmd } (B_1^*)}{\Delta E\ (B_1^*)}$$

$$g_{zz} = 2.0023 - \frac{8a^2 \xi_v \alpha_1^{*2} \text{ Pmd } (A_2^*)}{\Delta E\ (A_2^*)} \qquad 2.8$$

The Pmd values are the d-orbital populations in the various excited state molecular orbitals, the ΔE values are the differences in energies between the ground and excited states, and ξ_v is the vanadium ion spin-orbit coupling constant.

The expressions for the hyperfine tensor components, which are also derived in appendix C, are

$$A_{xx} = P(-K + \frac{2}{7}(a^2-b^2)\alpha_1^{*2} - \frac{4\sqrt{3}}{7} ab\alpha_1^{*2} - \Delta g_{xx} + \frac{(3a + b\sqrt{3})}{14(a - b\sqrt{3})} \Delta g_{yy} + \frac{b}{7a} \Delta g_{zz})$$

$$A_{yy} = P(-K + \frac{2}{7}(a^2-b^2)\alpha_1^{*2} + \frac{4\sqrt{3}}{7} ab\alpha_1^{*2} - \Delta g_{yy} + \frac{(3a - b\sqrt{3})}{14(a + b\sqrt{3})} \Delta g_{xx} - \frac{b}{7a} \Delta g_{zz})$$

$$A_{zz} = P(-K - \frac{4}{7}(a^2-b^2)\alpha_1^{*2} - \frac{(3a + b\sqrt{3})}{14(a - b\sqrt{3})} \Delta g_{yy} - \frac{(3a - b\sqrt{3})}{14(a + b\sqrt{3})} \Delta g_{xx} - \Delta g_{zz}) \qquad 2.9$$

where $P = g_e g_N \beta_e \beta_N \langle d_{x^2-y^2} | r^{-3} | d_{x^2-y^2} \rangle$, $\Delta g_{ii} = 2.0023 - g_{ii}$, and $-PK$ is the isotropic contribution to the hyperfine coupling arising from the Fermi contact interaction. These equations are similar to those used by Belford et al[11], which in turn are simply those of McGarvey,[21] with covalency allowed for. The 4s orbital contribution to the ground state, which was not considered previously, contributes only to the value of $-PK$, although this contribution is very important, as will be seen later.

These equations, therefore, are those appropriate to a complex with C_{2v} symmetry. It has been shown that if the effective symmetry falls below

C_{2v} due to an inequivalence of the basal ligand atoms, then the relationships above become more complex.[23] In systems with lower than C_{2v} symmetry, mixing of the $d_{x^2-y^2}$ with the d_{xy} and of the d_{xz} with the d_{yz} orbital becomes allowed. As a result, the out-of-plane orbitals derived from the d_{xz} and d_{yz} orbitals no longer point along the same axes as the in-plane orbitals derived from the $d_{x^2-y^2}$ and d_{xy} orbitals. This results in the principal axis systems for the g and hyperfine tensors becoming non-coincident, so that the observed e.p.r. spectra can not be interpreted in terms of a spin Hamiltonian in which both tensors are diagonalised. This effect has, however, been shown to be fairly small in the case of vanadyl benzoylacetonate doped into single crystals of palladium benzoylacetonate,[11] and this, together with the fact that all the spectra recorded here could in fact be interpreted in terms of a Hamiltonian in which the g and hyperfine tensors were simultaneously diagonalised, suggests that this effect is small for vanadyl chelates in general, and that the effective symmetry can be taken as C_{2v}.

The equations 2.8 and 2.9 cannot be solved directly, since they have too many unknowns, therefore it is necessary to estimate reasonable values for ζ_v and P for the vanadium ion having the charge and configuration which it possesses in the complexes. Values of ζ_v can be estimated for various states of ionisation of vanadium from atomic spectroscopy[24,1], and values of P can be estimated from the values of $\langle d_{x^2-y^2} | r^{-3} | d_{x^2-y^2} \rangle$ obtained from Hartree-Fock calculations[25]. The values of ζ_v and P which will be used in the calculations are those for the V^{+2} $(3d^3)$ ion[6], ie

$$\zeta_v = 170 \text{ cm}^{-1}$$

$$P = 0.0127 \text{ cm}^{-1}$$

since Kivelson and Lee[5] pointed out that Ballhausen and Grey's calculation on vanadyl pentahydrate gave the vanadium a configuration $3d^3\ 4s^{\frac{1}{2}}\ 4p^{\frac{1}{2}}$, and the values of S and P for this will be closer to those for V^{+2} than those for V^{+1}, as used by Ballhausen and Grey.

It is now possible to proceed with the calculation of the molecular orbital coefficients.

2.6 Molecular orbital coefficients and bonding in vanadyl chelates

(a) In-plane π-bonding.

Combining the three equations 2.9 gives

$$\langle A \rangle = -PK - \tfrac{3}{7}(2.0023 - \langle g \rangle) \qquad 2.10$$

from which it is possible to calculate values of -PK, and hence K for each of the chelates. The values of -PK can then be used, together with the expression for A_{zz} to obtain the α_1^{*2} values. The resulting values of K and α_1^{*2} are summarised in table 2.6.

In calculating K it was assumed that $\langle A \rangle$ is negative, although the sign of $\langle A \rangle$ cannot be determined directly from the e.p.r. spectrum. It can, however, be inferred from the fact that the spin-dipolar contribution to the value of A_{zz} for an electron in a $d_{x^2-y^2}$ orbital can be shown to be negative, and since for vanadyl chelates $|A_{zz}| > |\langle A \rangle|$, the isotropic coupling must be negative.

The variation in the calculated values of K parallels the variation in $\langle A \rangle$, as would be expected, since the isotropic hyperfine coupling arises almost exclusively from the Fermi contact interaction, with only a small contribution from the orbital-dipolar interaction. The values of α_1^{*2} show that the unpaired electron in all of the complexes studied is localised almost completely on the vanadium ion, so that in-plane π bonding between the mainly $3d_{x^2-y^2}$ orbital and the ligand p_π orbitals

is very slight in all cases. This fact is of some importance in the later discussion of the variation of the isotropic hyperfine coupling constant in the complexes.

(b) In-plane σ-bonding

Information about the extent of the in-plane σ-bonding between the metal ion $3d_{xy}$ orbital and the s and p_σ orbitals of the basal ligands can be obtained from the $Pmd(A_2^*)$ values, which give the metal $3d_{xy}$ orbital populations in the A_2^* antibonding molecular orbitals. The calculation of the $Pmd(A_2^*)$ values can only be carried out, however, if the values of $\Delta E(A_2^*)$ are known. These values can be estimated from the u.v.-visible spectra of the complexes if it is known which of the maxima in the spectra correspond to the $A_1^* \longrightarrow A_2^*$ electronic transitions. There are, however, two alternative assignments of the bands present in the u.v.-visible spectrum of vanadyl acetylacetonate listed in table 2.3, one due to Ballhausen and Grey,[4] and the other to Selbin et al[7]. The two schemes are shown schematically in figure 2.9.

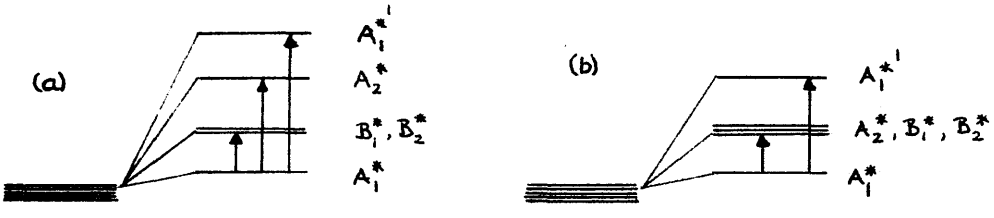

Figure 2.9 Alternative energy level schemes for vanadyl complexes (a) Ballhausen-Grey (b) Selbin et al.

According to Ballhausen and Grey the lowest energy band in the spectrum contains the $A_1^* \longrightarrow B_1^*$ and $A_1^* \longrightarrow B_2^*$ transitions, the next lowest is the $A_1^* \longrightarrow A_2^*$ transition and the highest energy band is assigned to the $A_1^* \longrightarrow A_1^{*\prime}$ transition where the $A_1^{*\prime}$ molecular orbital is that derived from the metal ion $3d_{z^2}$ orbital.

In the scheme of Selbin et al the transitions $A_1^* \longrightarrow A_2^*$, $A_1^* \longrightarrow B_1^*$ and $A_1^* \longrightarrow B_2^*$ are all assigned to the lowest energy band, the next lowest band is assigned to the $A_1^* \longrightarrow A_1^{*'}$ transition and the highest band is thought to be a ligand-to-metal charge transfer band. The evidence for this scheme is that at 77K, the low frequency band can be seen to consist of several overlapping bands, although it has been suggested that this may simply be the result of vibronic coupling with the vanadyl V-O stretching mode, which has a frequency roughly equal to that observed for the separation between the bands observed at low temperature in the u.v.-visible spectrum.

In order to decide between the alternative schemes, therefore, the $Pmd(A_2^*)$ values were calculated according to both schemes as shown below for vanadyl acetylacetonate and its adducts.

Complex	$\Delta E(A_2^*)$		$Pmd(A_2^*)$	
	(a)	(b)	(a)	(b)
$VO(acac)_2$	16,800	15,100	0.75	0.68
$VO(acac)_2$ Py	17,200	13,000	0.74	0.57
$VO(acac)_2$ EtOH	17,200	12,800	0.72	0.42

Table 2.4 Values of $Pmd(A_2^*)$ calculated according to (a) Ballhausen and Grey, (b) Selbin et al for vanadyl acetylacetonate and its pyridine and ethanol adducts.

From these results it can be seen that assigning the lowest band in the spectrum to the $A_1^* \longrightarrow A_2^*$ transition leads to an excessively large variation in $Pmd(A_2^*)$ between the complex and its adducts, and leads to covalency parameters which are chemically unreasonable, for instance in the ethanol adduct there is more electron density on the metal in the bonding orbital than there is on the more electronegative ligands. Assigning the higher frequency band to the $A_1^* \longrightarrow A_2^*$ transition on the

other hand leads to values of $Pmd(A_2^*)$ which are both chemically reasonable, and show a reasonable variation between the complexes, and so on this basis the Ballhausen-Grey scheme is the more likely of the two alternatives.

In the case of the five-membered ring chelates there are three bands in the 10,000-20,000 cm^{-1} region of the visible spectrum compared with the two found in the six-membered ring chelates, and again each of the bands was used in turn to calculate the value of $Pmd(A_2^*)$ as shown for vanadyl maltolate.

Complex	$\Delta E(A_2^*)$	$Pmd(A_2^*)$
VO $(malt)_2$	(a) 18,200 (b) 16,600 (c) 13,300	(a) 0.74 (b) 0.67 (c) 0.54
VO $(malt)_2$ Py	(a) 16,400 (b) 13,000 (c) 11,800	(a) 0.71 (b) 0.57 (c) 0.51
VO $(malt)_2$ EtOH	(a) 16,400 (b) 13,000 (c) 11,800	(a) 0.72 (b) 0.58 (c) 0.52

Table 2.5 Values of $Pmd(A_2^*)$ calculated for different assignments of the $A_1^* \longrightarrow A_2^*$ transition for vanadyl maltolate and its pyridine and ethanol adducts.

On the basis of these results the most reasonable values of $Pmd(A_2^*)$ are obtained by assigning the $A_1^* \longrightarrow A_2^*$ transition to the highest frequency band in the spectrum. This assignment leads to values of $Pmd(A_2^*)$ which are acceptable both chemically and in terms of the variation in values between the uncomplexed species and its adducts.

Thus, to summarise, values of $Pmd(A_2^*)$ were calculated for all the complexes using the values ΔE_3 of table 2.3 for $\Delta E(A_2^*)$ and the results are tabulated in table 2.6. The values obtained show that there is a considerable degree of covalency in the in-plane σ-bonding for both the five and six-membered ring chelates, and that the degree of covalency is similar for all the complexes, as might be expected.

The molecular orbital coefficients α_2^* could be calculated if the chelate oxygens were assumed to be sp^2 hybridised from the equation

$$Pmd(A_2^*) = \alpha_2^{*2} + \alpha_2^{*I}S \qquad 2.11$$

where $S = -2\langle d_{xy}|(p_\sigma^1 + s^1)/\sqrt{2}\rangle$

The values of α_2^* calculated in this way, using a value of S of 0.25, are also given in table 2.6.

(c) Out-of-plane π-bonding.

The extent of the out-of-plane π-bonding between the metal d_{xz} and d_{yz} orbitals and the ligand π-orbitals, primarily the vanadyl oxygen π-orbitals, can be estimated from the values of $Pmd(B_1^*)$ and $Pmd(B_2^*)$. These can be obtained by first calculating values for the parameters a and b from the expressions for A_{xx} and A_{yy} of equations 2.9 and then using these values, together with the expressions for g_{xx} and g_{yy} of equations 2.8 to calculate the $Pmd(B_1^*)$ and $Pmd(B_2^*)$ values. The values of $Pmd(B_1^*)$, $Pmd(B_2^*)$ and b calculated in this way are listed in table 2.6. It should be noted that since it is impossible to say which of the experimentally determined g-values corresponds to g_{xx} and which to g_{yy} of the axis system of figure 2.5, it is impossible to determine the relative signs of the a and b values, so that the labelling of the g-tensor values in table 2.2 is quite arbitrary.

In calculating the values of $Pmd(B_1^*)$ and $Pmd(B_2^*)$, the energy differences $\Delta E(B_1^*)$ and $\Delta E(B_2^*)$ were equated to the transition energies ΔE_1 and ΔE_2 of table 2.3. Assigning the $A_1^* \longrightarrow B_1^*$, B_2^* transitions to bands at higher frequencies in the u.v.-visible spectra of the chelates leads to values of the metal orbital populations greater than one, therefore these transitions must be assigned to the lowest frequency bands in the spectra. In the six-membered ring chelates, where there is only one low frequency

band in the spectra, the same value was used in the calculations for $\Delta E(B_1^*)$ and $\Delta E(B_2^*)$. The fact that the $A_1^* \longrightarrow B_1^*$ and $A_1^* \longrightarrow B_2^*$ transitions are resolved in the five-membered ring chelates but not in the six-membered ring chelates is consistent with the greater anisotropy in the e.p.r. spectra of the former type of complex.

The values of $Pmd(B_1^*)$ and $Pmd(B_2^*)$ listed in table 2.6 are individually reliable only to ± 0.05, so there is no significant difference in the π-bonding in the XZ and YZ planes. Despite the large errors on these values, however, the overall results do indicate a fairly high degree of out-of-plane π-bonding, which is almost certainly mainly due to bonding with the vanadyl oxygen, and this is consistent with the known multiple bond character of the vanadyl V-O bond. Overall, also, there appears to be slightly more π-bonding in the five-membered ring chelates than in the six-membered ring chelates.

The equations 2.8 and 2.9 can also be used to check the validity of the form assumed for the ground state orbital for the chelates, by showing that the parameters a and b calculated from equation 2.9 have the same magnitude and relative signs as those obtained from equation 2.8. This was done for all the chelates studied here, and in all cases consistent sets of values were in fact obtained from the two equations, so showing that the correct form for the ground state had been used.

Inspection of the equations 2.8 and 2.9 shows that although various factors may produce an anisotropy in the X and Y values of the e.p.r. parameters for the chelates, the mixing of d_{z^2} character into the ground state is by far the most important factor and it requires only a very small degree of d_{z^2} mixing to produce a very large anisotropy.

Table 2.6

Molecular orbital coefficients and orbital populations for vanadyl chelates and their adducts with ethanol and pyridine. Limits of error α_1^{*2} ±0.005, Pmd (A_2^*) ±0.015, Pmd (B_1^*), Pmd (B_2^*) ±0.05, K ±0.002.

Complex	K	$(\alpha_1^*)^2$	|b|	Pmd (A_2^*)	$(\alpha_2^*)^2$	Pmd (B_2^*)	Pmd (B_1^*)
VO $(acac)_2$	0.77	0.989	0.0034	0.75	0.90	0.83	0.94
VO $(benzac)_2$	0.78	0.995	0.0094	0.76	0.91	0.83	0.90
VO $(trop)_2$	0.64	0.965	0.041	0.76	0.90	0.95	0.83
VO $(maltolate)_2$	0.68	0.984	0.033	0.74	0.89	0.91	0.84
VO $(acac)_2$ EtOH	0.72	0.985	0.018	0.72	0.87	0.99	1.02
VO $(benzac)_2$ EtOH	0.72	0.995	0.022	0.71	0.86	0.99	1.01
VO $(trop)_2$ EtOH	0.73	0.979	0.013	0.76	0.91	0.80	0.82
VO $(bromotrop)_2$ EtOH	0.72	0.982	0.013	0.75	0.90	0.80	0.82
VO $(maltolate)_2$ EtOH	0.73	0.989	0.014	0.72	0.87	0.87	0.84
VO $(acac)_2$ Py	0.74	0.972	*	0.74	0.89	0.89	0.89
VO $(benzac)_2$ Py	0.74	0.965	0.0078	0.76	0.91	0.87	0.94
VO $(trop)_2$ Py	0.70	0.950	0.0068	0.74	0.89	0.77	0.79
VO $(bromotrop)_2$ Py	0.71	0.953	0.0072	0.73	0.88	0.77	0.79
VO $(maltolate)_2$ Py	0.72	0.970	0.009	0.71	0.86	0.83	0.81
VO $(kojate)_2$ Py	0.72	0.970	0.008	0.71	0.86	0.90	0.84

2.7 Adduct formation and its effects on the spectral properties and electron distributions in vanadyl chelates

The following changes occur in the spectral parameters of the vanadyl chelates on adduct formation.

(a) In the u.v.-visible spectra of the chelates the energy of the $A_1^* \longrightarrow A_2^*$ transition increases slightly for the six-membered ring chelates and decreases slightly for the five-membered ring chelates. The energies of the $A_1^* \longrightarrow B_1^*$ and $A_1^* \longrightarrow B_2^*$ transitions decrease in all cases.

(b) In the e.p.r. spectra, the values of g_{zz} decrease in the case of the five-membered ring chelates while those of the six-membered ring chelates increase.

(c) The anisotropic contributions to the hyperfine coupling constants remain unchanged in all cases. The isotropic contributions, on the other hand, increase for the five-membered ring chelates and decrease for the six-membered ring chelates. The overall changes in the hyperfine coupling tensor components therefore simply reflect the changes in the isotropic coupling contributions.

The changes in the positions of the band maxima in the u.v.-visible spectra of the chelates on adduct formation cannot be explained in terms of one single effect.

In the case of square planar copper complexes, which form adducts in the same way as vanadyl complexes, the changes in the u.v.-visible spectra could be explained by considering the effects of the solvating base to be equivalent to those that would be produced by placing a dipole μ along the symmetry axis of the molecule with its negative end pointing towards the metal ion.[26] The changes in the spectra could then

be explained in terms of the effects of the additional electrostatic interaction on the energies of the molecular orbitals of the complexes.

The Hamiltonian for this dipolar interaction is given by

$$\mathcal{H} = \frac{e\mu}{a^2}\left[1 - \frac{2r\cos\theta}{a} - \frac{3r^2}{2a^2}\left(1 - 3\cos^2\theta\right)\right] \qquad 2.12$$

where the dipole is considered to be at a distance a along the -Z axis direction of figure 2.4, and the usual form of the polar coordinates is used.

If the first order contributions to the energies of the molecular orbitals of the complexes due to the electrostatic interaction with the dipole are evaluated, the predicted changes in the transition energies of the vanadyl complexes studied here are given by

$$\Delta E'\ (A_1^* \longrightarrow A_2^*) = \left[\frac{e\mu}{a^2} - 108\,\frac{e\mu a_o^2}{a^4 c^2}\right]\left[\alpha_2^{*2} - \alpha_1^{*2}\right]\ (hc)^{-1}\ \text{cm}^{-1}$$

$$\Delta E'\ (A_1^* \longrightarrow B_1^*) = \left[\frac{e\mu}{a^2}\left(\alpha_1^{*2} - \beta_1^{*2}\right) + 54\,\frac{e\mu a_o^2}{a^4 c^2}\left(2\alpha_1^{*2} + \beta_1^{*2}\right)\right]\ (hc)^{-1}\ \text{cm}^{-1}$$

$$\Delta E'\ (A_1^* \longrightarrow B_2^*) = \left[\frac{e\mu}{a^2}\left(\alpha_1^{*2} - \beta_2^{*2}\right) + 54\,\frac{e\mu a_o^2}{a^4 c^2}\left(2\alpha_1^{*2} + \beta_2^{*2}\right)\right]\ (hc)^{-1}\ \text{cm}^{-1} \qquad 2.13$$

If these expressions are evaluated, using reasonable values for μ and a, together with the molecular orbital coefficients listed in table 2.6, they predict an increase in the frequency of the $A_1^* \longrightarrow B_1^*$ and $A_1^* \longrightarrow B_2^*$ transitions and a slight decrease in the $A_1^* \longrightarrow A_2^*$ transition. Although some of the predictions agree with the experimentally observed changes, on the whole this simple model does not satisfactorily account for the changes in the spectra of the vanadyl chelates, although it did

prove satisfactory in the case of the copper chelates. It is therefore very probable that there are other factors which must be taken into account in explaining the changes in the transition energies. It is known, for instance, that there is a decrease in the V-O vanadyl bond stretching frequency on adduct formation, and it has been suggested[6] that this is due to a decrease in the extent of the π-bonding in the vanadyl V-O bond, which would be expected to result in a decrease in the $A_1^* \longrightarrow B_1^*$ and $A_1^* \longrightarrow B_2^*$ transition frequencies, as observed. It is therefore possible that changes in the bonding in the complex are important in deciding the changes in the transition frequencies.

Changes in the geometry of the complexes may also be of some importance in changing the energy levels. The x-ray structure analysis of vanadyl acetylacetonate[27,28] shows that the vanadium atom in vanadyl complexes does not lie in the plane of the basal ligands, but slightly above the plane, as shown in figure 2.10 below.

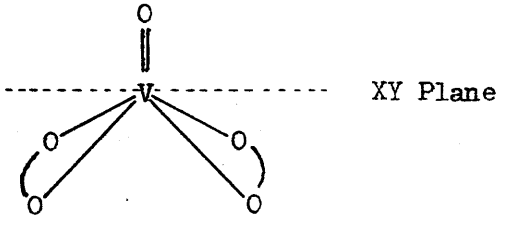

Figure 2.10

The complex probably assumes this geometry to minimise steric interactions between the vanadyl oxygen and the chelate ligands. On adduct formation, however, the added steric interaction with the incoming base would be expected to cause the chelating ligands to swing upwards, closer to the XY plane, and the resulting change in the geometry would cause changes in the energy levels of the complex.

Thus changes in the electrostatic interactions, geometry, and bonding in these complexes on adduct formation may all contribute to the changes

in the energy levels of the molecular orbitals, and the resulting transition energies, so that the observed changes in the u.v.-visible spectra will depend very much on the type of complex involved.

The effect of adduct formation on the g_{zz} values for the chelates can be seen from equation 2.8 to depend on changes in α_2^{*2}, $Pmd(A_2^*)$ and $\Delta E(A_2^*)$. In fact it can be seen from the data in table 2.6 that the molecular orbital coefficients remain fairly constant, so that the g_{zz} value changes are determined by the changes in the values of $\Delta E(A_2^*)$.

Thus the differences in the way in which the g_{zz} values of the five- and six-membered ring chelates change can simply be traced back to the differences in the way in which the $\Delta E(A_2^*)$ values change. In the case of the g_{xx} and g_{yy} values, it is not possible to say that changes in one single parameter are mainly responsible for the changes observed in these, since the values of a, b, the orbital populations and the transition energies, are all important to some extent.

The differences in the isotropic hyperfine coupling constants A_o, between the five- and six-membered ring chelates and the differences in the way in which these alter on adduct formation are particularly interesting. The values of A_o for the uncomplexed five-membered ring chelates are much smaller than those of the six-membered ring chelates, and whereas the A_o values for the former increase on adduct formation, those of the latter decrease.

The isotropic hyperfine coupling in vanadyl complexes, as noted earlier, arises almost exclusively from the Fermi contact interaction. This interaction depends on the presence of unpaired spin density at the vanadium nucleus, and in these complexes there may be two types of contribution to this.

(a) The unpaired electron in the complexes repels electrons of similar spin more strongly than it does those of opposite spin. This results in paired electrons in filled s orbitals having slightly different wavefunctions, so that one may have a higher probability of being found at the metal nucleus than the other.

This spin polarisation effect has been shown[25] by unrestricted Hartree-Fock calculations to produce a value of A_o for transition metal ions which is negative in sign.

(b) In vanadyl chelates with C_{2v} symmetry, such as those studied here, it is possible as noted already, to have a direct contribution to the molecular orbital containing the unpaired electron from the metal 4s orbital. This would yield a positive contribution to A_o. Contributions of this type to A_o are unimportant in chelates with effective C_{4v} symmetry.

The A_o values for the five-membered ring chelates are markedly smaller than those for the six-membered ring chelates, as shown in table 2.2, yet the near constancy of the α_1^{*2} values in table 2.6 shows that the differences are not due to different degrees of delocalisation of the unpaired electron onto the ligands in the five- as compared with the six-membered ring species.

The differences in the A_o values can be accounted for if the five-membered ring chelates have a direct 4s contribution to the A_1^* orbital containing the unpaired electron. If this is the only reason for the difference, this direct contribution would amount to about 0.001 and 0.0017 cm^{-1} for the maltolate and tropolonate respectively. Clementi's wavefunctions[30] lead to direct contributions per 4s electron of 0.085 and 0.156 cm^{-1} respectively for the vanadium configurations $V(3d^3\ 4s^2)$ and $V^+(3d^2\ 4s^2)$. Hence the 4s contribution to hyperfine coupling in the configuration

appropriate to the vanadyl chelates is about 0.110 cm^{-1}. Thus the A_1^* molecular orbital in the vanadyl chelates contains about 1% 4s character.

The fall in the value of A_o observed for the six-membered ring chelates is almost certainly due to changes in the spin polarisation contribution to A_o, and although several reasons for this change have been discussed[29], the exact mechanism is still uncertain. It is probable, however, that this mechanism should contribute to the observed changes in A_o in both the five- and six-membered ring chelates.

The fact that the A_o values for the five-membered ring chelates are observed to increase on adduct formation can also be explained in terms of a direct 4s contribution to the A_1^* molecular orbital. On adduct formation there is a large decrease in the anisotropy of the e.p.r. spectral parameters in these chelates, corresponding to a large decrease in the $3d_{z^2}$ orbital contribution to the ground state. Since the $3d_{z^2}$ and 4s orbital contributions to the ground state are both due to the C_{2v} component of the crystal field, it is reasonable that the fall in the $3d_{z^2}$ contribution to the ground state should be accompanied by a reduction in the 4s orbital contribution. The net changes in A_o are therefore the resultant of the combined changes in the polarisation and direct contributions, with the changes in the direct contribution predominating, and causing the observed increase in the case of the five-membered ring chelates.

The decrease in the anisotropy of the chelates on adduct formation is almost certainly due to changes in the geometry of the chelates. If it is accepted that the anisotropy is due to the deviation of the basal O-V-O angles from 90^o, one possible mechanism for the change is shown in figure 2.11 below.

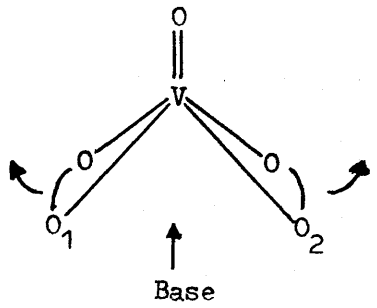

Figure 2.11

The approach of the complexing base would be expected to cause the chelating ligands to swing closer to the XY plane, and if the O_1-V-O_2 angle was less than 90^o initially, this process would lead to a decrease in the anisotropy of the complex.

2.8 Summary of part II

In this study the X-band e.p.r. spectra of some five- and six-membered ring chelates of the VO^{2+} ion have been recorded in solution at room temperature, and in magnetically dilute glasses at 77K. These studies indicate that the chelates form adducts with ethanol and with pyridine, and that they are readily oxidised, especially in hydroxylic solvents, to oxovanadium (V) complexes. The oxidation may be reversible in some cases. A method is described for deriving very accurate values of the spin Hamiltonian parameters from glassy spectra of these complexes, which have effective C_{2v} symmetry, and the parameters which were derived in this way are listed, together with the band maxima in the u.v.-visible spectra of the complexes. The spin Hamiltonian parameters are equated to the atomic orbital coefficients in some of the molecular orbitals involved in bonding in the complexes, and it is thereby shown that whereas the in-plane σ-bonding and the out-of-plane π-bonding in the complexes is fairly covalent, the delocalisation of the unpaired electron onto the ligands via in-plane π-bonding is very slight. The weak C_{2v} component of the ligand field in these complexes mixes a small

amount of $3d_{z^2}$ and 4s orbital character into the $3d_{x^2-y^2}$ orbital, which contains the unpaired electron, and the magnetic resonance data is used to estimate the extent of the mixing. Mixing $3d_{z^2}$ character into the orbital containing the unpaired electron accounts for the in-plane anisotropy of the g and hyperfine tensor components. Mixing in 4s character accounts for characteristic differences between the hyperfine tensor components observed for the five- and six-membered ring chelates, and for the differences in the changes which occur in these when additional complexing with solvent molecules takes place. The principal values of the hyperfine tensor components and the isotropic contribution to hyperfine coupling can be used to distinguish between five- and six-membered ring chelates.

PART III

AN ELECTRON PARAMAGNETIC RESONANCE STUDY OF THE BIS - (π - CYCLOPENTADIENYL) VANADIUM (IV), BIS - (π - CYCLOPENTADIENYL) NIOBIUM (IV) AND BIS - (π - CYCLOPENTADIENYL) TANTALUM (IV) COMPLEXES $(\pi - C_5H_5)_2 VX_2$, $(\pi - C_5H_5)_2 NbX_2$ AND $(\pi - C_5H_5)_2 TaX_2$

3.1 Introduction

Although the paramagnetic resonance properties of systems containing the oxovanadium (IV) species have been fairly thoroughly studied, d^1 systems which contain the vanadium (IV) ion in sites of tetrahedral, or pseudotetrahedral, symmetry are less common, and have been less extensively studied by e.p.r. methods. The only magnetically dilute systems for which detailed analyses of the e.p.r. properties of vanadium (IV) in a tetrahedral environment have been made are the chloride[1], alkoxide[2-4], and amino[3-5], derivatives, VCl_4, $V(OBu^t)_4$, and $V(NR_2)_4$, where in each case the unpaired electron lies essentially in the $3d_{x^2-y^2}$ orbital of the metal ions.

Other than niobium doped into a molybdenum sulphide host lattice[6], the only magnetically dilute systems containing niobium (IV) in a tetrahedral environment which have been studied in detail are the amino derivatives[7] $Nb(NR_2)_4$. No e.p.r. studies at all have been carried out on derivatives of tantalum (IV).

It was therefore decided to study a selection of the bis - (π - cyclopentadienyl) complexes $(\pi - C_5H_5)_2 MX_2$ for which the metal ion M = V(IV), Nb(IV), or Ta(IV) and the sigma bonded ligands X = $\sigma - C_5H_5^-$, Cl^-, CN^-, SCN^-, and OCN^- where σ-$C_5H_5^-$ indicates a cyclopentadienide ring bonded to the metal through a σ bond to one of the carbon atoms. These complexes have the general pseudotetral structure shown in figure 3.1 below.

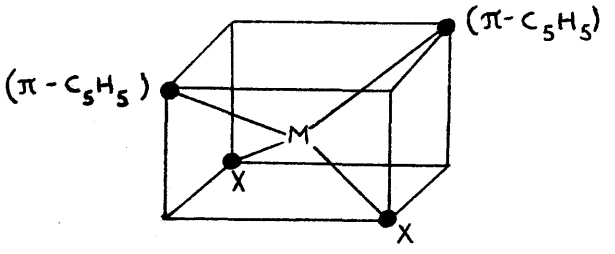

Figure 3.1

The π-cyclopentadienide groups in the complexes are symmetrically bonded to the metal ion, which lies on the normal through the centre of the ring, such that the metal-to-carbon bond distances are all equal.

The studies were carried out with the following two objectives.

(a) To see whether values of the anisotropic spin Hamiltonian parameters could be extracted from the spectra of magnetically dilute glasses of the complexes, in the same way as for the oxovanadium (IV) complexes.

(b) To use these spin Hamiltonian parameters to obtain detailed quantitative information about the electronic structures and the bonding in these complexes. Previous discussions of the electronic structures of complexes of this type[8,9] had been completely qualitative, and little reliance can be placed on deductions based on these arguments.

The e.p.r. spectra of some of the vanadium complexes had been studied previously in solution at room temperature[10], and well resolved eight-line spectra had been obtained. The e.p.r. spectra of the corresponding niobium (IV) and tantalum (IV) complexes had not been studied, previously. Complexes containing the ^{93}Nb ($I = 9/2$) and ^{181}Ta ($I = 7/2$) nuclei should, however, give rise to well resolved ten- and eight-line spectra respectively.

3.2 Experimental

Dichlorobis - (π-cyclopentadienyl) vanadium (IV), $(\pi\text{-}C_5H_5)_2\ VCl_2$, was prepared[11] by allowing vanadium tetrachloride to react with sodium cyclopentadienide in diglyme solution. The product was isolated by removal of the solvent under reduced pressure, and extraction of the residue with boiling chloroform saturated with hydrogen chloride. The crude product obtained in this way was re-extracted two more times in the same way, and finally recrystallised from chloroform saturated with hydrogen chloride.

The corresponding dithiocyanate, dicyanate, and dicyanide complexes were prepared from the purified dichloride by reaction with KSCN, KOCN, and KCN respectively.[10]

Tetracyclopentadienyl niobium (IV), $(\pi\text{-}C_5H_5)_2\ Nb(\sigma\text{-}C_5H_5)_2$, was prepared[12,13,14] by allowing niobium pentachloride to react with a suspension of sodium cyclopentadienide in benzene. Dichlorobis-(π-cyclopentadienyl) niobium (IV) was then prepared by treating the $(C_5H_5)_4\ Nb$ with a saturated solution of hydrogen chloride in ether.[13,14] The product was purified by vacuum sublimation, ($270^{\circ}C/100\mu$). The corresponding dithiocyanate and dicyanide complexes were prepared by stirring a solution of the dichloride with KSCN or KCN for 1 and 4 hours respectively.

Tetracyclopentadienyl tantalum (IV), $(\pi\text{-}C_5H_5)_2Ta\ (\sigma\text{-}C_5H_5)_2$ was prepared in the same way as the corresponding niobium complex,[12] by allowing tantalum pentachloride to react with a suspension of sodium cyclopentadienide in benzene. It was, however, found to be impossible to convert $(C_5H_5)_4Ta$ to the chloride complex in the same way as was done for the niobium (IV) complex. Reaction of $(C_5H_5)_4Ta$ with dry hydrogen chloride in ether produces only diamagnetic products.

The purity of the complexes was checked by comparing their i.r. spectra with published spectra in the case of those complexes which had been reported previously.[10,13] The purity of the niobium (IV) complexes which had not been reported previously was checked by comparing their i.r. spectra with those of the corresponding vanadium (IV) complexes.[10]

The vanadium (IV) complexes are stable indefinitely as solids, but are unstable in some cases in solution, especially in the presence of light, where the dichloride, for instance, is slowly oxidised.[15] The niobium (IV) complexes are very unstable with respect to oxidation to niobium (V). $(C_5H_5)_4$ Nb ignites spontaneously in air, while the other complexes decompose more slowly, over a period of a day or two, to give diamagnetic products. $(C_5H_5)_4$ Ta is similarly very rapidly decomposed in air.

Because of the instability of these complexes, therefore, all the solvents used were dried and degassed beforehand, and the complexes themselves were stored and handled in a nitrogen-filled drybox.

With the exception of $(C_5H_5)_4$ Nb and $(C_5H_5)_4$ Ta, the e.p.r. spectra of the complexes were recorded at room temperature in 10^{-3}M chloroform solutions, and at 77K in 10^{-2}M glasses of chloroform containing 10% ethanol, which helped in forming the glass. The complexes $(C_5H_5)_4$ Ta and $(C_5H_5)_4$ Nb were unstable in solutions containing ethanol, and so their spectra were recorded in toluene. It was found that the replacement of the σ-bonded ligands in $(\pi\text{-}C_5H_5)_2$ Nb Cl_2 occurs sufficiently slowly to enable the ligand exchange reactions to be followed in the e.p.r. spectrometer, and although they were not isolated, e.p.r. spectra of the redistribution complexes $(\pi\text{-}C_5H_5)_2$ Nb Cl (SCN), $(\pi\text{-}C_5H_5)_2$ Nb Cl (CN) and $(\pi\text{-}C_5H_5)_2$ Nb Cl ($\sigma\text{-}C_5H_5$) were observed and characterised at room temperature. Under no conditions was superhyperfine coupling observed in the spectra of any of the complexes.

The u.v.-visible spectra of the complexes were recorded on Unicam SP700C and 800 spectrometers in both dichloromethane and in dimethylformamide solutions where possible, although because of solubility difficulties not all of the spectra could be recorded in dichloromethane. Because of the instability of some of the complexes in air, their u.v.-visible spectra were recorded by placing some of the solid complex in one of the quartz cells used, evacuating the cell on a vacuum line and distilling the solvent into it, so that the spectra could thus be recorded in the complete absence of air.

3.3. Analysis of the e.p.r. spectra

The complexes of vanadium (IV) and niobium (IV) gave well-resolved eight- and ten-line spectra in solution at room temperature as expected, and these could be interpreted using the usual isotropic spin Hamiltonian.[16]

$$\mathcal{H} = g_o \beta_e \underline{H}.\underline{S} + A_o \underline{S}.\underline{I} \qquad 3.1$$

The values of g_o and A_o obtained from the solution spectra of each of the complexes are listed in table 3.1.

The e.p.r. spectra obtained from magnetically dilute glasses of $(\pi\text{-}C_5H_5)\ V\ Cl_2$ and $(\pi\text{-}C_5H_5)_2\ Nb\ Cl_2$ are shown in figure 3.2. As indicated in the figure, it is possible to distinguish peaks in the spectra corresponding to the cases where the applied magnetic field lies along each of the X, Y and Z principal axes of the complexes. For complexes of this type, which have effective C_{2v} symmetry, the principal axes are those shown in figure 3.3 below.

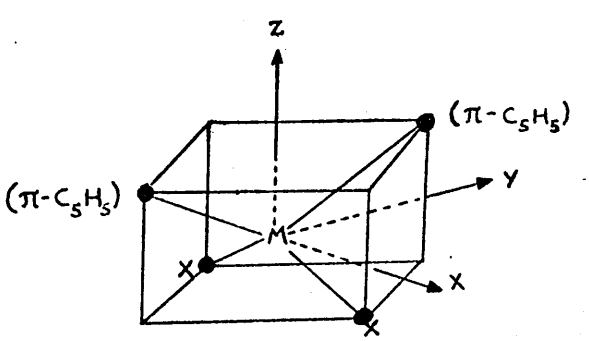

Figure 3.3

Table 3.1

Isotropic spin Hamiltonian parameters for the complexes $(\pi\text{-}C_5H_5)_2$ MXY in solution at room temperature. The A_o values are in units of cm^{-1}. Limits of error are $g_o \pm 0.0005$, $A_o \pm 0.00002\ cm^{-1}$.

Complex	g_o	A_o
$(\pi\text{-}C_5H_5)_2\ VCl_2$	1.988	0.00687
$(\pi\text{-}C_5H_5)_2\ V(SCN)_2$	1.986	0.00681
$(\pi\text{-}C_5H_5)_2\ V(OCN)_2$	1.980	0.00708
$(\pi\text{-}C_5H_5)_2\ V(CN)_2$	1.984	0.00565
$(\pi\text{-}C_5H_5)_2\ Nb\ Cl_2$	1.976	0.01064
$(\pi\text{-}C_5H_5)_2\ Nb\ Cl(SCN)$	1.976	0.01057
$(\pi\text{-}C_5H_5)_2\ Nb\ Cl(\sigma\text{-}C_5H_5)$	1.984	0.00982
$(\pi\text{-}C_5H_5)_2\ Nb\ Cl(CN)$	1.984	0.00973
$(\pi\text{-}C_5H_5)_2\ Nb(SCN)_2$	1.975	0.01027
$(\pi\text{-}C_5H_5)_2\ Nb(\sigma\text{-}C_5H_5)_2$	1.988	0.00923
$(\pi\text{-}C_5H_5)_2\ Nb(CN)_2$	1.995	0.00839

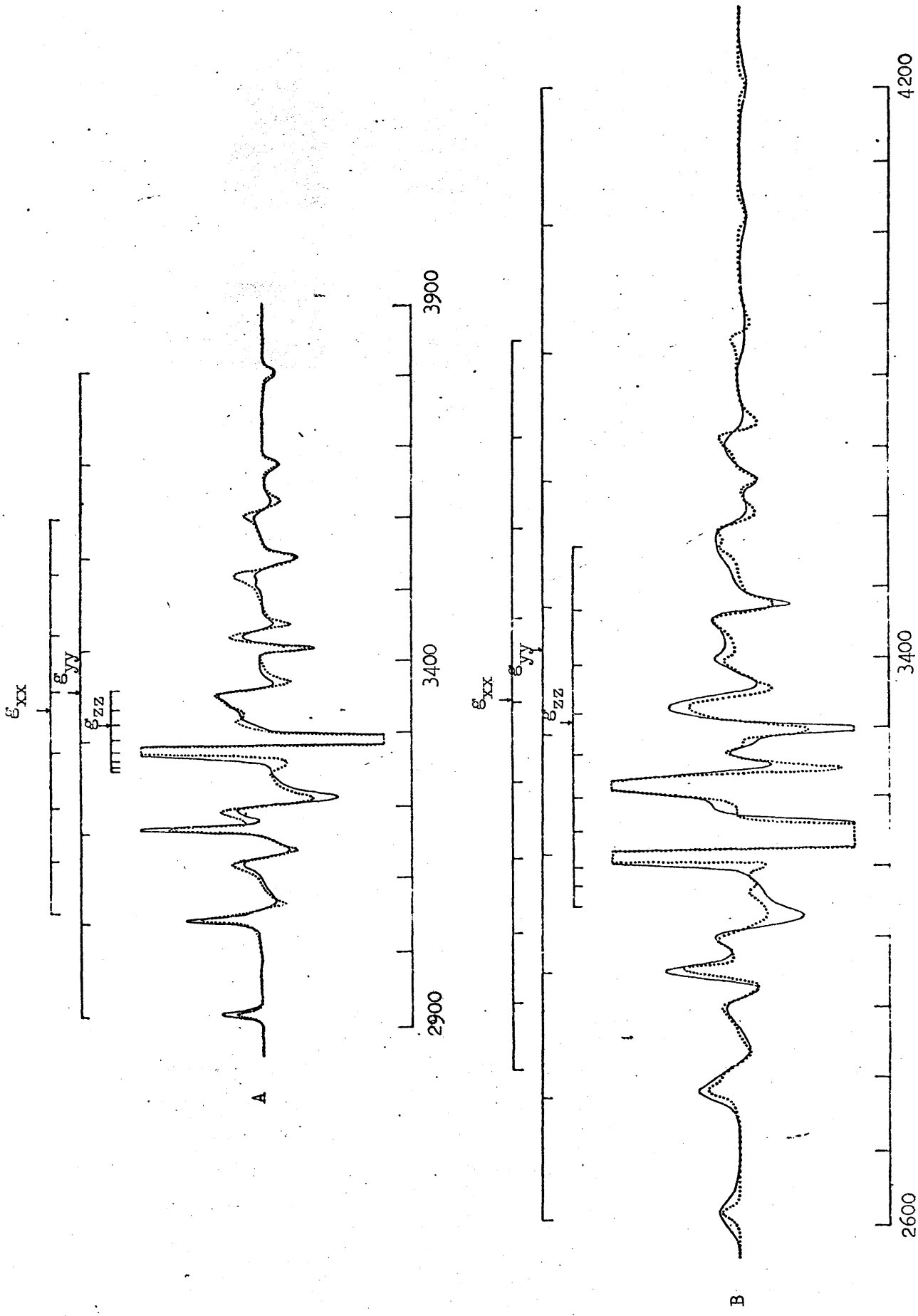

Figure 3.2 Observed (—) and calculated (--) e.p.r. spectra of 10^{-3}M solutions of $(\pi\text{-}C_5H_5)_2VCl_2$, A, and of $(\pi\text{-}C_5H_5)_2NbCl_2$, B, in $CHCl_3$: EtOH glass (9:1) at 77K.

The glassy spectra of the complexes could therefore be interpreted in terms of the totally anisotropic spin Hamiltonian of the form.[16]

$$\mathcal{H} = \beta_e \underline{H}.g.\underline{S} + \underline{S}.A.\underline{I} \qquad 3.2$$

where, once again, g and A are the anisotropic g and hyperfine tensors, and it is assumed that the two tensors can be simultaneously diagonalised.

As shown in appendix B, the general expression for the allowed $\Delta m_S = +1$, $\Delta m_I = 0$ transitions, for the case where the applied magnetic field lies along one of the principal axis directions is given by[17]

$$H_i = h\nu_o(g_{ii}\beta_e)^{-1} - hc(g_{ii}\beta_e)^{-1} A_{ii} m_I - hc^2(4g_{ii}\beta_e\nu_o)^{-1} (A_{jj}^2+A_{kk}^2)(I(I+1)-m_I^2) \qquad 3.3$$

where i, j, k = x, y, or z, and the coupling constants are in units of cm^{-1}.

The glassy spectra of the complexes were interpreted using the computer simulation method described for vanadyl chelates, and the best fitting values of the resonant fields H_x, H_y, and H_z were used together with equation 3.3 to calculate values of the anisotropic spin Hamiltonian parameters for each of the complexes. The values obtained in this way, together with the best fitting value of the Gaussian line-broadening parameter β, are listed in table 3.2.

The fact that the g_{zz} values for each of the complexes listed in table 3.2 are approximately equal to the spin-only value, shows immediately that in each complex the unpaired electron occupies a molecular orbital which is primarily metal ion d_{z^2} in character, since for any other orbital all the g-tensor values would deviate from the spin-only value. The marked deviation from axial symmetry in both the g and A tensor values, however, show that the metal ion $d_{x^2-y^2}$ orbitals, which belongs to the same irreducible representation as the d_{z^2} orbital

Table 3.2

Spin Hamiltonian parameters for the complexes $(\pi\text{-}C_5H_5)_2\,MX_2$ at 77K. All hyperfine tensor components are in units of cm^{-1}. Limits of error are g_{xx} and $g_{yy} \pm 0.0005$, $g_{zz} \pm 0.001$, A_{xx}, A_{yy}, $A_{zz} \pm 0.00002\ cm^{-1}$. β values are in units of gauss.

Complex	g_{xx}	g_{yy}	g_{zz}	A_{xx}	A_{yy}	A_{zz}	$\langle g \rangle$	$\langle A \rangle$	β
$(\pi\text{-}C_5H_5)_2\,VCl_2$	1.986	1.971	2.000	-0.00740	-0.01170	-0.00152	1.986	-0.00687	3.5
$(\pi\text{-}C_5H_5)_2\,V(SCN)_2$	1.988	1.958	2.000	-0.00712	-0.01153	-0.00192	1.982	-0.00686	3.0
$(\pi\text{-}C_5H_5)_2\,V(OCN)_2$	1.985	1.957	2.000	-0.00734	-0.01194	-0.00186	1.981	-0.00708	3.0
$(\pi\text{-}C_5H_5)_2\,V(CN)_2$	1.994	1.986	2.000	-0.00587	-0.00998	-0.00110	1.993	-0.00562	3.0
$(\pi\text{-}C_5H_5)_2\,NbCl_2$	1.980	1.940	2.000	-0.01066	-0.01598	-0.00528	1.974	-0.01064	6.0
$(\pi\text{-}C_5H_5)_2\,Nb(SCN)_2$	1.987	1.935	2.000	-0.01005	-0.01536	-0.00528	1.975	-0.01023	4.5
$(\pi\text{-}C_5H_5)_2\,Nb(\sigma\text{-}C_5H_5)_2$	1.982	1.979	1.999	-0.00908	-0.01431	-0.00437	1.987	-0.00925	3.5
$(\pi\text{-}C_5H_5)_2\,Nb(CN)_2$	1.997	1.976	2.003	-0.00771	-0.01293	-0.00534	1.992	-0.00834	4.0

in these complexes, also contributes to the ground state, so that the overall metal ion contribution to the molecular orbital containing the unpaired electron in these complexes is similar to that in the vanadyl chelates, ie $(ad_{x^2-y^2} + bd_{z^2})$. In these complexes, however, $b > a$.

The e.p.r. spectrum obtained from a magnetically dilute glass of $(C_5H_5)_4$ Ta in toluene could not be interpreted in terms of the usual spin Hamiltonian 3.2, and a discussion of the spectrum of this complex will be reserved until the end of this chapter. The discussion in the following sections therefore deals only with the complexes of vanadium (IV) and niobium (IV).

3.4 U.v.-visible spectra

The u.v.-visible spectra of the complexes were all rather similar, and various types of bands could be distinguished. These can be summarised as

(a) In the region 10,000-20,000 cm^{-1} there are weak absorptions which, from their position and intensity, are almost certainly ligand field transitions, involving the transfer of the unpaired electron in the complexes into empty antibonding molecular orbitals. In all of the complexes, except for the dichlorides there is only one very broad band in this region. In $(\pi\text{-}C_5H_5)_2 VCl_2$ and $(\pi\text{-}C_5H_5)_2 Nb Cl_2$, this peak was resolved into one strong absorption, with a weaker shoulder at higher frequency, and in the latter complex there was also a third weak band at 20,400 cm^{-1}.

(b) All the complexes have a stronger absorption band in the region 25,000-30,000 cm^{-1}. In the vanadium (IV) complexes this was at about 26,000 cm^{-1} and in the niobium (IV) complexes at about 28,000 cm^{-1}. As shown later, this is assignable to a transition in which an electron

is transferred from a filled bonding orbital which is derived mainly from a cyclopentadienyl ring molecular orbital, to the orbital containing the unpaired electron. The fact that the frequency of this band is almost independent of the nature of the X ligands would appear to support this assignment.

(c) There are various other bands at higher frequencies which are more difficult to assign. In the thiocyanate complexes there is a band at 21,600 and 22,600 cm^{-1} in the vanadium (IV) and niobium (IV) complexes respectively which is thought to be due to the internal $\pi \rightarrow \pi^*$ transition of the thiocyanato group.[18]

(d) The ligand field bands in the complexes $(C_5H_5)_4$ Nb and $(C_5H_5)_4$ Ta are obscured by a very intense charge transfer band, which may be due to the transfer of the unpaired electron from the metal ion into the π^* orbitals of the σ-bonded cyclopentadienide rings.

The frequencies of the band maxima in the u.v.-visible spectra of the complexes are summarised in table 3.3. The frequencies were almost independent of solvent for those complexes whose spectra could be recorded in both dichloromethane and dimethylformamide. Of the spectra listed only the u.v. spectra of $(\pi\text{-}C_5H_5)_2\ VCl_2$ and $(\pi\text{-}C_5H_5)_2\ V(SCN)_2$ had already been reported elsewhere.[19]

3.5 Extended Huckel molecular orbital calculations on the complex $(\pi\text{-}C_5H_5)_2\ VCl_2$

Before the spin Hamiltonian parameters could be used to obtain information about the electronic distributions in the complexes, it was necessary to estimate values of ζ, the spin-orbit coupling constant, and $P = g_e g_N \beta_e \beta_N \langle d_{z^2} | r^{-3} | d_{z^2} \rangle$, for the vanadium and niobium ions with the charges and configurations found in these complexes.

Table 3.3

Band maxima (cm^{-1}) in the u.v.-visible absorption spectra of the complexes $(\pi\text{-}C_5H_5)_2\ MX_2$.

Complex	d-d transition	Metal ion ← Ring charge transfer	Other bands
$(\pi\text{-}C_5H_5)_2\ VCl_2$	11,800	26,300	35,400
	13,600		
$(\pi\text{-}C_5H_5)_2\ V(SCN)_2$	14,000	25,000	21,600
			28,900
			37,800
$(\pi\text{-}C_5H_5)_2\ V(OCN)_2$	13,300	26,800	36,100
$(\pi\text{-}C_5H_5)_2\ V(CN)_2$	16,900	25,000	32,700
			40,000
$(\pi\text{-}C_5H_5)_2\ NbCl_2$	14,500	28,500	41,000
	17,000		
	20,400		
$(\pi\text{-}C_5H_5)_2\ Nb(SCN)_2$	17,000	27,500	22,600
			38,500
$(\pi\text{-}C_5H_5)_2\ Nb(CN)_2$	20,300	29,800	

Since no estimates of the charge and configuration of the metal ions were available, for complexes of this type, an extended Huckel molecular orbital calculation was therefore carried out on the complex $(\pi\text{-}C_5H_5)_2\ VCl_2$.

The general method used for the calculation is discussed more fully in references 20 and 21, but the main steps involved can be summarised as follows.

(a) The metal ion orbitals are assigned to the various irreducible representations of the point group of the molecule, which is assumed to be C_{2v}. The form of the corresponding ligand group orbitals is worked out.

(b) The overlap integrals between the metal ion and ligand atomic orbitals are calculated. Hence the overlap integrals between the metal ion atomic orbitals and the ligand group orbitals of the various symmetry types are calculated.

(c) The coulomb integrals for the various atomic orbitals are calculated by setting them equal to the valence state ionisation energies. The energies of the metal ion atomic orbitals are very dependent on the charge and configuration of the metal ion, so an initial charge and configuration must be assumed, and the energies corresponding to this are used.

(d) The exchange integrals between basis orbitals are expressed as a function of the coulomb integrals of the two orbitals, and the overlap integral between them.

(e) The molecular orbitals for the complex are assumed to be linear combinations of the metal ion orbitals and ligand group orbitals of the same symmetry. Knowing the values of the coulomb, exchange and overlap integrals H_{ii}, H_{ij} and S_{ij}, the secular determinants can now be solved

for sets of orbitals of the same symmetry, and the eigenvalues and eigenfunctions obtained.

(f) The electrons available to the complex are fed into the molecular orbitals according to the Aufbau principle, a population analysis is carried out, and the charge and configuration of the metal ion are determined.

(g) On the basis of the previous calculation, a new charge and configuration are chosen for the metal ion, a new set of coulomb integrals are worked out, and the whole cycle is repeated until the input and output charge and configuration are identical.

The geometry assumed for the complex was that shown in figure 3.4. The chlorine atoms lie in the XZ plane, and the centres of the rings in the YZ plane of the complex. In the absence of X-ray data for this complex, the following bond lengths and angles were assumed

V - C bond length = 2.25 Å

V - Cl bond length = 2.10 Å

C - C bond length = 1.35 Å

$(\pi\text{-}C_5H_5)\text{-}V\text{-}(\pi\text{-}C_5H_5)$ bond angle = 125°

Cl - V - Cl bond angle = 95°

The values were estimated from X-ray and electron diffraction structural data which is available for similar complexes.[22-25]

The basis orbitals used in forming the molecular orbitals were

(a) vanadium ion 3d, 4s and 4p orbitals

(b) chloride ion 3p orbitals

(c) cyclopentadienide ring π molecular orbitals. The form of these, and their energies are obtainable from the usual Huckel calculations,[26,9] and these are given below.

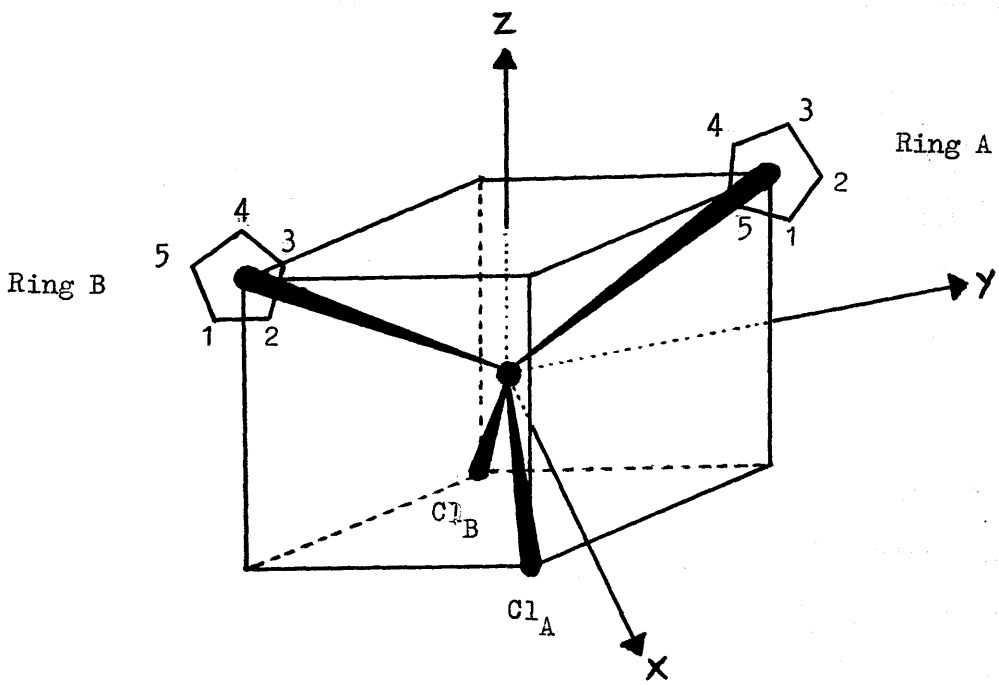

Figure 3.4

$$cp(1) = (1/5)^{\frac{1}{2}} (\phi_1 + \phi_2 + \phi_3 + \phi_4 + \phi_5) \qquad cp_o \text{ orbital}$$

$$cp(2) = (2/5)^{\frac{1}{2}} (\phi_1 + \cos 2\pi/5(\phi_2 + \phi_5) + \cos \tfrac{4\pi}{5} (\phi_3 + \phi_4)) \qquad cp_{\pm 1} \text{ orbitals}$$

$$cp(3) = (2/5)^{\frac{1}{2}} (\sin \tfrac{2\pi}{5} (\phi_2 - \phi_5) + \sin \tfrac{4\pi}{5} (\phi_3 - \phi_4)) \qquad cp_{\pm 1} \text{ orbitals}$$

$$cp(4) = (2/5)^{\frac{1}{2}} (\phi_1 + \cos \tfrac{4\pi}{5} (\phi_2 + \phi_5) + \cos \tfrac{2\pi}{5} (\phi_3 + \phi_4)) \qquad cp_{\pm 2} \text{ orbitals}$$

$$cp(5) = (2/5)^{\frac{1}{2}} (\sin \tfrac{4\pi}{5} (\phi_2 - \phi_5) - \sin \tfrac{2\pi}{5} (\phi_3 - \phi_4)) \qquad cp_{\pm 2} \text{ orbitals}$$

Seen from the side of the ring away from the metal ion, these have the form

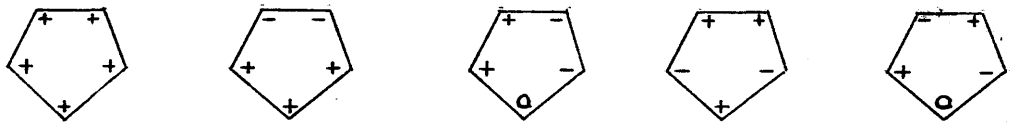

cp(1) cp(2) cp(3) cp(4) cp(5)

Thus the cp_o, $cp_{\pm 1}$ and $cp_{\pm 2}$ orbitals can be seen to be similar in form to s, p, and d orbitals.

The metal ion orbitals and the ligand group orbitals derived from the above ligand basis orbitals can now be assigned to the various irreducible representations of the C_{2v} point group, as shown below.

Class	A_1	A_2
Metal ion orbitals	$4s,\ 4p_z,\ 3d_{z^2},\ 3d_{x^2-y^2}$	$3d_{xy}$
Chloride ion orbitals	$p_x(A_1) = \frac{1}{\sqrt{2}} (p_{XA} - p_{XB})$	$p_y\ (A_2) = \frac{1}{\sqrt{2}} (p_{YA} - p_{YB})$
	$p_z(A_1) = \frac{1}{\sqrt{2}} (p_{ZA} \pm p_{ZB})$	
Cyclopentadienide ion orbitals	$Cp_0\ (A_1) = \frac{1}{\sqrt{2}} (cp(1)_A + cp(1)_B)$	$cp_1\ (A_2) = \frac{1}{\sqrt{2}} (cp(3)_A - cp(3)_B)$
	$Cp_1\ (A_1) = \frac{1}{\sqrt{2}} (cp(2)_A + cp(2)_B)$	$cp_2\ (A_2) = \frac{1}{\sqrt{2}} (cp(5)_A - cp(5)_B)$
	$Cp_2\ (A_1) = \frac{1}{\sqrt{2}} (cp(4)_A + cp(4)_B)$	

Class	B_1	B_2
Metal ion orbitals	$3d_{XZ}$, $4p_X$	$3d_{YZ}$, $4p_Y$
Chloride ion orbitals	$p_X(B_1) = \frac{1}{\sqrt{2}}(p_{XA} + p_{XB})$	$p_Y(B_2) = \frac{1}{\sqrt{2}}(p_{YA} + p_{YB})$
	$p_Z(B_1) = \frac{1}{\sqrt{2}}(p_{ZA} - p_{ZB})$	
Cyclopentadienide ion orbitals	$cp_1(B_1) = \frac{1}{\sqrt{2}}(cp(3)_A + cp(3)_B)$	$cp_0(B_2) = \frac{1}{\sqrt{2}}(cp(1)_A - cp(1)_B)$
	$cp_2(B_1) = \frac{1}{\sqrt{2}}(cp(5)_A + cp(5)_B)$	$cp_1(B_2) = \frac{1}{\sqrt{2}}(cp(2)_A - cp(2)_B)$
		$cp_2(B_2) = \frac{1}{\sqrt{2}}(cp(4)_A - cp(4)_B)$

The wave functions used in calculating the overlap integrals for the complex were those of Cusachs[27,28]. These are single exponent Slater-type atomic orbitals of the form $Nr^{n-1}e^{-\zeta r}$, in which the values of the principal quantum number n, and the orbital exponent ζ, are chosen to give the best agreement with the overlap properties of Clementi's multi-exponent wave functions.[29] Being single-exponent wave functions these are considerably easier to work with than Clementi's functions. The best values of ζ and n for the various atoms are given below.

Carbon	2p	n = 2.0	ζ = 1.42
Chlorine	3p	n = 2.0	ζ = 1.38
Vanadium	4s	n = 3.0	ζ = 0.96
"	4p	n = 3.0	ζ = 0.58
"	3d	n = 3.0	ζ = 2.00

The group overlap integrals obtained using these values are listed in table 3.4.

The coulomb integrals for the various groups in the complex were set equal to the valence state ionisation energies[30], obtained as follows

Table 3.4

Group overlap integrals for the complex $(\pi\text{-}C_5H_5)_2\ VCl_2$

A_1 Symmetry

	$p_z(A_1)$	$p_x(A_1)$	$cp_0(A_1)$	$cp_1(A_1)$	$cp_2(A_1)$
4s	0.215	-0.234	-0.565	0	0
$4p_z$	0.164	0.146	0.047	0.197	0
$3d_{z^2}$	0.153	0.074	0.059	0.123	-0.020
$3d_{x^2-y^2}$	0.155	-0.030	0.121	0.140	0.025

A_2 Symmetry

	$p_y(A_2)$	$cp_1(A_2)$	$cp_2(A_2)$
$3d_{xy}$	0.139	-0.270	-0.057

B_1 Symmetry

	$p_z(B_1)$	$p_x(B_1)$	$cp_1(B_1)$	$cp_2(B_1)$
$4p_x$	0.146	0.138	-0.206	0
$3d_{xz}$	-0.142	0.180	-0.173	-0.035

B_2 Symmetry

	$p_y(B_2)$	$cp_0(B_2)$	$cp_1(B_2)$	$cp_2(B_2)$
$4p_y$	0.205	0.084	-0.092	0
$3d_{yz}$	-0.128	-0.119	0.178	0.055

(a) The ionisation energies for chlorine 3p orbitals are

in atomic chlorine - 13.6 eV in chloride ion in H Cl - 12.8 eV.

The value of 12.8 eV was used as being a better approximation in view of the state of the chlorine in the complex.

(b) Simple Huckel calculations show that the ring molecular orbitals have energies of

$$cp_0 = \alpha + 2\beta \qquad cp_{\pm 1} = \alpha + 2\cos\frac{2\pi}{5}\beta \qquad cp_{\pm 2} = \alpha - 2\cos\frac{\pi}{5}\beta$$

respectively. The first ionisation potential of the cyclopentadienyl radical is - 8.8 eV, and this can be equated to the energy of the $cp_{\pm 1}$ orbitals. The value of β which has been observed to give the best agreement with spectroscopic properties in other complexes[21] is - 2.5 eV. Using these values, the energies of the cyclopentadienyl radical molecular orbitals become cp_0 = - 12.8 eV, $cp_{\pm 1}$ = - 8.8 eV, $cp_{\pm 2}$ = 3.2 eV. Preliminary calculations, however, showed that there was a slight positive charge on the carbon atoms in the complex, and to compensate for this the energies used were adjusted to

$$cp_0 = -13.5 \text{ eV}$$

$$cp_{\pm 1} = -9.5 \text{ eV}$$

$$cp_{\pm 2} = -3.9 \text{ eV}$$

(c) The ionisation energies for the metal ion atomic orbitals were obtained using the method of Ballhausen and Grey.[20] The ionisation potential for a particular type of configuration can be expressed as a function of the charge on the ion by fitting the experimental ionisation potential data to an equation of the form

$$\text{I. P.} = A + Bq + Cq^2 \qquad 3.4$$

where q is the charge on the ion. If this is done for the vanadium ion data, the following equations result.

1) d - electron ionisation energies.

d^n configuration : $E = 31.4 + 68q + 15.8q^2$

$d^{n-1}s$ " : $E = 51.4 + 87q + 14q^2$

$d^{n-1}p$ " : $E = 61.4 + 101.3q$ 3.5

2) s - electron ionisation energies

$d^{n-1}s$ configuration : $E = 51.0 + 54.2q + 8.5q^2$

$d^{n-2}s^2$ " : $E = 60.4 + 71.5q$

$d^{n-2}sp$ " : $E = 70.6 + 66.1q$ 3.6

3) p - electron ionisation energies

$d^{n-1}p$ configuration : $E = 27.7 + 45.4q + 7.5q^2$

$d^{n-2}sp$ " : $E = 36.4 + 58.3q$

$d^{n-2}p^2$ " : $E = 36.8 + 65q$ 3.7

For the metal ion having a charge q and configuration $d^x s^s p^p$, the ionisation energies for the various electrons are given by the expressions

$$\text{d - electron I.P.} = (1 - s - p)\,E(d^n) + sE(d^{n-1}s) + pE(d^{n-1}p)$$

$$\text{s - electron I.P.} = (2 - s-p)\,E(d^{n-1}s) + (s - 1)\,E(d^{n-1}s^2) + pE(d^{n-2}sp)$$

$$\text{p - electron I.P.} = (2 - s-p)\,E(d^{n-1}p) + (p - 1)\,E(d^{n-2}p^2) + sE(d^{n-2}sp) \qquad 3.8$$

The above equations give the energies in units of 1000 cm^{-1} and these were converted to eV for the calculations.

The exchange integrals were calculated using the Wolfsberg-Helmholtz approximation[31]

$$H_{ij} = 0.85\,(H_{ii} + H_{jj})\,S_{ij} \qquad 3.9$$

3.6 Molecular orbital calculation: results and discussion

The molecular orbital calculation was cycled as indicated above, and the most important final results are listed below.

(1) The final self-consistent charge and configuration for the vanadium ion are +0.356 ($d^{4.016}$ $s^{0.524}$ $p^{0.104}$). The overall charge distribution is

Atom or group	V	(π -C_5H_5)	Cl
Charge	+0.356	+0.457	-0.645

The final eigenvalues and eigenfunctions are listed in table 3.5 and the resultant energy level diagram is shown in figure 3.5.

(2) The unpaired electron in the complex is predicted to occupy the essentially non-bonding metal ion d_{z^2} / $d_{x^2-y^2}$ hybrid orbital shown in table 3.5. It can be seen that the only ligand group orbital which contributes appreciably to this molecular orbital is the p_x (A_1) orbital, which contributes about 3% to its character. This agrees with the deduction made earlier from the g-tensor values about the metal ion contribution to the orbital containing the unpaired electron.

(3) It will be shown later that the coefficients a and b of the $d_{x^2-y^2}$ and d_{z^2} orbitals in the above d_{z^2} / $d_{x^2-y^2}$ hybrid orbital are affected very little by the nature of the X ligands in the complexes. This is because by the end of the calculation the input energy for the metal ion d-orbitals is similar to that of the cyclopentadienide ring $cp_{\pm 1}$ orbitals. The d_{z^2} and $d_{x^2-y^2}$ orbitals therefore hybridise so as to form one hybrid which bonds strongly to the $cp_{\pm 1}$ orbitals, and the other, containing the unpaired electron, which is almost non-bonding with respect to the ligands. The form of the hybrid is therefore dominated by the bonding to the rings. The orbitals on the X ligands, which are of much lower energy, only have a small effect.

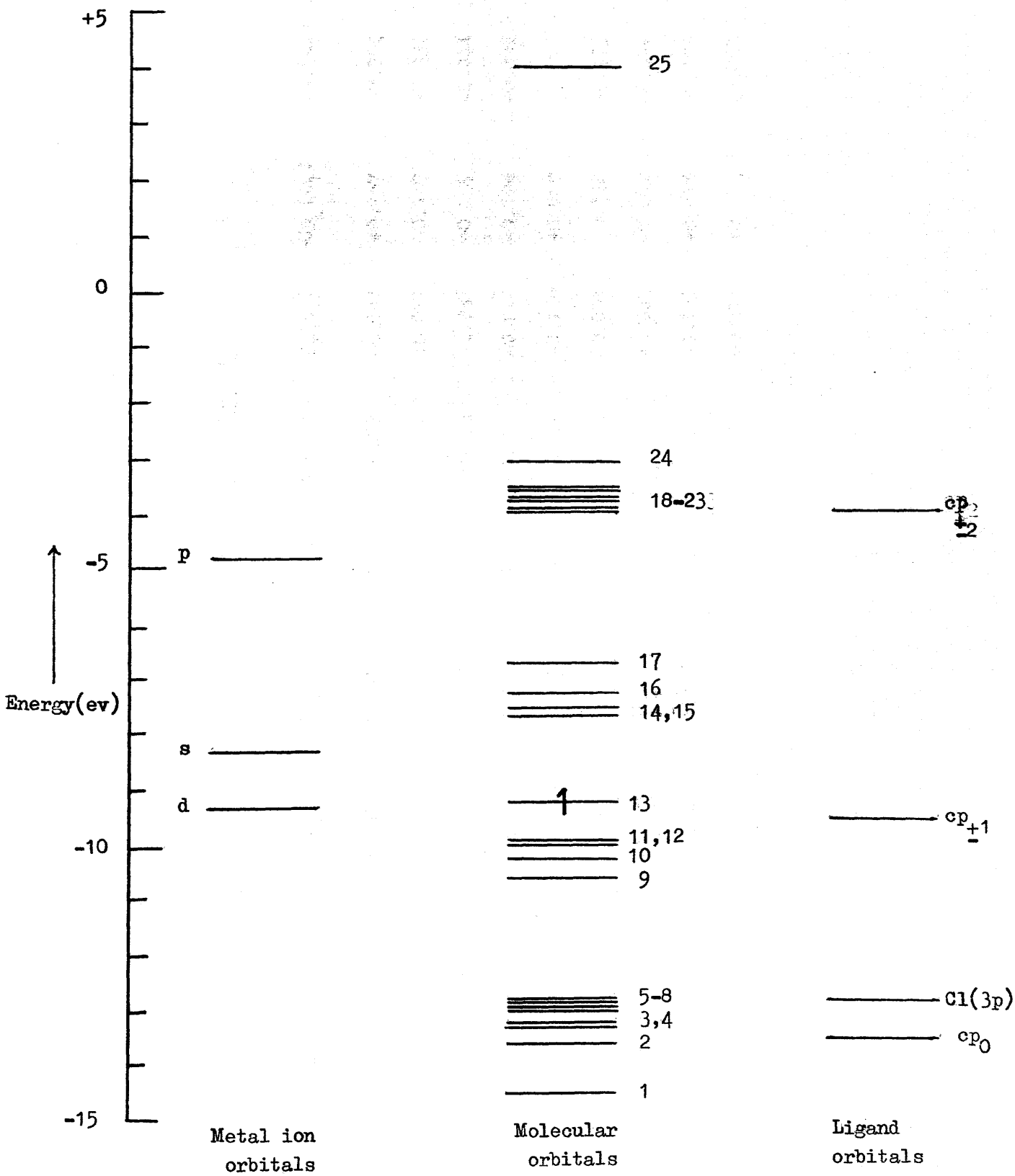

Figure 3.5 Molecular orbital energy level diagram for $(\pi\text{-}C_5H_5)_2\,VCl_2$

Table 3.5

Energy levels and atomic orbital coefficients in the L.C.A.O. molecular orbital description of $(\pi\text{-}C_5H_5)_2 V Cl_2$ Molecular orbitals are in symmetry classes appropriate to the C_{2v} group. Energies are in units of eV. The unpaired electron is in the starred A_1 orbital. The orbital numbers refer to the labelling in figure 3.5.

A_1 symmetry

Orbital Number	Energy	Atomic Orbital Coefficients								
		4s	$4p_z$	d_{z^2}	$d_{x^2-y^2}$	$p_z(A_1)$	$p_x(A_1)$	$Cp_o(A_1)$	$Cp_1(A_1)$	$Cp_2(A_1)$
1	-14.50	-0.305	+0.004	+0.041	+0.073	-0.088	+0.147	+0.757	+0.004	0.000
3	-13.33	-0.090	-0.023	-0.190	-0.223	-0.847	+0.097	-0.167	-0.037	0.000
7	-12.93	+0.042	-0.034	-0.123	+0.064	-0.133	-0.931	+0.237	-0.004	0.000
11	-10.03	+0.025	+0.013	+0.247	+0.299	-0.287	-0.016	-0.104	+0.832	0.000
13*	- 9.21	-0.010	-0.036	+0.755	-0.645	-0.027	-0.199	+0.069	+0.009	-0.012
16	- 7.24	+0.063	-0.339	+0.543	+0.656	-0.336	+0.054	-0.132	-0.475	+0.007
19	- 3.89	+0.002	-0.009	-0.027	+0.039	-0.001	+0.008	-0.002	-0.001	-1.000
24	- 2.99	+0.173	+0.982	+0.267	+0.247	-0.380	-0.132	+0.018	-0.405	-0.007
25	+ 4.09	+1.262	-0.161	-0.093	-0.123	-0.279	+0.416	+0.953	+0.080	+0.002

Table 3.5 (Contd.)

A_2 Symmetry

Atomic Orbital Coefficients

Orbital Number	Energy	d_{xy}	$p_y(A_2)$	$Cp_1(A_2)$	$Cp_2(A_2)$
5	-12.99	-0.224	-0.939	+0.053	-0.002
9	-10.64	+0.538	-0.284	-0.687	-0.003
17	- 6.67	+0.865	-0.239	+0.774	-0.082
20	- 3.84	+0.135	-0.032	+0.079	+0.998

B_1 Symmetry

Atomic Orbital Coefficients

Orbital Number	Energy	$4p_x$	d_{xz}	$p_y(B_1)$	$p_x(B_1)$	$Cp_1(B_1)$	$Cp_2(B_1)$
4	-13.23	-0.002	-0.299	+0.548	-0.697	+0.031	+0.007
8	-12.82	+0.051	-0.001	+0.778	+0.610	+0.003	0.000
12	- 9.91	-0.064	-0.368	-0.146	+0.220	-0.852	-0.009
15	- 7.53	-0.153	+0.895	+0.304	-0.317	+0.470	+0.101
21	- 3.79	+0.479	-0.121	-0.115	-0.045	+0.170	+0.891
23	- 3.47	+0.912	+0.230	-0.109	-0.222	+0.335	-0.456

B_2 Symmetry

Table 3.5 (Contd.)

Atomic Orbital Coefficients

Orbital Number	Energy	$4p_y$	d_{yz}	$p_y(B_2)$	$Cp_o(B_2)$	$Cp_1(B_2)$	$Cp_2(B_2)$
2	-13.63	-0.020	+0.179	-0.149	-0.945	+0.018	-0.002
6	-12.94	+0.039	-0.154	+0.938	-0.227	-0.024	+0.002
10	-10.17	+0.024	+0.500	+0.203	+0.163	+0.768	+0.005
14	- 7.67	+0.212	+0.837	+0.173	+0.177	-0.635	+0.044
18	- 3.91	+0.432	-0.012	-0.112	-0.046	+0.063	-0.907
22	- 3.64	+0.911	-0.257	-0.284	-0.141	+0.218	+0.423

(4) If electron-electron repulsions are ignored, then the calculation predicts the one-electron transitions in the visible region of the spectrum to be

Transition	Type	Energy (cm^{-1})
1	$B_2^* \leftarrow A_1^*$	12,100
2	$B_1^* \leftarrow A_1^*$	13,500
3	$A_1^{*\prime} \leftarrow A_1^*$	16,100
4	$A_2^* \leftarrow A_1^*$	20,100

If these predictions are now compared with the experimental data in table 3.3, then the stronger absorption band observed at 11,800 cm^{-1} in the spectrum of $(\pi\text{-}C_5H_5)_2$ V Cl_2 can be assigned to the transitions 1 and 2 and the weaker band at 13,600 cm^{-1} to transition 3. Transition 4 is forbidden in C_{2v} symmetry, and no peak is observed in the 20,000 cm^{-1} region of the $(\pi\text{-}C_5H_5)_2$ V Cl_2 spectrum, but a weak absorption is observed in this region of the spectrum of $(\pi\text{-}C_5H_5)_2$ Nb Cl_2, in addition to the stronger bands at lower frequencies. In all the other complexes the single broad band in the visible region of the spectrum probably contains transitions 1, 2, and 3.

The four highest energy filled bonding orbitals in the complex, shown in figure 3.5 arise mainly from the ring $cp_{\pm 1}$ orbitals. The difference in one-electron energies between these and the orbital containing the unpaired electron is only about 10,000 cm^{-1}. It seems reasonable, therefore, to assign the band at about 26,000 cm^{-1} in the spectra of these complexes to transitions from this group of levels to the orbital containing the unpaired electron. There are, in fact, three of these levels within 2,000 cm^{-1} of each other which probably contribute to this

band, while the A_2 orbital lies at lower energy. Again, however, the $A_2 \longleftarrow A_1^*$ transition is forbidden in C_{2v} symmetry, and should therefore be weak.

(5) The molecular orbital calculation suggests that there is a reasonably high degree of covalency in the metal-ligand bonds. The values of the metal d-orbital populations estimated from this calculation are

$$\text{Pmd } (B_1^*) = 0.66$$

$$\text{Pmd } (B_2^*) = 0.57$$

These are the quantities which will be calculated independently of the molecular orbital calculation from the e.p.r. data later.

(6) Knowing the charge and configuration of the vanadium ion, the values of P and ζ can now be estimated. The plot of the free ion values of the spin-orbit coupling constants [32,33], for vanadium ions, against the charges on the ions, shown in figure 3.6 shows that for a vanadium ion with a charge of +0.356 and a configuration $3d^{4.644}$, $\zeta = 115\ cm^{-1}$. For vanadium (0) in a $3d^5$ configuration $\zeta = 91\ cm^{-1}$; for vanadium (0) in a $3d^3\ 4s^2$ configuration, $\zeta = 158\ cm^{-1}$. Promoting an electron from a 3d to a 4s orbital therefore increases ζ by $33\ cm^{-1}$, and hence promoting 0.6 of an electron from $V^{+0.356}\ (3d^{4.644})$ to $V^{+0.356}\ (3d^{4.106}\ 4s^{0.524}\ 4p^{0.104})$ increases ζ to $133\ cm^{-1}$. Figure 3.7 shows a plot of ζ against $\frac{4}{7}P$ for various ions of vanadium, from which it can be seen that the value of P corresponding to $\zeta = 133\ cm^{-1}$ is $0.01065\ cm^{-1}$.

Thus the values of ζ and P for the vanadium ion in these complexes are

$$P = 0.01065\ cm^{-1}$$

$$\zeta = 133\ cm^{-1}.$$

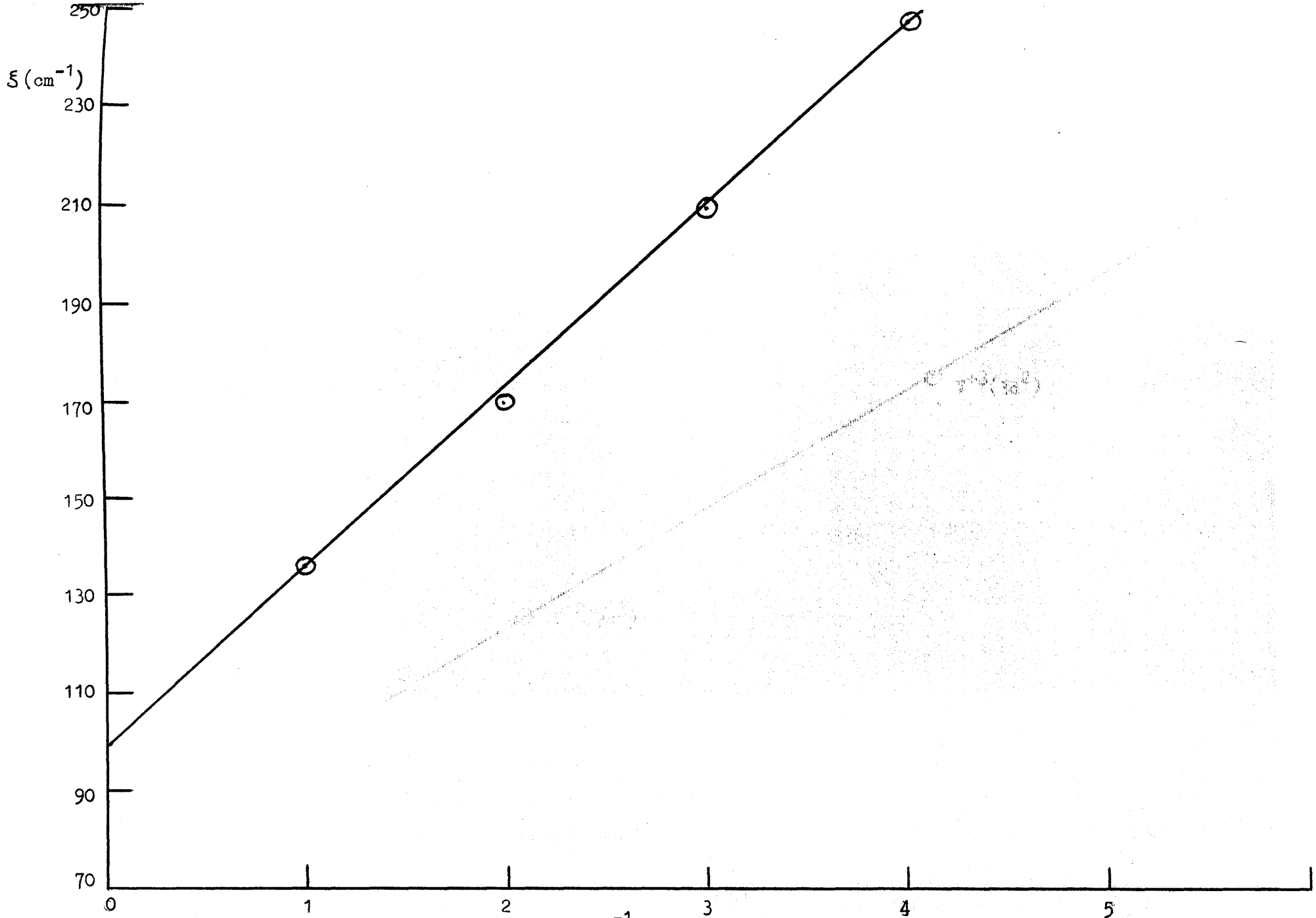

Figure 3.6 Spin-orbit coupling constants ζ(cm^{-1}) for $3d^n$ ions of vanadium vs ionic charge Z.

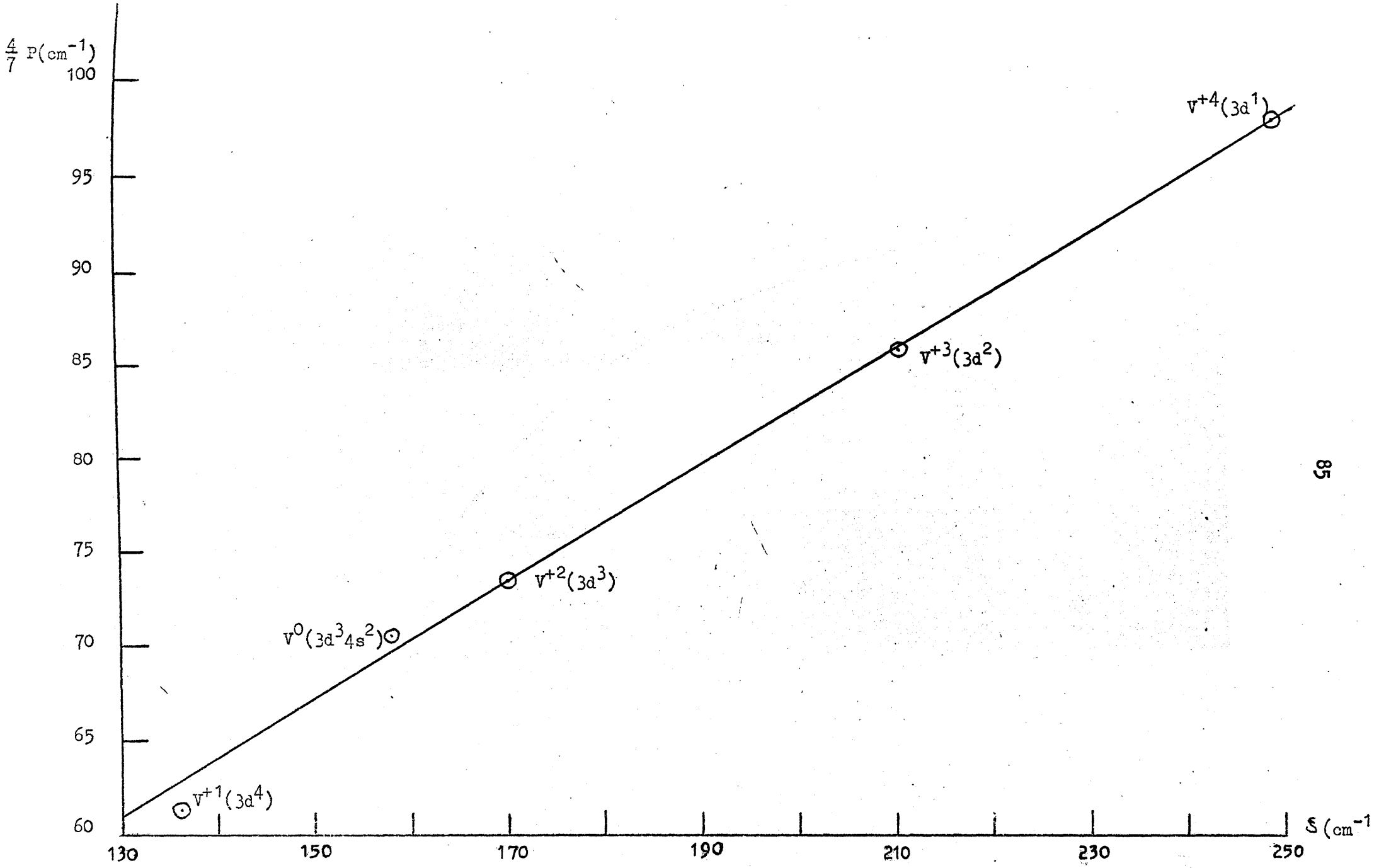

Figure 3.7 Spin-orbit coupling constants ζ(cm^{-1}) for various vanadium ion configurations VS $\frac{4}{7}$ P(cm^{-1})

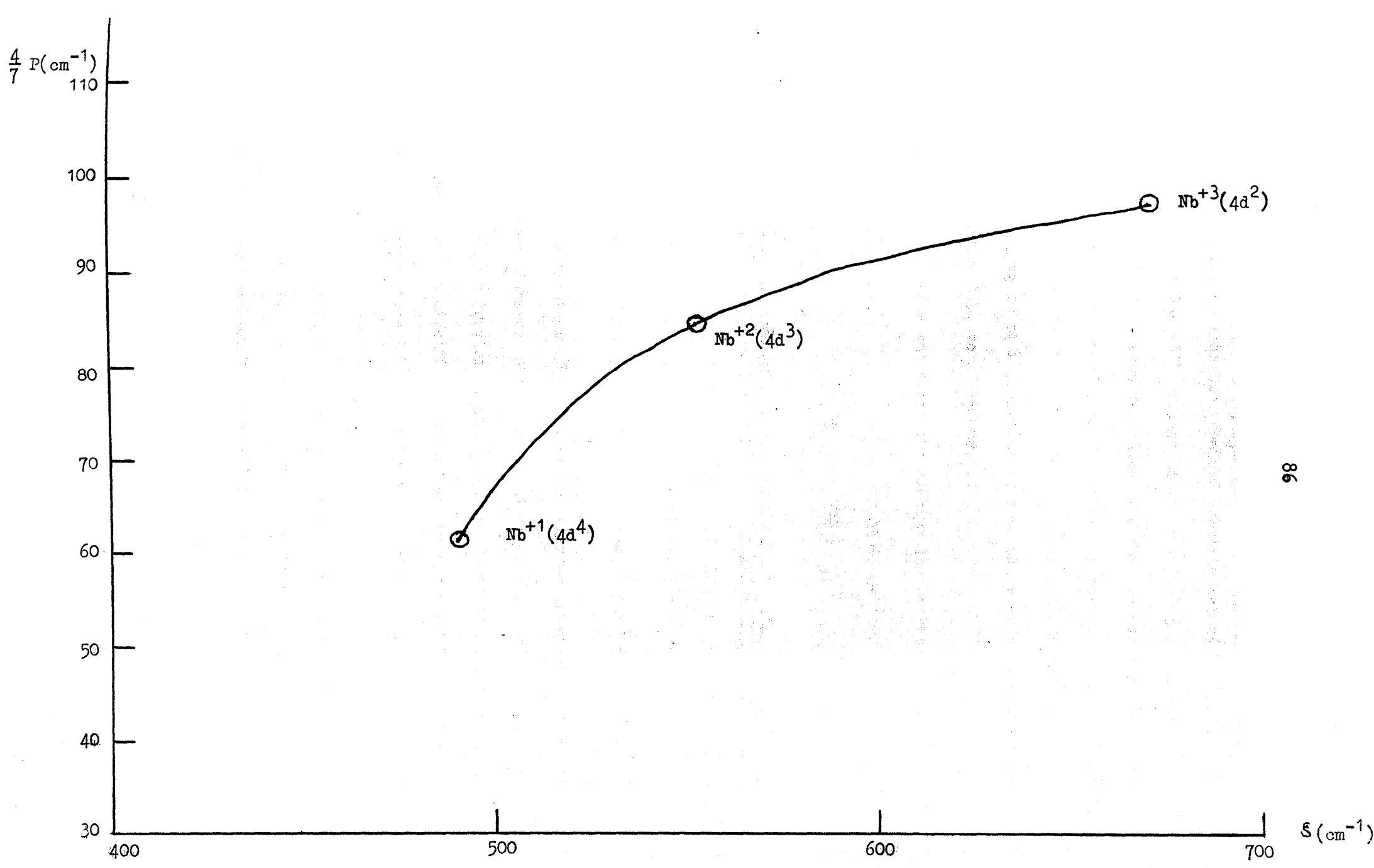

Figure 3.8 Spin-orbit coupling constants $\zeta(cm^{-1})$ for various niobium ion configurations vs $\frac{4}{7}$ P(cm^{-1})

As noted above, the d_{z^2} and $d_{x^2-y^2}$ orbitals in these complexes always hybridise so that the unpaired electron occupies an orbital which is non-bonding with respect to the ring molecular orbitals. Assuming that this is true the value of P for the niobium ion in these complexes can be estimated from the values of the anisotropic hyperfine coupling constants in $(\pi\text{-}C_5H_5)_2\ Nb\ Cl_2$ to be 0.01086 cm^{-1}, and the corresponding value of ζ is estimated from the plot of ζ against $\frac{4}{7}P$, shown in figure 3.8, to be 490 cm^{-1}.

Thus the values of P and ζ for the niobium ion in these complexes are

$$P = 0.01086\ cm^{-1}$$

$$\zeta = 490\ cm^{-1}.$$

3.7 Equations relating the spin Hamiltonian parameters to the molecular orbital coefficients in the complexes $(\pi\text{-}C_5H_5)_2MX_2$

As can be seen from table 3.5, the unpaired electron in these complexes occupies the A_1^* orbital, which has the form

$$A_1^* = \alpha_1^* (a d_{x^2-y^2} + b d_{z^2}) + \alpha_1^{*I} p_x (A_1)$$

where the contributions from the other basis orbitals of A_1 symmetry can be ignored because of the small values of their coefficients in this particular molecular orbital. It was found that spin orbit coupling causes a significant mixing of two types of excited state into the ground state in these complexes: these excited states are produced by promoting the unpaired electron into the empty antibonding orbitals of B_1 and B_2 symmetry lying immediately above A_1^* in figure 3.5, or promoting an electron from the filled bonding orbitals of B_1 and B_2 symmetry lying immediately below A_1^* into the A_1^* orbital.

These orbitals have the general form shown below, where * denotes an antibonding molecular orbital.

$$B_2^* = \beta_2^* d_{yz} + \beta_2^{*I} cp_0(B_2) + \beta_2^{*II} cp_1(B_2) + \beta_2^{*III} cp_2(B_2) + \beta_2^{*IV} P_y(B_2)$$

$$B_1^* = \beta_1^* d_{xz} + \beta_1^{*I} cp_1(B_1) + \beta_1^{*II} cp_2(B_1) + \beta_1^{*III} p_z(B_1) + \beta_1^{*IV} P_x(B_1)$$

$$B_2 = \beta_2 d_{yz} + \beta_2^{I} cp_0(B_2) + \beta_2^{II} cp_1(B_2) + \beta_2^{III} cp_2(B_2) + \beta_2^{IV} p_y(B_2)$$

$$B_1 = \beta_1 d_{xz} + \beta_1^{I} cp_1(B_1) + \beta_1^{II} cp_2(B_1) + \beta_1^{III} p_z(B_1) + \beta_1^{IV} p_x(B_1)$$

The metal ion 4p orbital contribution to these orbitals is ignored, since it does not affect the magnetic properties.

If the matrix elements of the true Zeeman and hyperfine Hamiltonians are equated to the corresponding matrix elements of the spin Hamiltonian[34], the following equations relating the spin Hamiltonian parameters to the molecular orbital coefficients for the complexes are obtained. The derivation of these equations is given in appendix C.

$$g_{xx} = 2.0023 - 2(a + b\sqrt{3})^2 \alpha_1^{*2} \zeta_m \left[\frac{Pmd(B_2^*)}{\Delta E(B_2^*)} - \frac{Pmd(B_2)}{\Delta E(B_2)} \right]$$

$$g_{yy} = 2.0023 - \frac{2(a - b\sqrt{3})^2 \alpha_1^{*2} \zeta_m Pmd(B_1^*)}{\Delta E(B_1^*)} \left[1 + \frac{\alpha_1^{*I} \beta_1^{*III} \zeta_x}{\alpha_1^* \beta_1^* (a - b\sqrt{3}) \zeta_m} \right] + \frac{2(a - b\sqrt{3})^2 \alpha_1^{*2} \zeta_m Pmd(B_1)}{\Delta E(B_1)} \left[1 + \frac{\alpha_1^{*I} \beta_1^{III} \zeta_x}{\alpha_1^* \beta_1 (a - b\sqrt{3}) \zeta_m} \right]$$

$$g_{zz} \simeq 2.0023 \qquad 3.10$$

ζ_m and ζ_x are the metal and ligand spin orbit coupling constants respectively. Small contributions to g_{zz} of the order of -0.002, which are due to spin-orbit mixing of orbitals of A_2 symmetry have been

omitted from the above equation, although the form of these is considered in appendix C.

The equations for the hyperfine coupling tensor components are the same as those for vanadyl complexes, ie

$$A_{xx} = P\left(-K + \frac{2}{7}(a^2 - b^2)\alpha_1^{*2} - \frac{4\sqrt{3}}{7}ab\alpha_1^{*2} - \Delta g_{xx} + \frac{(3a + b\sqrt{3})}{14(a - b\sqrt{3})}\Delta g_{yy} + \frac{b}{7a}\Delta g_{zz}\right)$$

$$A_{yy} = P\left(-K + \frac{2}{7}(a^2 - b^2)\alpha_1^{*2} + \frac{4\sqrt{3}}{7}ab\alpha_1^{*2} - \Delta g_{yy} + \frac{(3a - b\sqrt{3})}{14(a + b\sqrt{3})}\Delta g_{xx} - \frac{b}{7a}\Delta g_{zz}\right)$$

$$A_{zz} = P\left(-K - \frac{4}{7}(a^2 - b^2)\alpha_1^{*2} - \frac{(3a + b\sqrt{3})}{14(a - b\sqrt{3})}\Delta g_{yy} - \frac{(3a - b\sqrt{3})}{14(a + b\sqrt{3})}\Delta g_{xx} - \Delta g_{zz}\right) \qquad 3.11$$

where $\Delta g_{ii} = 2.0023 - g_{ii}$.

The above equations are not directly soluble since they contain too many unknowns, and to get them into a tractable form it is necessary to assume

(a) that $Pmd(B_2^*) + Pmd(B_2) \simeq 1$ and that $Pmd(B_1^*) + Pmd(B_1) \simeq 1$

(b) that contributions to the g-factors from spin-orbit coupling on the ligands is negligible.

With these approximations, the equations 3.10 become

$$g_{xx} = 2.0023 - 2\alpha_1^{*2}(a + b\sqrt{3})^2 \xi_m \left[\frac{Pmd(B_2^*)}{\Delta E(B_2^*)} - \frac{Pmd(B_2)}{\Delta E(B_2)}\right]$$

$$g_{yy} = 2.0023 - 2\alpha_1^{*2}(a - b\sqrt{3})^2 \xi_m \left[\frac{Pmd(B_1^*)}{\Delta E(B_1^*)} - \frac{Pmd(B_1)}{\Delta E(B_1)}\right]$$

$$g_{zz} \simeq 2.0023 \qquad 3.12$$

3.8 Calculation of molecular orbital coefficients for the complexes $(\pi\text{-}C_5H_5)_2MX_2$

The e.p.r. parameters for the complexes can be used to deduce the following information

(1) The equations 3.11 can be solved to yield values of K, a, b and α_1^{*2} for each of the complexes, and the resulting values of these parameters are listed in table 3.6.

(2) If the energy differences in the equations for g_{xx} and g_{yy} are set equal to the frequencies of the band maxima in the u.v.-visible spectra of the complexes, using the assignments given in section 3.6, then these equations can be solved to yield the values of $Pmd(B_1^*)$ and $Pmd(B_2^*)$ listed in table 3.6.

From the e.p.r. data alone it is impossible to say what the relative signs of the parameters a and b are, and hence which of the observed g-tensor values corresponds to g_{xx} and which to g_{yy}, referred to the axis system of figure 3.4. The molecular orbital calculation, however, indicates that a and b are opposite in sign, so that g_{xx} corresponds to the larger of the two g-factors. The values of g_{xx} and g_{yy} reflect the bonding of the ligands with the d_{yz} and the d_{xz} orbitals respectively. The d_{yz} orbital is most strongly bound to the cyclopentadienide ring orbitals, whereas the d_{xz} orbital interacts most strongly with the orbitals of the X ligands.

Since no u.v.-visible spectral data were available for $(C_5H_5)_4Nb$, the molecular orbital coefficients were estimated by setting its $Pmd(B_2^*)$ value equal to the average value of $Pmd(B_2^*)$ for the other niobium complexes. Using the expression for g_{xx} and an estimated value of 28,000 cm^{-1} for $\Delta E(B_2)$, a value of 14,200 cm^{-1} was estimated for $\Delta E(B_2^*)$. Setting the values of $\Delta E(B_1)$ and $\Delta E(B_1^*)$ equal to the values of $\Delta E(B_2)$ and $\Delta E(B_2^*)$ estimated in this way, a value of $Pmd(B_1^*)$ could then be

Table 3.6

Molecular orbital coefficients and metal ion d-orbital populations for the complexes $(\pi\text{-}C_5H_5)_2\,VX_2$ and $(\pi\text{-}C_5H_5)_2\,Nb\,X_2$. Bracketed data are obtained if the charge-transfer terms in equations 3.12 are omitted in estimating the metal d-orbital populations. Limits of error, $(\alpha_1^*)^2$ ±0.005, $Pmd(B_1^*)$, $Pmd(B_2^*)$ ±0.015.

	K	|a|	|b|	$(\alpha_1^*)^2$	$Pmd(B_2^*)$		$Pmd(B_1^*)$	
$(\pi\text{-}C_5H_5)_2\,VCl_2$	0.64	0.223	0.975	0.970	0.553	(0.348)	0.582	(0.392)
$(\pi\text{-}C_5H_5)_2\,V(SCN)_2$	0.64	0.247	0.969	0.917	0.586	(0.370)	0.776	(0.658)
$(\pi\text{-}C_5H_5)_2\,V(OCN)_2$	0.66	0.237	0.971	0.946	0.605	(0.425)	0.762	(0.643)
$(\pi\text{-}C_5H_5)_2\,V(CN)_2$	0.53	0.237	0.971	0.830	0.577	(0.296)	0.595	(0.333)
$(\pi\text{-}C_5H_5)_2\,NbCl_2$	0.98	0.274	0.963	1.000	0.456	(0.166)	0.520	(0.350)
$(\pi\text{-}C_5H_5)_2\,Nb(SCN)_2$	0.94	0.294	0.956	0.942	0.475	(0.149)	0.585	(0.324)
$(\pi\text{-}C_5H_5)_2\,Nb(\sigma\text{-}C_5H_5)_2$	0.85	0.276	0.962	0.915	0.455		0.440	
$(\pi\text{-}C_5H_5)_2\,Nb(CN)_2$	0.77	0.325	0.946	0.808	0.438	(0.072)	0.504	(0.167)

calculated.

Having now obtained values of the molecular orbital coefficients for the complexes from the e.p.r. parameters, it is now of interest to compare the information obtained in this way with that obtained from the molecular orbital calculation on $(\pi\text{-}C_5H_5)_2\ VCl_2$.

Although the e.p.r. parameters confirm that the unpaired electron in these complexes lies in an orbital of A_1 symmetry, localised mainly on the metal ion, the values of a and b listed in table 3.6 show that the molecular orbital calculation overestimates the $d_{x^2-y^2}$ orbital contribution to this orbital. From the data in table 3.6, it can also be seen that the values of a and b are fairly insensitive to changes in the nature of the X ligands, and as explained earlier this is because the hybridisation of the metal ion d_{z^2} and $d_{x^2-y^2}$ orbitals is a function of the bonding to the cyclopentadienide ring orbitals, which does not change much from complex to complex.

The values of α_1^{*2} in table 3.6 which indicate the degree of delocalisation of the unpaired electron in these complexes onto the ligands show that the unpaired electron is localised mainly on the metal ion in most of these complexes, and is only delocalised to any great extent in the cyanide complexes. The value of 0.97 for α_1^{*2} in $(\pi\text{-}C_5H_5)_2\ VCl_2$ is in excellent agreement with the value obtained from the molecular orbital calculation.

The $Pmd(B_2^*)$ values, which reflect the bonding between the metal ion d_{yz} orbitals and the cyclopentadienide ring orbitals are, as expected, fairly constant for a particular metal ion, whereas the $Pmd(B_1^*)$ values vary with the nature of the X ligands, again as expected. The values also indicate a high degree of covalency in the bonds between the metal ion and the cyclopentadienide rings and the X ligands, with the bond to

cyclopentadienide rings being the more covalent. The values of $Pmd(B_1^*)$ and $Pmd(B_2^*)$ for $(\pi\text{-}C_5H_5)_2\ VCl_2$ estimated using equations 2.11 are 0.553 and 0.58, in good agreement with the values of 0.57 and 0.66 obtained from the molecular orbital calculation. The bracketed values of $Pmd(B_1^*)$ and $Pmd(B_2^*)$ in table 3.6 are those obtained if the contribution to the g-factors from charge-transfer states are ignored. These values show an excessive degree of covalency in the metal-ligand bonds, and show how important the charge transfer states are in these complexes.

Thus there is a very good correlation between the values of the molecular orbital coefficients obtained from the e.p.r. parameters and those obtained from the molecular orbital calculation.

3.9 E.p.r. properties of the complex $(\pi\text{-}C_5H_5)_2\ Ta\ (\sigma\text{-}C_5H_5)_2$

The e.p.r. spectra of the complex $(C_5H_5)_4\ Ta$, recorded in toluene solution at room temperature, and in a magnetically dilute glass at 77K, are shown in figure 3.9. Although the solution spectrum can easily be analysed in terms of the usual isotropic spin Hamiltonian 3.1, giving values of the isotropic g-value and hyperfine coupling constant of 1.954 and 0.00982 cm^{-1} respectively, it was not possible to fit the observed resonant field values in the glassy spectrum of the complex to a set of equations of the general type given in equation B10 of appendix B.

The most probable reason for this is that the ^{181}Ta nucleus has a very large quadrupole moment, and provided that there is a non-zero electric field gradient at the tantalum ion nucleus, it is quite possible that the quadrupolar interaction in this complex could be of the same order of magnitude as the hyperfine interaction. This would produce several effects.

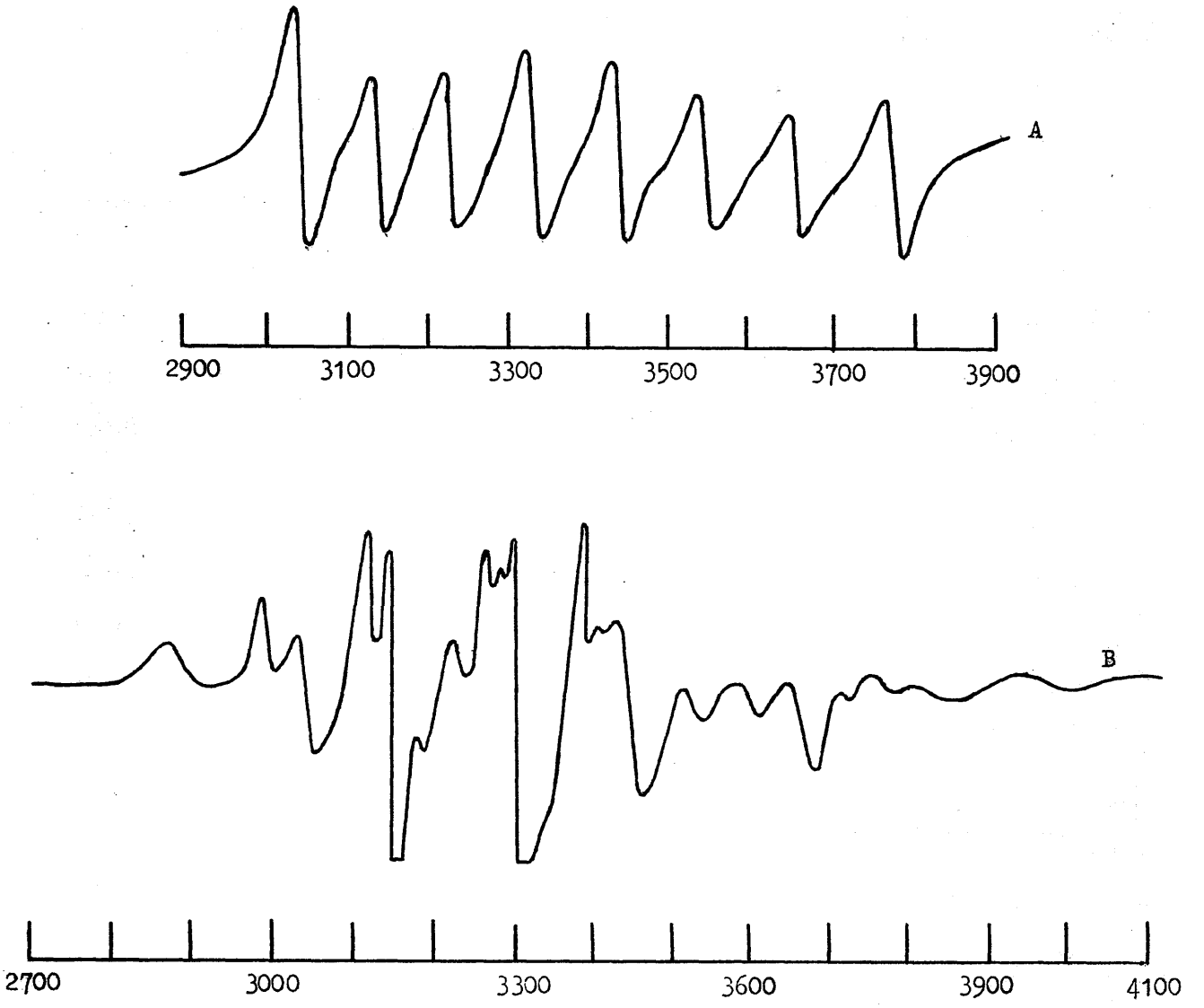

Figure 3.9 E.p.r. spectra of a 10^{-2}M solution of $(\pi\text{-}C_5H_5)_2\ Ta(\sigma\text{-}C_5H_5)_2$ in toluene at 298K, A, and in toluene glass at 77K, B.

(1) As noted earlier, the general form of the spin Hamiltonian, including quadrupolar terms is

$$\mathcal{H} = \beta_e \underline{H}.g.\underline{S} + \underline{S}.A.\underline{I} + \underline{I}.P.\underline{I} \qquad 3.13$$

As shown in appendix B, the derivation of analytical expressions for the energy levels and resonant fields for a complex using this Hamiltonian, involves the assumption that the quadrupolar terms are small enough to be considered simply as a perturbation on the eigenfunctions of the Hamiltonian containing only the Zeeman and hyperfine interactions.[17] If the quadrupolar terms were to become large, however, this assumption would no longer be valid, and the analytical equations for the resonant field values given in equation B10 would no longer hold; this is in fact observed in the glassy spectrum of $(C_5H_5)_4$ Ta.

(2) The presence of a large quadrupolar term in the spin Hamiltonian mixes together states of the form $|m_S, m_I\rangle$ and $|m_S, m_I \pm 2\rangle$. This results in transitions of the type $\Delta m_S = \pm 1$, $\Delta m_I = \pm 2$ becoming allowed[35] and these contribute to the glassy spectrum. Again, extra transitions are in fact observed in the spectrum of $(C_5H_5)_4$ Ta.

(3) The quadrupolar coupling tensor is traceless, so that there is no quadrupolar term in the isotropic spin Hamiltonian, which explains why the solution spectrum can be analysed in terms of the usual Hamiltonian. The quadrupolar terms in 3.13 could, however, contribute to the linewidths in the solution e.p.r. spectrum of $(C_5H_5)_4$ Ta, through modulation of these terms by the rotation of the complex in solution.[36] Ordinarily, the e.p.r. spectra of transition metal ions exhibit a smooth gradation of the solution linewidths as a function of m_I value, with the narrowest lines being in the centre of the spectrum and the broadest in the wings. The irregular gradation of the linewidths in the solution spectrum of $(C_5H_5)_4$ Ta may be due to an important contribution to the linewidths from quadrupolar relaxation.

Thus the evidence above indicates that the differences between the e.p.r. spectra of the vanadium (IV) and niobium (IV) complexes on the one hand, and those of tantalum (IV) on the other are due to a large quadrupolar interaction in the latter.

The glassy spectrum of $(C_5H_5)_4$ Ta could be interpreted by choosing reasonable values for the spin Hamiltonian parameters and solving the problem numerically to obtain values for the energy levels and the resonant field values for the complex. The values of the input parameters could then be varied systematically until agreement was reached between the observed and calculated resont field positions.

Because of the rather large number of variable parameters, however, this is a fairly lengthy procedure, and there was not enough time to carry this problem to its conclusion.

3.10 Summary of part III

In this study X-band e.p.r. spectra of the complexes $(\pi\text{-}C_5H_5)_2\ MX_2$, where M = vanadium (IV), niobium (IV) or tantalum (IV), and $X = Cl^-$, SCN^-, OCN^-, CN^- or $\sigma\text{-}C_5H_5^-$ have been recorded in solution at 298K and in magnetically dilute glasses at 77K, and these spectra are analysed in detail. From Huckel L.C.A.O. molecular orbital calculations carried out on the complex $(\pi\text{-}C_5H_5)_2\ VCl_2$, the metal ion spin-orbit coupling constants ζ_V and ζ_{Nb} in these complexes are estimated to be 133 cm^{-1} and 490 cm^{-1} respectively. Spin Hamiltonian parameters are listed for each substance, and are equated to the atomic orbital coefficients in some of the molecular orbitals involved in bonding in these complexes, and good agreement is obtained between the values derived in this way and those derived from the molecular orbital calculations. Except for the cyanides, in each case the unpaired electron lies essentially in a non-bonding nd_{z^2} metal ion orbital,

mixed with a small amount of the corresponding metal ion nd $_{x^2-y^2}$ orbital, the Z-axis coinciding with the C_2 axis of the compound. In the cyanides this unpaired electron is delocalised into p_x orbitals on the X ligands. The bonding of the metal ion to the cyclopentadienide rings and to the other ligands X is almost completely covalent, the bonding to the cyclopentadienide rings being stronger than that to the ligands X. Several redistribution complexes of the type $(\pi\text{-}C_5H_5)_2$ MXY have also been detected and characterised by their e.p.r. spectra. E.p.r. techniques can be used to distinguish compounds of the type $(\pi\text{-}C_5H_5)_2$ MX_2 from other compounds which contain vanadium (IV) and niobium (IV).

The difference between the e.p.r. spectra arising from complexes containing the tantalum (IV) ion and those containing vanadium (IV) or niobium (IV) may be due to the presence of a large quadrupolar interaction in the tantalum complexes.

PART IV

STUDIES OF THE E.P.R. LINEWIDTHS IN SOLUTION SPECTRA OF THE COMPLEXES $(\pi\text{-}C_5H_5)_2\ VCl_2$, $(\pi\text{-}C_5H_5)_2\ NbCl_2$ AND $(\pi\text{-}C_5H_5)_2\ Nb(\sigma\text{-}C_5H_5)_2$

4.1 Introduction

In the previous section it was shown that the unpaired electron in the complexes $(\pi\text{-}C_5H_5)_2\ VCl_2$ and $(\pi\text{-}C_5H_5)_2\ NbCl_2$ is localised almost completely on the metal ion. This information was obtained essentially from an analysis of the spin-dipolar interaction between the magnetic moment of the metal ion nucleus and the spin magnetic moment of the electron. It should be possible to obtain similar information about the delocalisation of the unpaired electron on to the ligands by an analysis of the ligand nuclear hyperfine interactions in these complexes. It should be possible to obtain information about the degree of delocalisation of the unpaired electron on to the π—cyclopentadienide rings and on to the chloride ligands by measuring the hyperfine interaction between the unpaired electron and the ring protons, and between the unpaired electron and the chlorine nuclei respectively.

Although no splitting of the e.p.r. lines in the spectra of these complexes due to a hyperfine interaction with ligand nuclei is in fact observed, it is nevertheless still possible to estimate the size of the isotropic hyperfine coupling constants for the chlorine and proton nuclei from the contribution which this coupling makes to the width of the lines in the e.p.r. spectra of these complexes in solution. To do this, a detailed analysis of the linewidths as a function of temperature is necessary, in order to separate out from the total linewidths the contributions from unresolved ligand hyperfine structure, and from various effects which cause relaxation of the electron's spin in solution and which thereby contribute to the linewidths.

A detailed analysis of the e.p.r. linewidths in these two complexes was therefore undertaken and the values of the ligand hyperfine coupling constants estimated in this way were then used to obtain an independent estimate of the extent of delocalisation of the unpaired electrons in these compounds. The estimates obtained in this way were then compared with the values obtained from the analysis of the spin Hamiltonian parameters described in the last chapter.

The complex $(\pi\text{-}C_5H_5)_2\ Nb(\sigma\text{-}C_5H_5)_2$ is also of interest because of the possibility that the σ and π bonded rings in this complex might be able to interchange, possibly through an equilibrium of the form

$$(\pi\text{-}C_5H_5)_2\ Nb(\sigma\text{-}C_5H_5)_2 \rightleftharpoons (\pi\text{-}C_5H_5)_3\ Nb(\sigma\text{-}C_5H_5)$$

A reaction of this type should affect the behaviour of the linewidths in this complex and for this reason it was decided to carry out a detailed analysis of the linewidths in the solution e.p.r. spectrum of this complex also.

4.2 Mechanisms of Electron Spin Relaxation in Solutions of Transition Metal Complexes

As shown in part I, the width of a magnetic resonance line is decided in most cases by the value of the transverse relaxation time T_2, which is defined in the equations

$$\frac{dM_x}{dt} = -\frac{M_x}{T_2}$$

$$\frac{dM_y}{dt} = -\frac{M_y}{T_2} \qquad 4.1$$

which describe the relaxation properties of the X and Y components of the macroscopic magnetic moment of a collection of spins in a magnetic field applied along the Z-axis direction.

The time-dependence of any property of a system can be explained in terms of the effect of the time-dependent terms in the Hamiltonian of the system. The Hamiltonian for any system can be written as

$$\mathcal{H} = \mathcal{H}_o + \mathcal{H}(t) \qquad 4.2$$

where $\mathcal{H}_o$ and $\mathcal{H}(t)$ are time-independent and time-dependent terms. The effect of $\mathcal{H}(t)$ is to cause the eigenfunctions, and hence the properties, of the system to be functions of time, ie it is the time-dependent terms in the Hamiltonian which cause relaxation.

In transition metal complexes of the type considered here, there are two main relaxing mechanisms.

(a) The Zeeman and hyperfine contributions to the energy of the complexes can be written as

$$\begin{aligned}\mathcal{H} &= \beta_e \underline{H}.g.\underline{S} + \underline{S}.A.\underline{I} \\ &= g_o \beta_e \underline{S}.\underline{H} + A_o \underline{S}.\underline{I} + \beta_e \underline{H}.g'.\underline{S} + \underline{S}.A'.\underline{I} \end{aligned} \qquad 4.3$$

where

$$g'_{ij} = g_{ij} - \delta_{ij} g_o \quad \text{and} \quad A'_{ij} = A_{ij} - \delta_{ij} A_o \qquad 4.4$$

g_o and A_o are the usual isotropic g-factor and hyperfine coupling constant.

Rotation of a paramagnetic complex in solution causes the g' and A' tensor components to be time-dependent, and the Brownian motion therefore modulates the Zeeman and hyperfine interactions. The time-dependent contribution to the Hamiltonian of the system from this effect is thus given by

$$\mathcal{H}(t) = \beta_e \underline{H}.\ g'(t).\ \underline{S} + \underline{S}.\ A'(t).\ \underline{I} \qquad 4.5$$

This mechanism for electron spin relaxation was suggested by McConnell,[1] and extended by Kivelson.[2,3] It is this mechanism which

leads to the m_I-dependent linewidths observed in complexes with large anisotropic g- and hyperfine tensor components.

(b) The second important electron relaxation mechanism, also proposed by Kivelson,[4] is called spin-rotational relaxation. When a complex rotates in solution, the motion of the electrons and nuclei in the complex produces magnetic fields which can interact with the magnetic moment of the unpaired electron, and since the magnitude and direction of these fields are time-dependent this leads to electron spin relaxation. This interaction can be written as

$$\mathcal{H}(t) = \underline{J}(t).\ C(t).\ \underline{S} \qquad 4.6$$

where $\underline{J}(t)$ is the rotational angular momentum operator for the molecule, and $C(t)$ is the spin-rotational interaction tensor. Both $J(t)$ and $C(t)$ are time-dependent, but in fact the modulation of $\underline{J}(t)$ by molecular collisions in solution is the more important relaxing mechanism.

The theoretical aspects of electron spin relaxation in systems of non-interacting spins acted upon by a random time-dependent perturbation are probably best treated using the density matrix approach.[5]

In this approach, the eigenfunctions of the Hamiltonian $\mathcal{H}$ of equation 4.2 are expanded as a linear combination of the eigenfunctions of $\mathcal{H}_o$, of the form

$$\psi = \sum_i c_i \phi_i \qquad 4.7$$

The time-dependence of the eigenfunctions ψ is thus contained in the coefficients c_i. The expectation value of any operator O is given by

$$\langle O \rangle = \sum_{i,j} c_i^* c_j \langle \phi_i | O | \phi_j \rangle \qquad 4.8$$

If an operator ρ is defined such that

$$\rho_{ij} = \langle \phi_j | \rho | \phi_i \rangle = c_i^* c_j \qquad 4.9$$

then

$$\langle O \rangle = \sum_{i,j} \langle \phi_j | \rho | \phi_i \rangle \langle \phi_i | O | \phi_j \rangle = \mathrm{Tr}\, \rho O \qquad 4.10$$

The elements of the operator ρ constitute what is known as the density matrix. The time-dependent of the operator O can thus be obtained by differentiating equation 4.10, to give

$$\frac{d\langle O \rangle}{dt} = \sum_{i,j} \frac{d\rho_{ij}}{dt} \langle \phi_i | O | \phi_j \rangle \qquad 4.11$$

The problem of obtaining an expression for the time-dependence of any property of the system thus reduces to one of deriving an equation describing the time-dependence of the elements of the density matrix, ie of the products $c_i^* c_j$.

Such an equation has, in fact, been derived using time-dependent perturbation theory by Redfield,[5,6] who obtained an expression for the time dependence of ρ_{ij} as a function of $\mathcal{H}(t)$. Using his equation it is possible to derive expressions for $\frac{dM_x}{dt}$ and $\frac{dM_y}{dt}$, and hence, by comparing these expressions with equations 4.1, to obtain expressions for the transverse relaxation time T_2. The T_2 value can then be related to the peak-to-peak linewidth ΔH for the first derivative of a Lorentzian line by the equation

$$\Delta H = \frac{2}{T_2 \sqrt{3}} \qquad 4.12$$

As noted above, the linewidth in the complexes studied here arises from rotational modulation of the g and hyperfine tensor components, the spin-rotational interaction, and unresolved ligand hyperfine coupling, and in this case the linewidth can be written in the form[3,7]

$$\Delta H = \alpha + \alpha' + \alpha'' + \beta m_I + \gamma m_I^2 \qquad 4.13$$

where the linewidth is in gauss and the other parameters are given by [3,7]

$$\alpha'' = \frac{2\beta_e H^2 \tau_c}{\sqrt{3}\, g_o \hbar}\left[\frac{2}{15} + \frac{1}{10(1+\omega_o^2\tau_c^2)}\right](g'^2_{xx} + g'^2_{yy} + g'^2_{zz})$$

$$+ \frac{4\pi h \tau_c}{\sqrt{3}\, g_o \beta_e}\left[\frac{1}{20} + \frac{7}{60(1+\omega_o^2\tau_c^2)}\right] I(I+1)\,(A'^2_{xx} + A'^2_{yy} + A'^2_{zz})$$

$$\beta = \frac{4\pi H \tau_c}{\sqrt{3}\, g_o}\left[\frac{4}{15} + \frac{1}{5(1+\omega_o^2\tau_c^2)}\right](g'_{xx} A'_{xx} + g'_{yy} A'_{yy} + g'_{zz} A'_{zz})$$

$$\gamma = \frac{4\pi h \tau_c}{\sqrt{3}\, g_o \beta_e}\left[\frac{1}{12} - \frac{1}{60(1+\omega_o^2\tau_c^2)}\right](A'^2_{xx} + A'^2_{yy} + A'^2_{zz}) \qquad 4.14$$

In the above expressions the hyperfine coupling constants are in units of sec^{-1}, and the subscripts X, Y, and Z refer to the principal axes of the g and A tensors.

The α'' term in the above expressions arises from the modulation of the g and A tensors, the γ term from the modulation of the A tensor and the β term from a cross term dependent on the modulation of both the g and A tensors. The α' term is the contribution from the spin-rotational interaction and the α term is the contribution from the unresolved hyperfine coupling, plus any other small contributions which have not been considered above.

The parameter τ_c is the rotational correlation time, and it is a measure of the rate at which the complex rotates in solution. It can be shown that this can be approximated by the relationship [8,9]

$$\tau_c = \frac{4\pi\eta a_o^3}{3kT} \qquad 4.15$$

where η is the viscosity of the solvent used and a_o is the effective radius of the rotating molecule.

It can be seen from the form of the equations 4.15 and 4.14 therefore, that in complexes where the term $\omega_o^2 \tau_c^2 \ll 1$, as it is in the complexes studied here, the α'', β and γ terms are proportional to ηT^{-1}. The spin-rotational term, on the other hand, can be shown[4] to be proportional to $T\eta^{-1}$.

In physical terms, the electron spin relaxation can be thought of as arising from the interaction of the magnetic moment of the electron with the X, Y and Z-axis components of the random magnetic fields generated in this case by the rotation of the complex in solution. The interaction of the magnetic moment of the electron with the Z component of these random fields causes the individual magnetic moments in the sample to precess at different rates, so that the rotation of the various spins becomes out of phase, and M_x and M_y tend towards zero. This effect is sometimes described as secular broadening, and it leads to the τ_c terms in equations 4.14. The interaction of the electron's magnetic moment with the X and Y components of the random fields, on the other hand, causes transitions between the allowed spin states and so leads to lifetime broadening. This effect is sometimes described as non-secular broadening and gives rise to the terms in $\tau_c(1 + \omega_o^2 \tau_c^2)^{-1}$ in equations 4.14.

4.3 Experimental

The complexes $(\pi\text{-}C_5H_5)_2\ VCl_2$, $(\pi\text{-}C_5H_5)_2\ NbCl_2$ and $(C_5H_5)_4\ Nb$ were prepared as described in the previous chapter [10-12]. Deuterated samples of $(\pi\text{-}C_5H_5)_2\ VCl_2$ and $(\pi\text{-}C_5H_5)_2\ NbCl_2$ were prepared in the same way, only using deuterated cyclopentadiene. The deuterated cyclopentadiene

was prepared[13] by stirring a mixture of monomeric cyclopentadiene, dimethyl formamide, and deuterated aqueous sodium hydroxide in carefully regulated proportions for one hour at 0°C. The partly deuterated cyclopentadiene obtained in this way was separated off, and the process was repeated two more times. This gave cyclopentadiene which was estimated from its i.r. spectrum to be about 90 atom % deuterated.

The linewidths of the complexes $(\pi\text{-}C_5H_5)_2\ VCl_2$ and $(\pi\text{-}C_5H_5)_2\ NbCl_2$ were measured in dried, degassed chloroform solution, while those of $(C_5H_5)_4\ Nb$ were measured in dried, degassed toluene. The measurements were made over a range of temperatures for the deuterated forms of the dichlorides, and for the undeuterated tetracyclopentadienide, and at one temperature only for the undeuterated forms of the chlorides. The deuterated form of the tetracyclopentadienide was not studied.

The temperature of the samples was varied using the gas flow system described in the introductory chapter, and the temperature was measured accurately using a copper-constantan thermocouple linked to a digital voltmeter.

The concentration of the solutions was about 10^{-3}M, which was sufficiently dilute to preclude the possibility of line broadening from intermolecular dipolar interactions in the solution, and the modulation amplitude and microwave power were small enough to prevent any broadening from these sources.

The linewidths were obtained by measuring the peak-to-peak width of one of the lines in a particular spectrum very accurately, and estimating the width of the other lines in the same spectrum from the relationship[3],

$$(\text{peak-to-peak width})^2 \quad (\text{peak-to-peak height}) = \text{constant}$$

The error involved in measuring the linewidths in this way was no greater than that involved in measuring them directly.

The effect on the e.p.r. spectra of these complexes of changing the temperature of the solution is illustrated in figure 4.1 which shows the spectrum of $(\pi\text{-}C_5H_5)_2\ VCl_2$ recorded at 260K and at 315K. The effect of reducing the temperature is to increase the linewidths due to increased broadening from the modulation of the g and A tensors. This effect also leads to an accentuation of the m_I dependence of the spectrum, which is more apparent at lower temperatures.

4.4 Results and Discussion for $(\pi\text{-}C_5H_5)_2\ VCl_2$ and $(\pi\text{-}C_5H_5)_2\ NbCl_2$

The value of the isotropic proton hyperfine coupling constants in $(\pi\text{-}C_5H_5)_2\ VCl_2$ and $(\pi\text{-}C_5H_5)_2\ NbCl_2$ was estimated by comparing the linewidths in the spectra of the deuterated samples of these complexes with the linewidths in the spectra of the corresponding undeuterated samples at the same temperature. Since the deuterium nucleus has a much smaller magnetic moment than that of the proton, it should be possible to estimate the value of the proton isotropic hyperfine coupling constant from the difference in the linewidths between the deuterated and undeuterated complexes.

In fact the spectra of these complexes recorded at 293K showed no detectable difference between the linewidths of the deuterated and undeuterated samples for either of them. The hyperfine coupling between the unpaired electron and the protons in both complexes is too small to be detected. This agrees with the conclusion reached in the last chapter, that the unpaired electron density at the cyclopentadienide rings is negligibly small in both complexes.

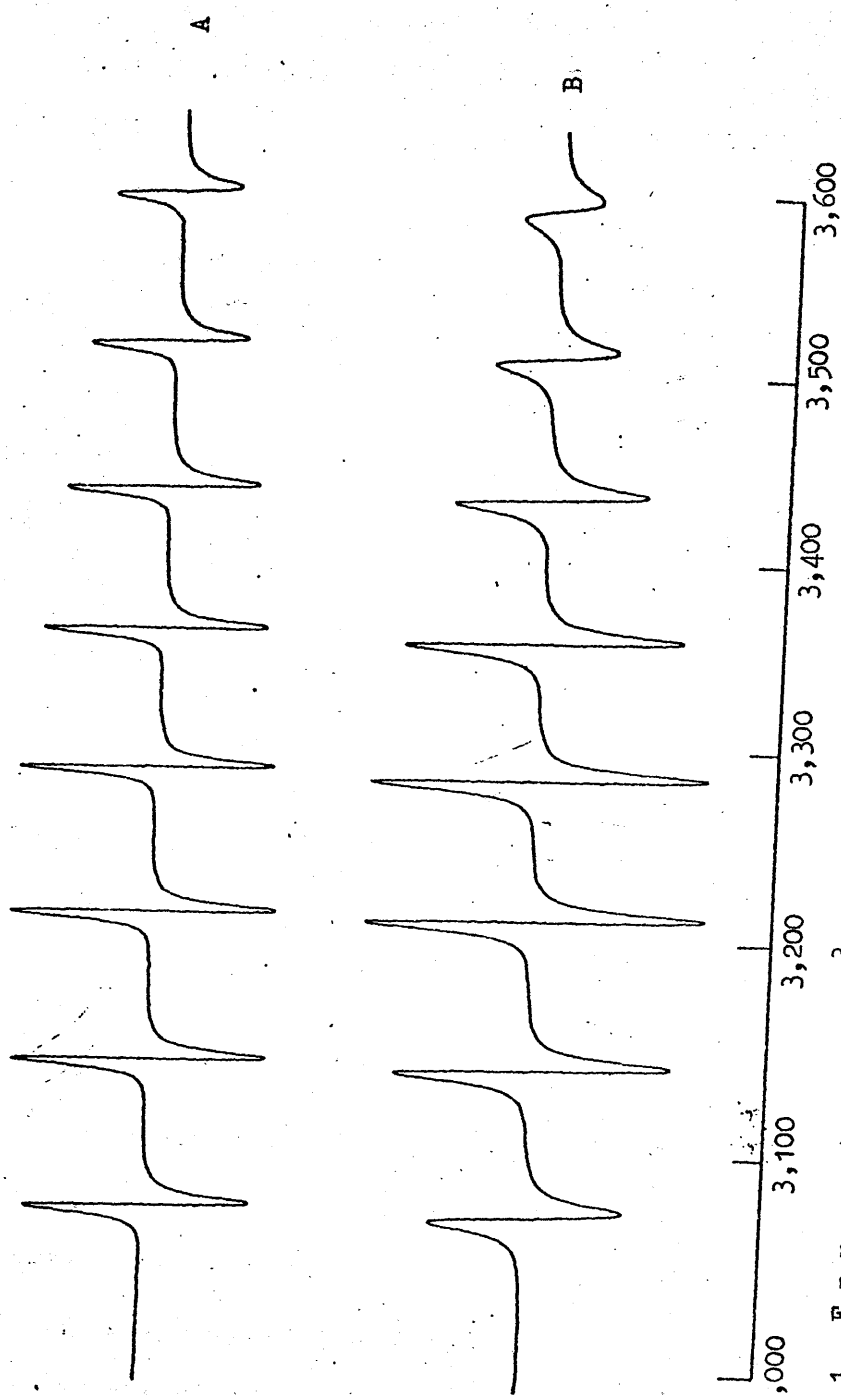

Figure 4.1 E.p.r. spectra of a 10^{-3}M solution of the complex $(\pi\text{-}C_5H_5)_2\ VCl_2$ in chloroform at 315K, A, and at 260K, B.

To estimate the chlorine nuclear hyperfine coupling constant, the linewidths in the spectra of the complexes were fitted, using a least squares procedure, to a function of the type shown in equation 4.13. The values of the parameters $\alpha + \alpha' + \alpha''$, β and γ obtained in this way are listed for the two complexes at various temperatures in tables 4.1 and 4.2 respectively. According to the theory discussed in section 4.2 the parameter β should be proportional to ηT^{-1} and to check, before proceeding further that the complexes were conforming to the theory, the values of β listed in tables 4.1 and 4.2 were plotted as a function of ηT^{-1}, and the resulting graphs are presented in figures 4.2 and 4.3. It can be seen from the graphs that for both complexes good straight lines, passing close to the origin are in fact obtained, so that both complexes do in fact conform well to the theory. The least squares fit of the data presented in figure 4.2 and 4.3 is given by

$$(\pi\text{-}C_5H_5)_2\,VCl_2 \qquad \beta = -0.056 + 18460\,\eta T^{-1}$$

$$(\pi\text{-}C_5H_5)_2\,NbCl_2 \qquad \beta = -0.035 + 42600\,\eta T^{-1} \qquad 4.16$$

The contribution to the linewidths at each temperature from the parameter α'' was calculated by using the spin Hamiltonian parameters for each complex together with the corresponding values of β at each temperature, and using the expression for β given in equation 4.14 to obtain values of the rotational correlation times τ_c. The values of τ_c were then used together with the spin Hamiltonian parameters to calculate values of α'', again from the expression given in equation 4.14.

The values of the residual linewidth $\alpha + \alpha'$ due to spin-rotational relaxation and unresolved hyperfine structure, could then be calculated since the values of $\alpha + \alpha' + \alpha''$ were already known.

Table 4.1

Parameters obtained from the least-squares fit of the e.p.r. linewidths of the complex $(\pi\text{-}C_5H_5)_2\ VCl_2$ in chloroform solution as a function of m_I: all values are in units of gauss.

Temperature (K)	$\alpha + \alpha' + \alpha''$	β	γ
332	3.846	0.172	0.065
325	4.049	0.214	0.069
313	4.052	0.220	0.085
304	4.195	0.214	0.095
293	4.273	0.292	0.125
283	4.409	0.348	0.154
270	4.706	0.436	0.208
260	5.030	0.538	0.267
243	5.354	0.684	0.349

Table 4.2

Parameters obtained from the least-squares fit of the e.p.r. linewidths of the complex $(\pi\text{-}C_5H_5)_2\ NbCl_2$ in chloroform solution as a function of m_I: all values are in units of gauss.

Temperature (K)	$\alpha + \alpha' + \alpha''$	β	γ
334	12.25	0.520	0.09
327	12.15	0.570	0.106
318	12.95	0.513	0.111
303	12.33	0.673	0.163
293	12.08	0.706	0.173
283	11.70	0.882	0.230
273	11.44	1.052	0.245
263	11.56	1.225	0.292

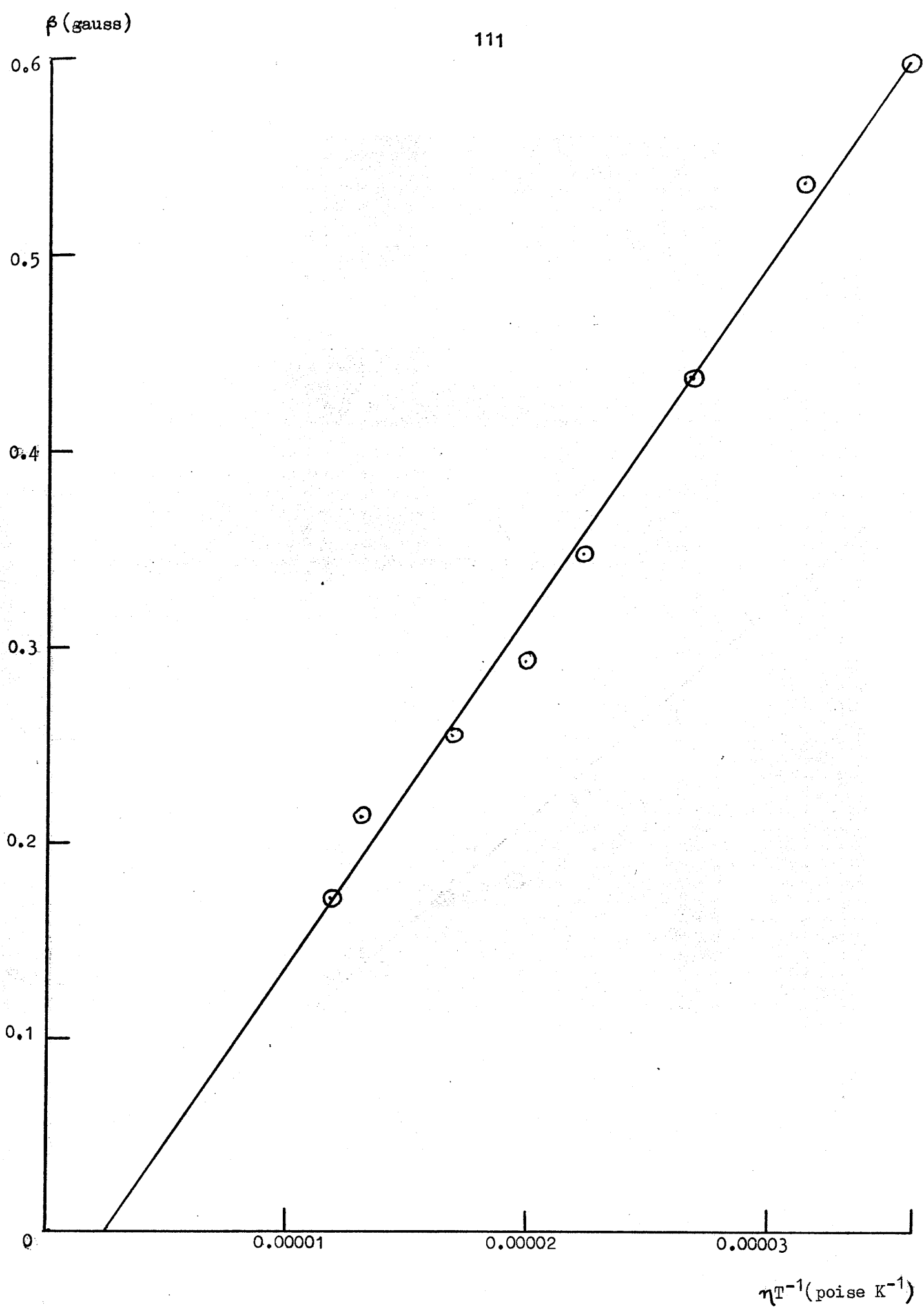

Figure 4.2 β(gauss) vs ηT^{-1} (poise K^{-1}) for $(\pi\text{-}C_5H_5)_2\ VCl_2$

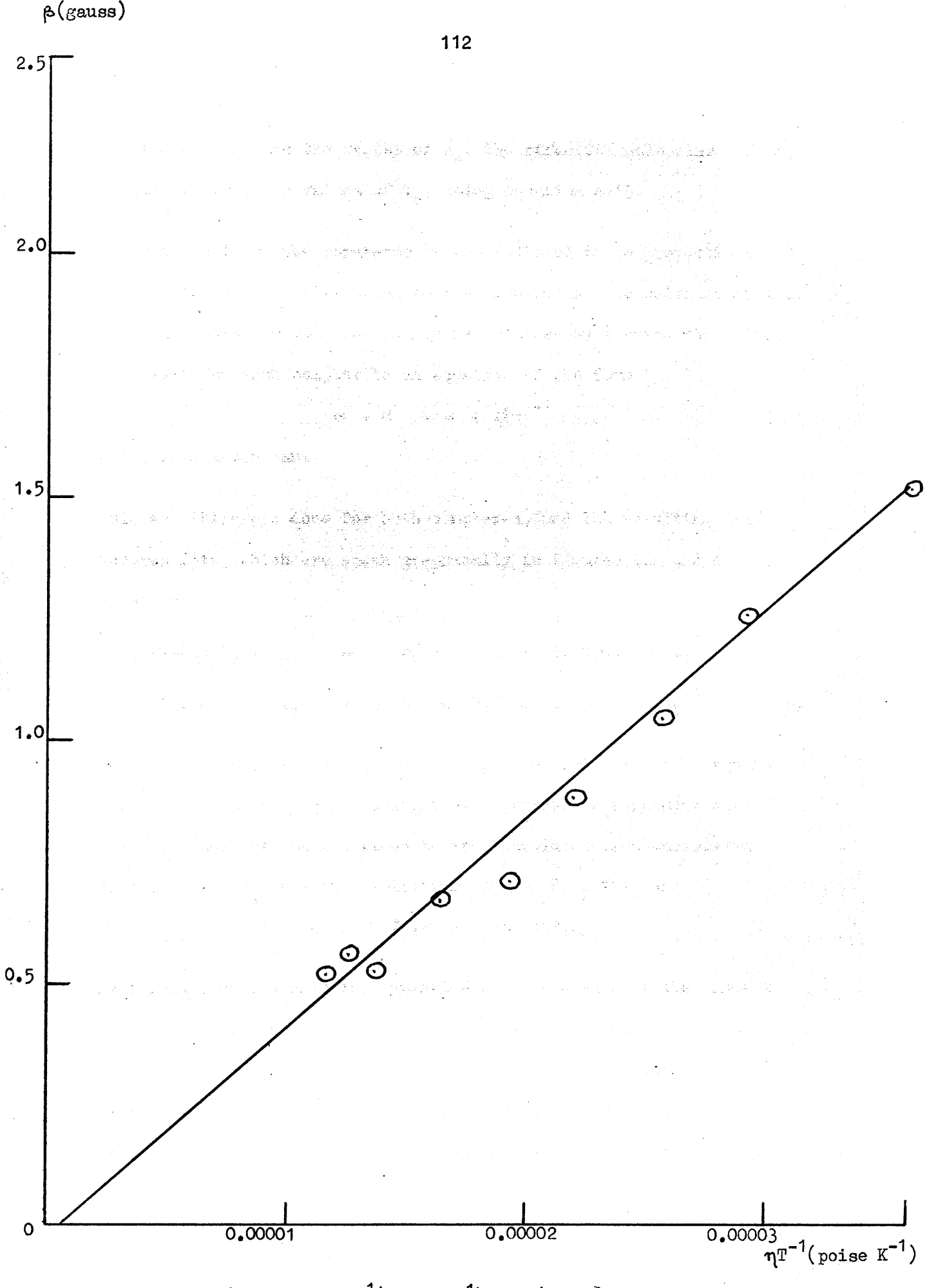

Figure 4.3 β(gauss) vs ηT^{-1}(poise K^{-1}) for $(\pi\text{-}C_5H_5)_2NbCl_2$

The values of $\alpha + \alpha'$, and τ_c obtained in this way are listed in tables 4.4 and 4.5, as are the values of a_o, the effective molecular radius, calculated from the values of τ_c, using equation 4.15.

As noted earlier, the parameter α' is predicted to be proportional to $T\eta^{-1}$, and so the contribution to the linewidths from chlorine nuclear hyperfine structure, α, can easily be obtained by fitting the values of $\alpha + \alpha'$ for each complex to an equation of the form

$$\alpha + \alpha' = \alpha + kT\eta^{-1} \qquad 4.17$$

where k is a constant.

This was therefore done for both complexes, and the resulting least-squares fits, which are shown graphically in figures 4.4 and 4.5 are given by

$$(\pi\text{-}C_5H_5)_2\ VCl_2 \qquad \alpha + \alpha' = 0.4 + 0.0000183\ T\eta^{-1}$$

$$(\pi\text{-}C_5H_5)_2\ NbCl_2 \qquad \alpha + \alpha' = 0.7 + 0.00008\ T\eta^{-1} \qquad 4.18$$

As can be seen from figures 4.4 and 4.5, the plots of $\alpha + \alpha'$ against $T\eta^{-1}$ are reasonably good straight line graphs, in agreement with theory. Thus the contributions to the linewidths from unresolved chlorine nuclear hyperfine splitting in $(\pi\text{-}C_5H_5)_2\ VCl_2$ and $(\pi\text{-}C_5H_5)_2\ NbCl_2$ is 0.4 and 0.7 gauss respectively.

As a result of the chlorine hyperfine coupling, each of the lines in the spectra of the chlorides consists of an unresolved 1 : 2 : 3 : 4 : 3 : 2 : 1 septet, and so to estimate the hyperfine coupling constant which would give rise to a particular contribution to the linewidths, use was made of a computer programme which plotted out the single curve arising from the superposition of seven peaks of this type. The spacing between the constituent peaks was simply varied until the width of the single

Table 4.3

Values of the viscosity (η), ηT^{-1} and $T\eta^{-1}$ for chloroform at various temperatures. Values of η are in units of poise, and were obtained by interpolation of values given in the International Critical Tables.[14]

Temperature (K)	η	ηT^{-1}	$T\eta^{-1}$
334	3.89×10^{-3}	1.16×10^{-5}	8.58×10^{4}
332	3.95×10^{-3}	1.19×10^{-5}	8.40×10^{4}
327	4.07×10^{-3}	1.25×10^{-5}	8.03×10^{4}
325	4.20×10^{-3}	1.29×10^{-5}	7.75×10^{4}
318	4.40×10^{-3}	1.38×10^{-5}	7.23×10^{4}
313	4.62×10^{-3}	1.47×10^{-5}	6.80×10^{4}
303	5.02×10^{-3}	1.65×10^{-5}	6.04×10^{4}
293	5.63×10^{-3}	1.92×10^{-5}	5.21×10^{4}
283	6.25×10^{-3}	2.21×10^{-5}	4.53×10^{4}
273	6.99×10^{-3}	2.56×10^{-5}	3.91×10^{4}
270	7.20×10^{-3}	2.67×10^{-5}	3.74×10^{4}
263	7.68×10^{-3}	2.92×10^{-5}	3.42×10^{4}
260	8.10×10^{-3}	3.12×10^{-5}	3.20×10^{4}
253	8.77×10^{-3}	3.46×10^{-5}	2.89×10^{4}

Table 4.4

Values of the residual linewidth ($\alpha + \alpha'$), in gauss, correlation time (τ_c) in seconds, and molecular radius (a_o) in angstroms for the complex $(\pi\text{-}C_5H_5)_2\ VCl_2$ at various temperatures.

Temperature (K)	$\alpha + \alpha'$	τ_c	a_o
332	1.89	8.1×10^{-12}	2.81
325	1.71	10.4×10^{-12}	2.96
313	1.66	10.7×10^{-12}	2.87
304	1.63	12.0×10^{-12}	2.85
291	1.36	15.1×10^{-12}	2.90
283	1.18	18.8×10^{-12}	3.02
270	1.06	24.9×10^{-12}	3.11
260	0.90	32.7×10^{-12}	3.20

Table 4.5

Values of the residual linewidth ($\alpha + \alpha'$) in gauss, correlation time (τ_c) in seconds, and molecular radius, (a_o) in angstroms, for the complex $(\pi\text{-}C_5H_5)_2\ NbCl_2$ at various temperatures.

Temperature (K)	$\alpha + \alpha'$	τ_c	a_o
334	7.24	1.06×10^{-11}	3.09
327	6.78	1.18×10^{-11}	3.14
318	7.97	1.05×10^{-11}	2.90
303	6.31	1.45×10^{-11}	3.05
293	5.87	1.53×10^{-11}	2.96
283	4.62	2.03×10^{-11}	3.10
273	3.65	2.53×10^{-11}	3.18
263	3.04	3.08×10^{-11}	3.25

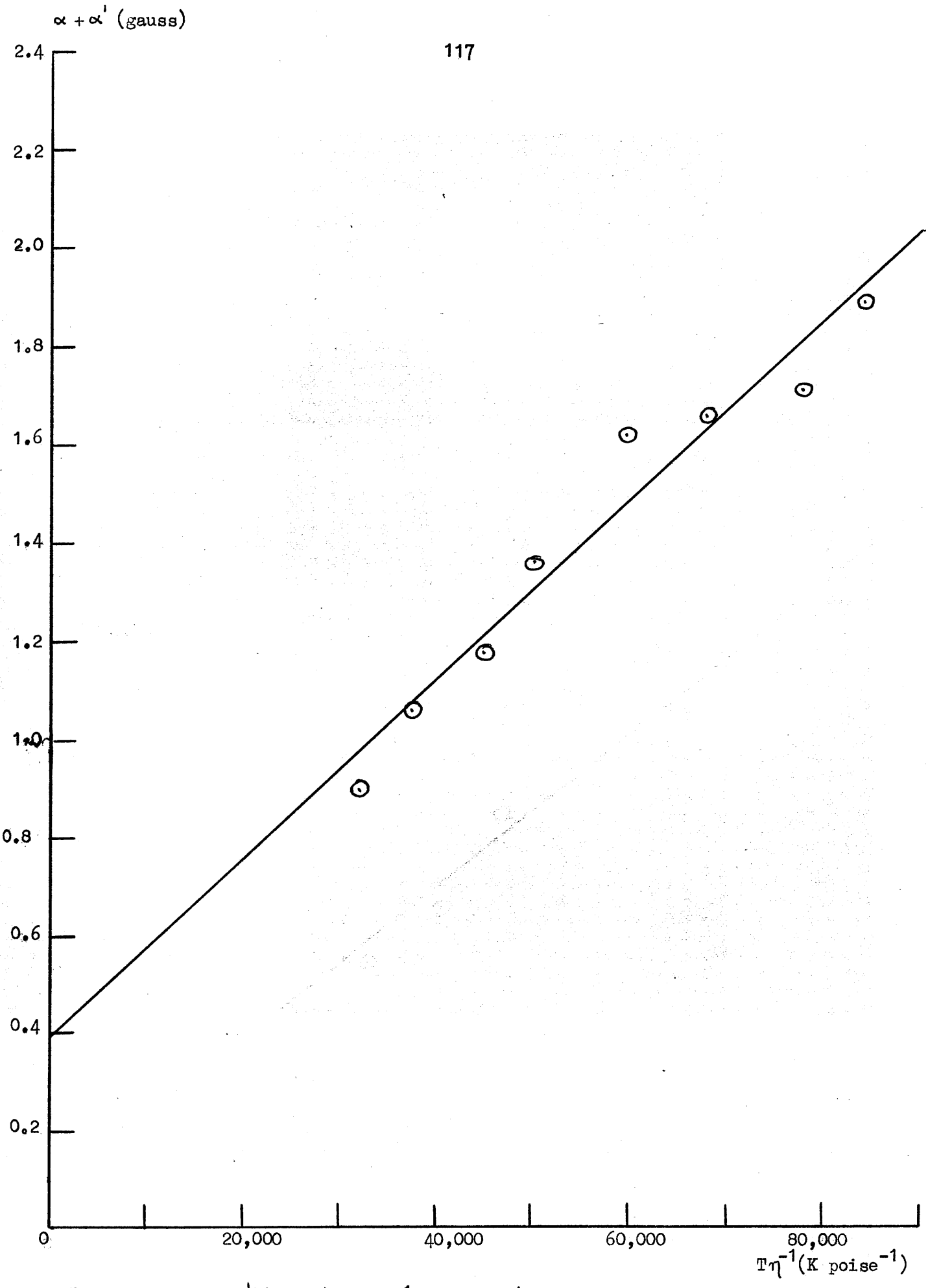

Figure 4.4 $\alpha + \alpha'$ (gauss) vs $T\eta^{-1}$(K poise $^{-1}$) for $(\pi\text{-}C_5H_5)_2\ VCl_2$

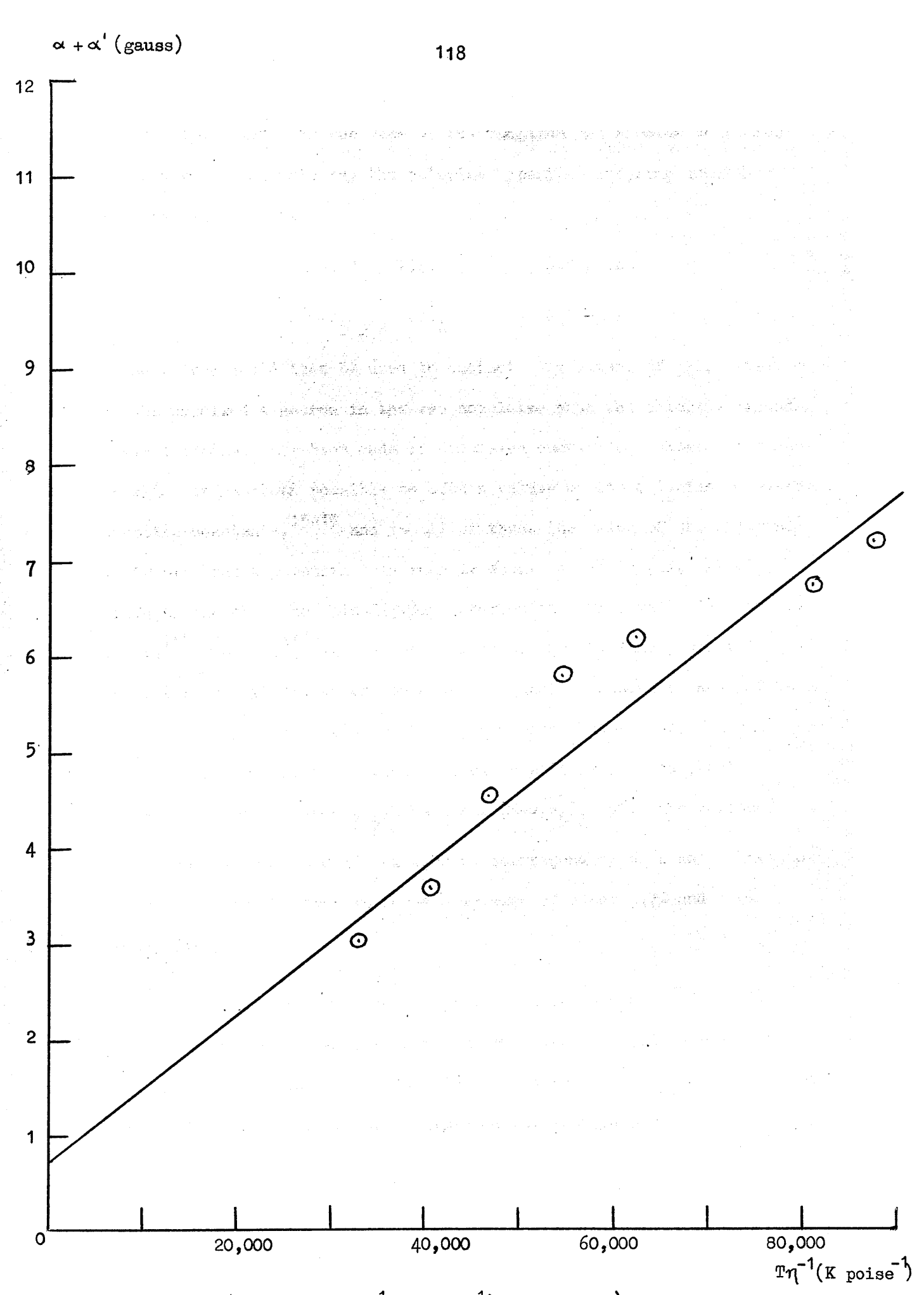

Figure 4.5 $\alpha + \alpha'$ (gauss) vs $T\eta^{-1}$(K poise^{-1}) for $(\pi\text{-}C_5H_5)_2$ $NbCl_2$

composite line was larger than that of the constituent lines by 0.4 gauss and 0.7 gauss in the case of the vanadium and niobium complexes respectively. In this way the chlorine hyperfine coupling constants were estimated to be

$(\pi\text{-}C_5H_5)_2\ VCl_2$	0.3 gauss
$(\pi\text{-}C_5H_5)_2\ NbCl_2$	0.6 gauss

These values could then be used to estimate the extent of delocalisation of the unpaired electron in the two complexes onto the chloride ligands. Several studies have been made of complexes containing chloride ligands in which it has been possible to obtain values of the chlorine anisotropic coupling constants,[15-19] and in all of these the value of the chlorine isotropic coupling constant is roughly equal to the largest principal value of the chlorine spin-dipolar interaction. This value is given by $\frac{4}{7} P \alpha_1^{I*2}$ where α_1^{I*2} is the coefficient of the chlorine p-orbital in the molecular orbital which contains the unpaired electron, and $\frac{4}{7} P$ is the largest principal value of the spin-diploar interaction for one electron in a chlorine p-orbital, which is estimated to be about 90 gauss. Thus, for $(\pi\text{-}C_5H_5)_2\ VCl_2$ and $(\pi\text{-}C_5H_5)_2\ NbCl_2$ the valuesof α_1^{I*2} must be about 0.0033 and 0.0066, corresponding to a delocalisation of the unpaired electron in these complexes of about 0.7% and 1.4% respectively.

Thus, to summarise, the values obtained from the analysis of the line-widths in both of these complexes confirm that the unpaired electrons are indeed localised on the metal ions, in agreement with the conclusions reached from the analysis of the spin Hamiltonian parameters described in the last chapter.

4.5 Results and Discussion for $(\pi\text{-}C_5H_5)_2$ Nb $(\sigma\text{-}C_5H_5)_2$

The results of the temperature dependence of the linewidths for this complex were analysed in exactly the same way as those of the dichlorides, and the results are presented in tables 4.6 to 4.8 and figures 4.6 and 4.7.

The least-squares fit of the data for β and $\alpha + \alpha'$ were of the form

$$\beta = 0.001 + 15{,}000\,\eta T^{-1}$$

$$\alpha + \alpha' = 0.9 + 0.00016\,T\eta^{-1} \qquad 4.19$$

From the results, it can be seen that the temperature dependence of the linewidths for the complex $(\pi\text{-}C_5H_5)_2$ Nb $(\sigma\text{-}C_5H_5)_2$ can be explained in terms of the usual relaxation mechanisms considered for the chlorides in the previous section, without the necessity for considering a dynamic equilibrium of the form

$$(\pi\text{-}C_5H_5)_2 \text{ Nb } (\sigma\text{-}C_5H_5)_2 \rightleftharpoons (\pi\text{-}C_5H_5)_3 \text{ Nb } (\sigma\text{-}C_5H_5)$$

It can be shown using a modified form of the Bloch equations that for an equilibrium between two paramagnetic species of the form

$$A \rightleftharpoons B$$

the observed value of T_2 is given by[20]

$$\frac{1}{T_2} = \frac{p_A}{T_{2A}} + \frac{p_B}{T_{2B}} \qquad 4.20$$

where p_A and p_B are the proportions of the species A and B in the mixture at equilibrium, and T_{2A} and T_{2B} are the transverse relaxation times for the separate species under conditions where no interconversion is taking place. Thus for a dynamic equilibrium of the type above the T_2 values would have a more complex temperature dependence than that which is involved in the usual broadening mechanisms.

Table 4.6

Parameters obtained from the least-squares fit of the e.p.r. linewidths of the complex $(\pi\text{-}C_5H_5)_2$ Nb $(\sigma\text{-}C_5H_5)_2$ in toluene solution as a function of m_I: all values are in units of gauss.

Temperature (k)	$\alpha + \alpha' + \alpha''$	β	γ
324	7.17	0.215	0.131
307	7.47	0.253	0.144
301	7.89	0.296	0.150
290	8.21	0.330	0.196
273	8.83	0.370	0.297
263	8.73	0.551	0.359

Table 4.7

Values of the viscosity (η), ηT^{-1} and $T\eta^{-1}$ for toluene at various temperatures. Values of η are in poise and were obtained by interpolation of values given in the International Critical Tables.[14]

Temperature (K)	η	ηT^{-1}	$T\eta^{-1}$
324	4.20×10^{-3}	1.30×10^{-5}	7.68×10^{4}
307	5.00×10^{-3}	1.63×10^{-5}	6.13×10^{4}
301	5.30×10^{-3}	1.76×10^{-5}	6.02×10^{4}
290	6.00×10^{-3}	2.07×10^{-5}	4.82×10^{4}
273	7.70×10^{-3}	2.82×10^{-5}	3.54×10^{4}
263	9.20×10^{-3}	3.50×10^{-5}	2.86×10^{4}

Table 4.8

Values of the residual linewidth ($\alpha + \alpha'$) in gauss, correlation time (τ_c) in seconds and molecular radius (a_o) in angstroms for the complex $(\pi\text{-}C_5H_5)_2$ Nb $(\sigma\text{-}C_5H_5)_2$ at various temperatures.

Temperature (K)	$\alpha + \alpha'$	τ_c	a_o
324	2.09	1.52×10^{-11}	3.36
307	1.78	1.94×10^{-11}	3.38
301	2.00	2.11×10^{-11}	3.39
290	1.82	2.55×10^{-11}	3.42
273	1.30	3.65×10^{-11}	3.47
263	0.06	4.68×10^{-11}	3.51

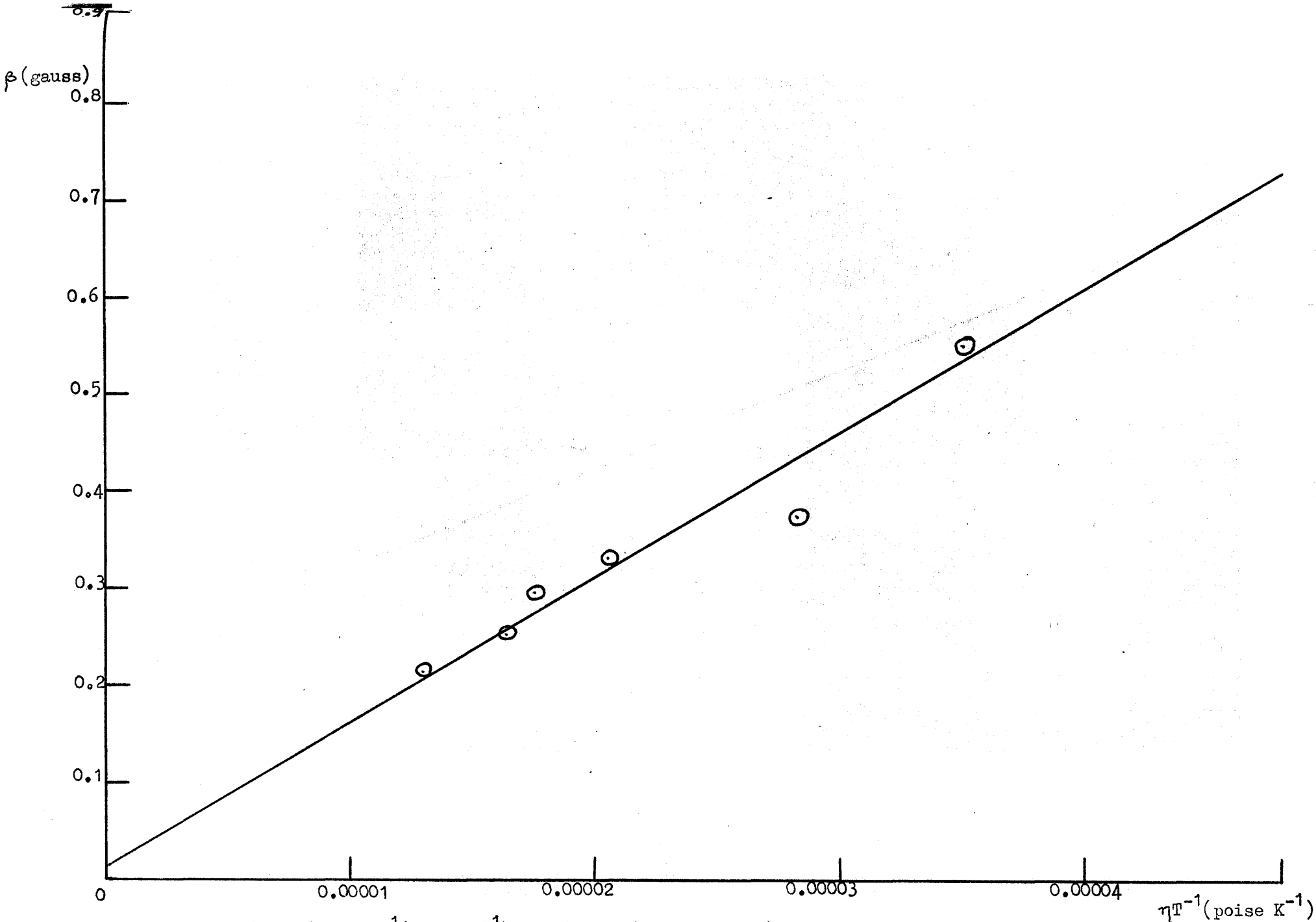

Figure 4.6 β (gauss) vs ηT^{-1} (poise K^{-1}) for $(\pi\text{-}C_5H_5)_2$ Nb $(\sigma\text{-}C_5H_5)_2$

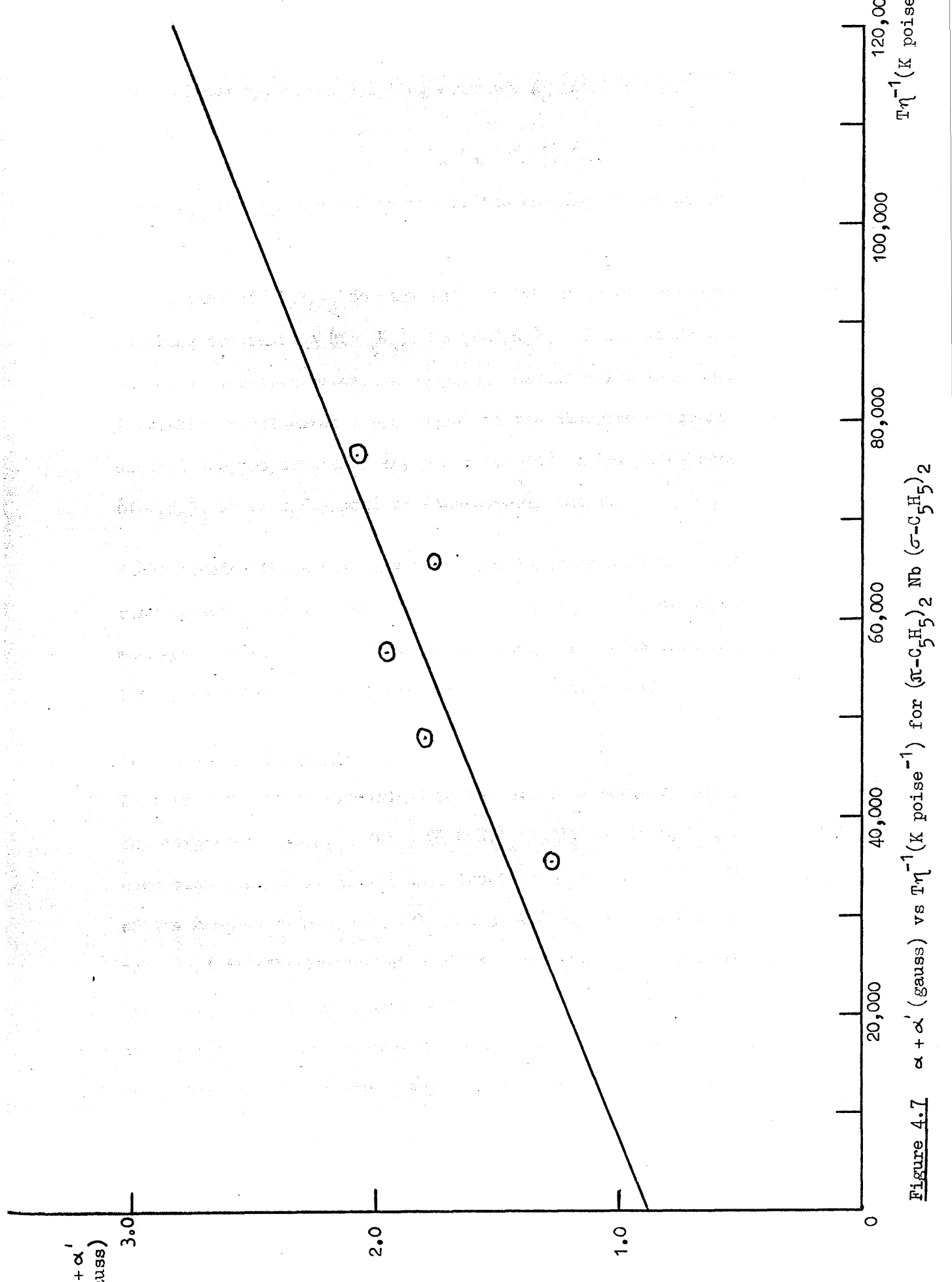

Figure 4.7 $\alpha + \alpha'$ (gauss) vs $T\eta^{-1}$(K poise^{-1}) for $(\pi\text{-}C_5H_5)_2$ Nb $(\sigma\text{-}C_5H_5)_2$

It can also be shown that for an equilibrium of this type, the observed value of any hyperfine coupling constant $\bar{A}_o$ is given by [20,21]

$$\bar{A}_o = p_A A_{oA} + p_B A_{oB} \qquad 4.21$$

where A_{oA} and A_{oB} are the values of the coupling constant in species A and B respectively.

In the case of $(C_5H_5)_4$ Nb the value of the niobium isotropic hyperfine coupling constant in $(\pi\text{-}C_5H_5)_2$ Nb $(\sigma\text{-}C_5H_5)_2$ calculated from the values of the anisotropic hyperfine coupling constants for this complex at 77K, is within experimental error, equal to the observed value in solution, so that the proportion of any other species in solution, such as $(\pi\text{-}C_5H_5)_3$ Nb $(\sigma\text{-}C_5H_5)$ must be immeasurably small.

These studies therefore show that if interconversion of the σ and π ring systems in this complex is taking place the amount of the intermediate species involved must be extremely small, so that the rate of interconversion is also likely to be very slow indeed.

4.6 Summary of Part IV

In this section the linewidths in the e.p.r. spectra of solutions of the complexes $(\pi\text{-}C_5H_5)_2$ VCl_2, $(\pi\text{-}C_5H_5)_2$ $NbCl_2$ and $(\pi\text{-}C_5H_5)_2$ Nb $(\sigma\text{-}C_5H_5)_2$ have been studied in detail as a function of temperature. In the case of the complexes $(\pi\text{-}C_5H_5)_2$ VCl_2 and $(\pi\text{-}C_5H_5)_2$ $NbCl_2$ these studies have been used to estimate the size of the proton and chlorine nuclear hyperfine coupling constants in these complexes, and hence to estimate the extent to which the unpaired electron in the complexes is delocalised on to the ligands. In this way it has been shown that the delocalisation of the unpaired electrons on to the cyclopentadienide groups in both compounds is negligibly small, and that they are delocalised on to the chloride ligands to the extent of about 0.7% and 1.4% in the vanadium and niobium complexes respectively.

In the case of the complex $(\pi\text{-}C_5H_5)_2$ Nb $(\sigma\text{-}C_5H_5)_2$ the studies show that the interconversion of the σ and π ring systems in this complex, if it occurs, is likely to be a very slow process, due to the low concentration of any intermediate which might be involved in the interconversion.

PART V

NUCLEAR QUADRUPOLE RESONANCE STUDIES OF SOME COMPLEXES OF NIOBIUM (V) WITH OXYGEN DONOR LIGANDS

5.1 Introduction

As noted earlier, nuclear quadrupole coupling constants obtained from pure n.q.r. spectroscopy can be used as very sensitive probes for transmitting information about the geometry of the molecules which contain the quadrupolar nuclei. This is because the size of the coupling constants depends mainly on the distribution of valence electrons about the nucleus, and this distribution in turn depends on the nature of the coordinating ligands, and on the geometry of the molecules.

Although compounds containing nitrogen and chlorine nuclei, for instance, have been extensively studied by n.q.r. methods,[1,2] the only compounds of niobium (V) which have been studied in this way are niobium pentachloride,[3] which is a dimer,[4] lithium and potassium niobate,[5,6] niobium pentafluoride,[7] which is tetrameric,[8] and some monomeric 1:1 adducts of NbF_5 with simple bases such as dimethyl ether and pyridine.[7]

It was therefore decided to study a selection of compounds of niobium (V) of various known structures in order to attempt to correlate the n.q.r. coupling constants of these complexes with their geometry. It was hoped that this correlation could be used to obtain information about other compounds of niobium (V) of unknown structure.

With one exception the complexes studied were penta-alkoxide derivatives of niobium (V) with the empirical formula $Nb(OR)_5$, where OR represents an alkoxide group. These have either one or other of two types of structure.

(a) Those complexes with R = methyl, ethyl or n-propyl have dimeric structures of the type shown in figure 5.1(a).

(b) Those complexes with R = isopropyl, phenyl or β-naphthyl are monomers, whose structures are as in figure 5.1(b).

The remaining complex, $Nb(OEt)_4$ Acac, where AcacH = acetylacetone, has the structure shown in figure 5.1(c).

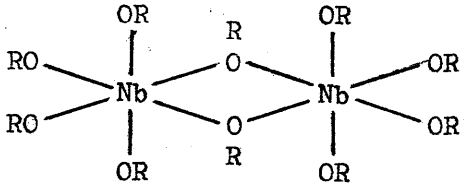

(a)

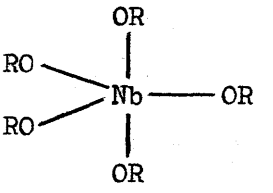

(b)

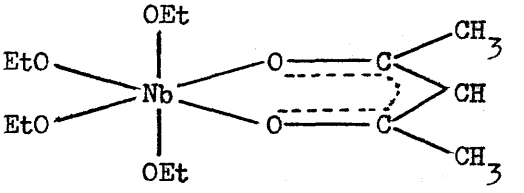

(c)

Figure 5.1

5.2 Experimental

The penta-alkoxide complexes $Nb(OR)_5$ with R = methyl, ethyl, n-propyl[9] and isopropyl[10] were all prepared by the same general method. Niobium pentachloride was allowed to react with an excess of the appropriate alcohol in benzene, giving the reaction 5.1 below.

$$Nb\,Cl_5 + 3ROH \longrightarrow Nb(OR)_3\,Cl_2 + 3HCl \qquad 5.1$$

The remaining chloride ligands were then replaced by treating the solution obtained in this way with an excess of dry ammonia gas, giving the reaction 5.2.

$$NbCl_2(OR)_3 + 2NH_3 + 2ROH \longrightarrow Nb(OR)_5 + 2NH_4Cl \qquad 5.2$$

The precipitated ammonium chloride was filtered off, and the solvent was removed under reduced pressure to give the crude products. These were then purified by distilling them under reduced pressure in the case of the methoxide, ethoxide and n-propoxide, or by vacuum sublimation, in the case of the isopropoxide. The ethoxide and n-propoxide complexes are viscous oils at room temperature, while the methoxide and isopropoxide are white solids. Since all of these compounds are extremely rapidly hydrolysed in moist air, all the above procedures were carried out either on a vacuum line or in an atmosphere of dry nitrogen, and solvents were dried and degassed before use.

Niobium penta-phenoxide was prepared[11] by allowing niobium pentachloride to react with a stoichiometric amount of molten phenol. The product was obtained by extracting the cold melt with carbon tetrachloride and recrystallising the crude product from the same solvent. The product is an orange crystalline solid, which is fairly stable in the presence of moist air.

Niobium penta-β-naphthoxide was prepared by refluxing a stoichiometric mixture of niobium pentachloride and β-naphthol in carbon tetrachloride[11] for four hours, allowing the mixture to cool, and filtering off the precipitated product, which is an orange-brown crystalline solid, which is completely unaffected by atmospheric moisture.

The complex $Nb(OEt)_4$ Acac was prepared by allowing niobium pentaethoxide to react with acetylacetone in benzene solution.[12] The mixture was refluxed for about eight hours, during which time the ethanol liberated in the reaction

$$Nb(OEt)_5 + AcacH \rightleftharpoons Nb(OEt)_4\,Acac + EtOH \qquad 5.3$$

was azeotroped out of the mixture, the azeotrope being collected at 68-80°C. At the end of the eight hours, the excess solvent was

removed under reduced pressure to give an orange-yellow liquid. This liquid was distilled to give, on cooling, an orange-yellow low-melting solid which was very rapidly hydrolysed in moist air.

The n.q.r. spectra of each of the complexes were recorded over the frequency range 5.5 to 17 MHZ, both at room temperature and at 77K. The recording of the spectra was hindered by the presence of two 'dead spots' on the spectrometer, one from about 5.5 to 6.2 MHZ, and the other from about 9.7 to 10.3 MHZ. At these frequencies the spectrometer produced spurious signals whether there was a sample in the coil of the oscillator or not, and also the oscillator ceased to function at all at certain points in these frequency ranges.

The spectra of niobium penta-ethoxide and niobium penta-n-propoxide were not recorded at room temperature since at that temperature both compounds are oils.

5.3 Analysis of the N.Q.R. Spectra

As shown in appendix A, the Hamiltonian for the quadrupolar interaction can be written as[13]

$$\mathcal{H}_Q = \frac{eQq}{4I(2I-1)} \left((3I_z^2 - \underline{I}^2) + \eta (I_x^2 - I_y^2)\right) \qquad 5.4$$

where η, the asymmetry parameter, is given by

$$\eta = \frac{V_{xx} - V_{yy}}{q} \qquad 5.5$$

q, V_{xx} and V_{yy} are the principal axis values of the electric field gradient at the quadrupolar nucleus and, by convention

$|V_{xx}| < |V_{yy}| < |q|$, so that $1 \geq \eta \geq 0$

The eigenfunctions and eigenvalues of the Hamiltonian 5.4 can be obtained by assuming the allowed functions to be linear combinations

of the basis set of nuclear spin functions $|m_I\rangle$, and applying the variation principle in the usual way. The resulting secular determinant for nuclei with half-integral values of I can be factorised into two identical determinants of degree $I + \frac{1}{2}$. For the ^{93}Nb nucleus, with $I = {}^9/_2$, these determinants can be multiplied out to give

$$E^5 - 11(3 + \eta^2)\,E^3 - 44(1 - \eta^2)\,E^2 + \frac{44}{3}(3 + \eta^2)\,E + 48(3 + \eta^2)(1 - \eta^2) = 0 \qquad 5.6$$

where E is in units of $\dfrac{3\,eQq}{2I(2I - 1)}$

Equation 5.6 can not be solved to give analytical expressions for the eigenvalues and transition energies, but it has been solved numerically[14] for various chosen values of η. The separation of the secular determinant into two identical determinants leads to the energy levels being doubly degenerate, with the $|+m_I\rangle$ and $|-m_I\rangle$ states having the same energy. Thus for the ^{93}Nb nucleus with $I = {}^9/_2$ there are four observed $\Delta m_I = \pm 1$ transitions, and it is found that the frequencies of the $|\pm {}^9/_2\rangle \leftrightarrow |\pm {}^7/_2\rangle$, $|\pm {}^7/_2\rangle \leftrightarrow |\pm {}^5/_2\rangle$, $|\pm {}^5/_2\rangle \leftrightarrow |\pm {}^3/_2\rangle$ and $|\pm {}^3/_2\rangle \leftrightarrow |\pm {}^1/_2\rangle$ transitions are roughly in the ratio of 4 : 3 : 2 : 1.

The energies of the $|\pm {}^9/_2\rangle$, $|\pm {}^7/_2\rangle$ and $|\pm {}^5/_2\rangle$ states given in reference 14, together with the energies of the $|\pm {}^9/_2\rangle \leftrightarrow |\pm {}^7/_2\rangle$ and $|\pm {}^7/_2\rangle \leftrightarrow |\pm {}^5/_2\rangle$ transitions are reproduced in table 5.1.

For a given set of observed frequencies, the value of η can most easily be obtained from the ratio of the $|\pm {}^9/_2\rangle \leftrightarrow |\pm {}^7/_2\rangle$ and $|\pm {}^7/_2\rangle \leftrightarrow |\pm {}^5/_2\rangle$ transition frequencies. This ratio is plotted as a function of η in figure 5.2. Knowing the value of η, the value of eQq can then be calculated using the data given in table 5.1.

Table 5.1

Eigenvalues and transition energies derived from the quadrupolar Hamiltonian 5.4 for various values of η. All values are in units of 3 eQq / 2I(2I-1). Data is reproduced from reference 14.

η	$E\|\pm\frac{9}{2}\rangle$	$E\|\pm\frac{7}{2}\rangle$	$E\|\pm\frac{5}{2}\rangle$	$\Delta E_1(\|\pm\frac{9}{2}\rangle \leftrightarrow \|\pm\frac{7}{2}\rangle)$	$\Delta E_2(\|\pm\frac{7}{2}\rangle \leftrightarrow \|\pm\frac{5}{2}\rangle)$	Ratio $\Delta E_1 / \Delta E_2$
0.1	6.00143	2.00467	-0.98972	3.99676	2.99439	1.3347
0.2	6.00572	2.01870	-0.95847	3.98702	2.97717	1.3392
0.3	6.01289	2.04218	-0.90522	3.97071	2.94740	1.3472
0.4	6.02297	2.07524	-0.82908	3.94773	2.90432	1.3593
0.5	6.03598	2.11809	-0.73017	3.91789	2.84826	1.3755
0.6	6.05199	2.17102	-0.61026	3.88097	2.78130	1.3954
0.7	6.07105	2.23440	-0.47275	3.83665	2.70715	1.4172
0.8	6.09323	2.30867	-0.32209	3.7846	2.63076	1.4386

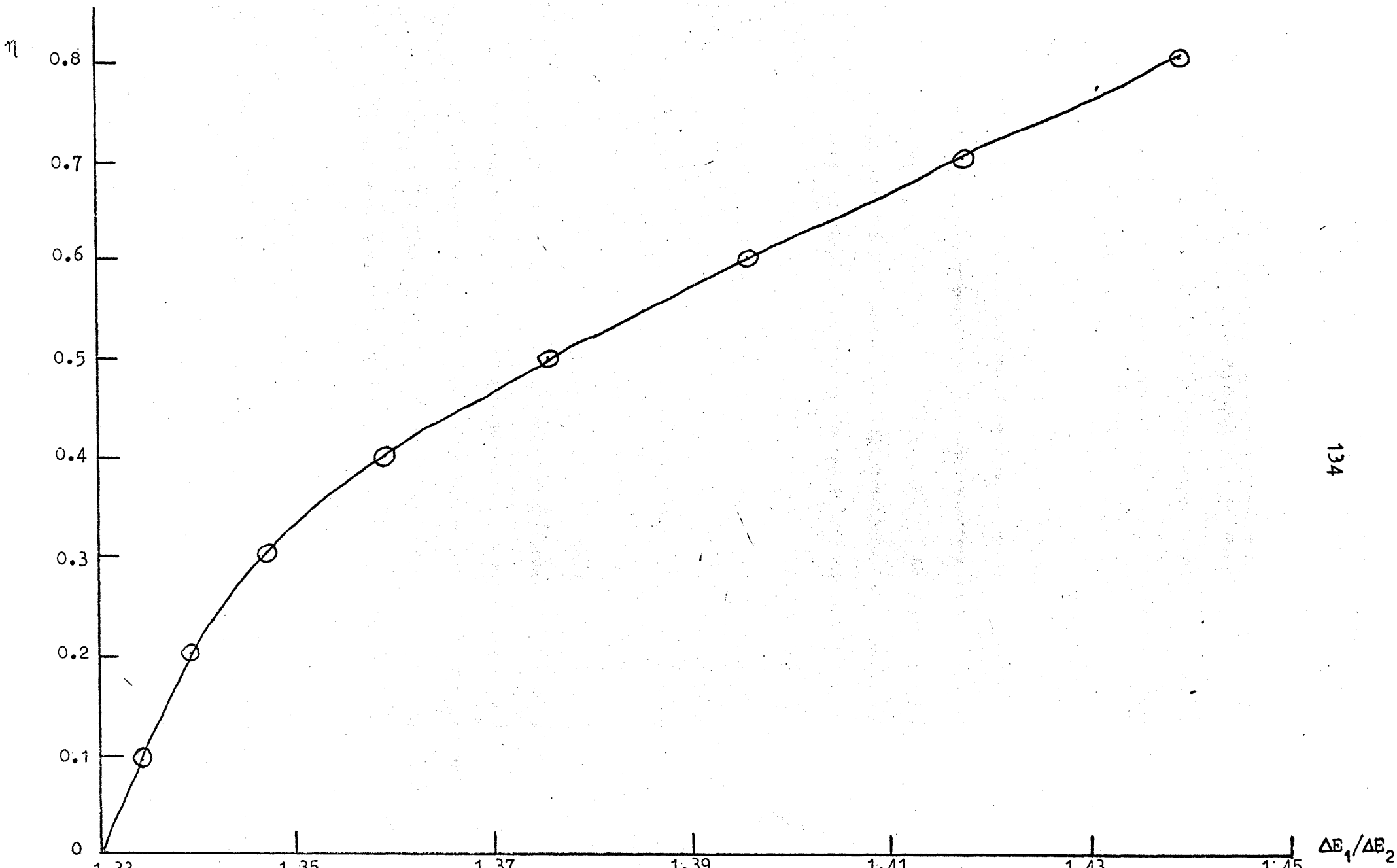

Figure 5.2 Ratio of the frequencies $\Delta E_1 \left(|\pm\frac{9}{2}\rangle \leftrightarrow |\pm\frac{7}{2}\rangle\right) : \Delta E_2 \left(|\pm\frac{7}{2}\rangle \leftrightarrow |\pm\frac{5}{2}\rangle\right)$ vs asymmetry parameter η

5.4 Results and Discussion

^{93}Nb n.q.r. signals were observed only in the case of the complexes $Nb(OMe)_5$ and $Nb(OEt)_4$ Acac at room temperature. No signals were obtained from any of the other complexes at room temperature, and no signals were obtained from any of the complexes studied at 77K.

Since niobium penta-ethoxide and niobium penta-n—propoxide exist as oils at room temperature and form glasses at 77K, it was not expected that any n.q.r. signals would be obtained from these complexes. This is because in solutions or glasses different quadrupolar nuclei experience different electric field gradients due to the random ordering of the surrounding molecules in the sample. As a result the n.q.r. signals become very broad, and can not be detected.

The absence of n.q.r. signals in the spectra of the monomeric alkoxides could be due to the presence of impurities or defects in the crystals of these complexes. These effects lead to regions of disorder in the crystal lattice and hence cause line broadening in the same way as in solutions or glasses. Alternatively it is possible that the signals lie outside the operating range of the spectrometer. In the case of antimony pentachloride, which can exist as a monomer or as a dimer, it is known that the ^{121}Sb and ^{123}Sb n.q.r. signals in the monomer occur at half the frequency of the corresponding signals in the dimer.[15] If this were also the case for the alkoxides studied here, the highest frequency signal in the monomers would occur at around 6 MHZ, and so would be undetectable on the instrument used in this work.

The n.q.r. signals observed for the complexes $Nb(OMe)_5$ and $Nb(OEt)_4$ Acac are shown in figure 5.3. Because of the low values of the quadrupole coupling constants, e^2qQ, in these complexes, only the two highest frequency transitions fall within the operating region of the spectrometer.

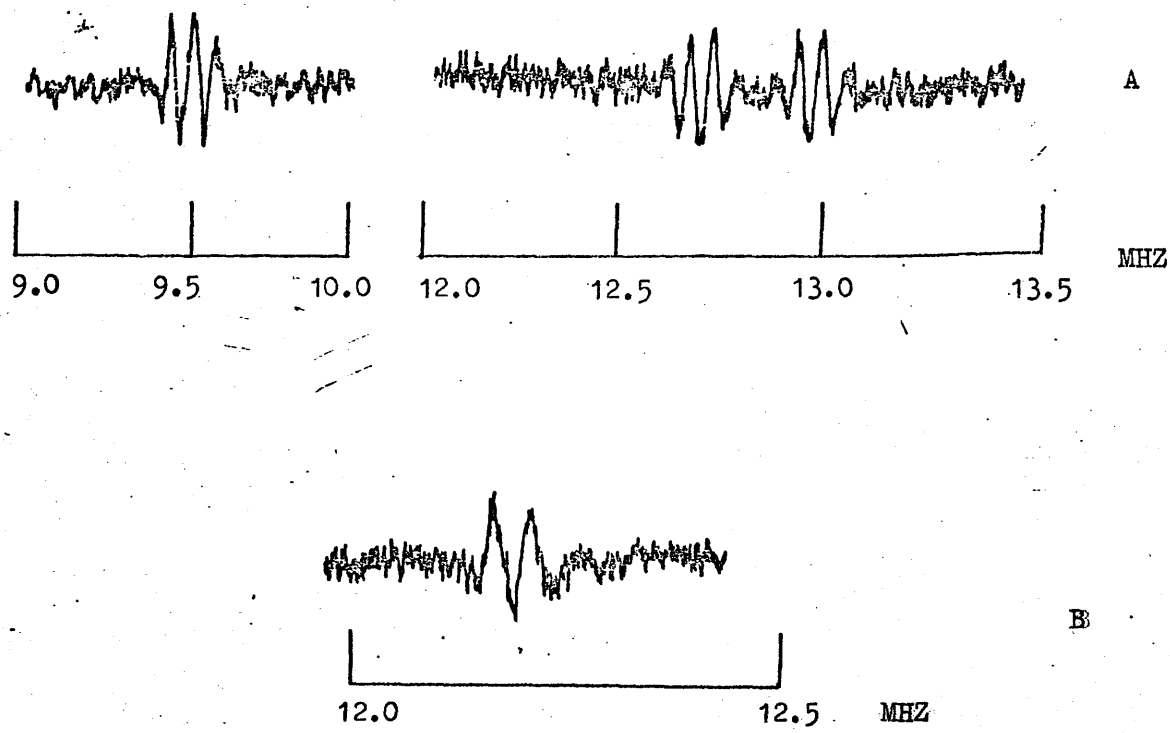

Figure 5.3 N.q.r. spectra at 298K of the complexes $Nb(OMe)_5$, A, and $Nb(OEt)_4$ Acac, B.

Thus the four signals above 12.5 MHZ, in the spectrum of $Nb(OMe)_5$ can all be assigned as $|\pm 9/2> \leftrightarrow |\pm 7/2>$ transitions, the fact that there are four such signals being due to the existence of four slightly different sites in the crystal lattice of this complex. The fact that only two $|\pm 7/2> \leftrightarrow |\pm 5/2>$ transitions are observed is probably because some of the signals are no longer resolved in this region.

The presence of two signals at just over 12 MHZ in the spectrum of $Nb(OEt)_4$ Acac would suggest that another signal should be detectable at about 9 MHZ, but despite repeated examination of this region of the spectrum this signal was not found, possibly due to the decreased sensitivity of the spectrometer in this frequency range.

The frequencies of the signals observed for the two complexes are listed in table 5.2, together with the values of eQq and η calculated from these frequencies. Since only one signal was detected in the spectrum of $Nb(OEt)_4$ Acac, the range of values of eQq given are those obtained if η is assumed to lie within the range 0 to 0.4. The resonant frequencies and quadrupole coupling constants for $NbCl_5$, given in reference 3, are also reproduced in table 5.2.

The object of this study was to show that complexes which contain niobium ions in similar environments have characteristic ^{93}Nb quadrupole coupling constants and it is now possible to show that this is, in fact, the case.

The environments of the niobium ions in the complexes $Nb(OMe)_5$, $Nb(OEt)_4$ Acac and $NbCl_5$ can all be represented by the same general structure, which is shown in figure 5.4 below.

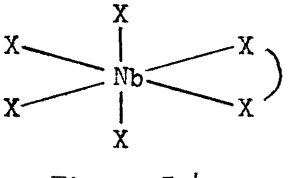

Figure 5.4

Table 5.2

^{93}Nb n.q.r. frequencies, eQq and η values for niobium-containing complexes.

The frequencies, and eQq values are in units of MHZ. Limits of error, observed frequencies $\pm$ 0.005 MHZ, eQq $\pm$ 0.04 MHZ.

Complex	Transition Frequencies $\left\|\pm\frac{9}{2}\right\rangle \leftrightarrow \left\|\pm\frac{7}{2}\right\rangle$	Transition Frequencies $\left\|\pm\frac{7}{2}\right\rangle \leftrightarrow \left\|\pm\frac{5}{2}\right\rangle$	eQq	η
$NbCl_5$	12.9	9.56	78.08	0.33
$Nb(OMe)_5$ (a)	12.6, 12.675	9.45	76.01	0.17
(b)	12.9, 12.975	9.525	78.56	0.39
$Nb(OEt)_4$ Acac	12.14, 12.195	-	73.02-74.02	0-0.4

It can be seen from the results in table 5.2 that these complexes do, in fact, have similar values of eQq and, to a lesser extent, of η. The values of eQq and η for these complexes are, moreover, significantly different from those of, for instance, the related group of compounds $NbF_5\ OMe_2$, NbF_5 Py and $NbF_5\ CH_2\ ClCN$, which have eQq values in the range 90-100 MHZ, and η values of about zero.[7] It would therefore be possible to differentiate between complexes of these two types on the basis of their n.q.r. coupling constants.

It should be possible to extend this work to obtain the characteristic ^{93}Nb n.q.r. coupling constants for other sets of related complexes, and hence to use this method to obtain information about the geometry of niobium-containing complexes of unknown structure.

5.5 Summary of Part V

The ^{93}Nb n.q.r. spectra of several complexes of niobium (V) with oxygen donor ligands have been recorded at room temperature and at 77K, and signals have been detected in two of these compounds, niobium penta-methoxide, $Nb(OMe)_5$, and niobium tetra-ethoxide acetylacetonate, $Nb(OEt)_4$ Acac.

It has been shown that the complexes $Nb(OMe)_5$, $Nb(OEt)_4$ Acac and $NbCl_5$ which are structurally related, have very similar ^{93}Nb n.q.r. coupling constants, and that it is possible to differentiate between complexes of this type and complexes of different structural types on the basis of their n.q.r. coupling constants.

The study suggests that it should be possible to use the characteristic ^{93}Nb n.q.r. coupling constants for complexes of known structures to obtain information about the geometry of niobium-containing complexes whose structures are not known.

APPENDIX A

THE SPIN HAMILTONIAN

The spin Hamiltonian is an artificial but useful concept which was first introduced by Abragam and Pryce.[1] For the systems discussed in this work, the form of this can be developed as follows.

(a) The Zeeman Interaction[2,3]

Kramer's theorem[4] states that in the absence of an applied magnetic field, the ground state of a molecule with one unpaired electron is a spin doublet.

Let the ground state wavefunctions in the absence of spin-orbit coupling $\phi_o\alpha$ and $\phi_o\beta$, be real wavefunctions with no orbital magnetic moment. Spin orbit coupling reinstates a small amount of orbital paramagnetism by mixing in of excited states $\phi_n\alpha$ and $\phi_n\beta$ into the ground state wavefunctions. The spin-orbit coupling Hamiltonian has the form

$$\mathcal{H}_{LS} = \xi\, \underline{L}.\underline{S} = \xi(L_zS_z + L_xS_x + L_yS_y) \qquad \text{A1}$$

where ξ is the spin-orbit coupling constant. First order perturbation theory yields the following form for the new ground state wavefunctions, which are still degenerate.

$$|+\rangle = |\phi_o\alpha\rangle - \frac{1}{2}\xi \sum_n \frac{\langle\phi_n|L_z|\phi_o\rangle}{E_n - E_o}|\phi_n\alpha\rangle - \frac{1}{2}\xi\sum_n \frac{\langle\phi_n|L_x + iL_y|\phi_o\rangle}{E_n - E_o}|\phi_n\beta\rangle$$

$$|-\rangle = |\phi_o\beta\rangle + \frac{1}{2}\xi \sum_n \frac{\langle\phi_n|L_z|\phi_o\rangle}{E_n - E_o}|\phi_n\beta\rangle - \frac{1}{2}\xi\sum_n \frac{\langle\phi_n|L_x - iL_y|\phi_o\rangle}{E_n - E_o}|\phi_n\alpha\rangle \qquad \text{A2}$$

If the molecule is in an applied magnetic field, the true form of the Zeeman Hamiltonian is

$$\mathcal{H}_z = \beta_e \underline{H}.(g_e \underline{S} + \underline{L})$$

$$= \beta_e H_z(g_e S_z + L_z) + \beta_e H_y(g_e S_y + L_y) + \beta_e H_x(g_e S_x + L_x) \qquad A3$$

where g_e, the spin-only g-factor, equals 2.0023.

The matrix elements of this Hamiltonian are thus

$$\langle + | \mathcal{H}_z | + \rangle = \beta_e(\langle + | g_e S_z + L_z | + \rangle H_z + \langle + | g_e S_y + L_y | + \rangle H_y + \langle + | g_e S_x + L_x | + \rangle H_x)$$

$$\langle + | \mathcal{H}_z | - \rangle = \beta_e(\langle + | g_e S_z + L_z | - \rangle H_z + \langle + | g_e S_y + L_y | - \rangle H_y + \langle + | g_e S_x + L_x | - \rangle H_x)$$

$$\langle - | \mathcal{H}_z | + \rangle = \beta_e(\langle - | g_e S_z + L_z | + \rangle H_z + \langle - | g_e S_y + L_y | + \rangle H_y + \langle - | g_e S_x + L_x | + \rangle H_x)$$

$$\langle - | \mathcal{H}_z | - \rangle = \beta_e(\langle - | g_e S_z + L_z | - \rangle H_z + \langle - | g_e S_y + L_y | - \rangle H_y + \langle - | g_e S_x + L_x | - \rangle H_x)$$

A4

The following relationships hold between the above matrix elements

1. $$\langle + | g_e S_j + L_j | + \rangle = - \langle - | g_e S_j + L_j | - \rangle \qquad A5$$

This can be shown by evaluation and comparison of these matrix elements.

2. $$\langle + | g_e S_j + L_j | - \rangle = \langle - | g_e S_j + L_j | + \rangle^* \qquad A6$$

This follows from the Hermitean property of angular momentum operators.

The following substitutions can now be made

$$\langle + | g_e S_j + L_j | + \rangle = - \langle - | g_e S_j + L_j | - \rangle = \tfrac{1}{2} g_{jz}$$

$$\langle - | g_e S_j + L_j | + \rangle = \langle + | g_e S_j + L_j | - \rangle^* = \tfrac{1}{2}(g_{jx} + i g_{jy}) \qquad A7$$

The form of the substitution is determined by the fact that diagonal matrix elements represent the expectation value of a real variable and so must be real, whereas off diagonal matrix elements may be imaginary.

The matrix elements thus become

$$\langle + |\mathcal{H}_z| + \rangle = \tfrac{1}{2} g_{zz}\beta_e H_z + \tfrac{1}{2} g_{yz}\beta_e H_y + \tfrac{1}{2} g_{xz}\beta_e H_x$$

$$\langle + |\mathcal{H}_z| - \rangle = \tfrac{1}{2}(g_{zx} - ig_{zy})\beta_e H_z + \tfrac{1}{2}(g_{yx} - ig_{yy})\beta_e H_y + \tfrac{1}{2}(g_{xx} - ig_{xy})\beta_e H_x$$

$$\langle - |\mathcal{H}_z| + \rangle = \tfrac{1}{2}(g_{zx} + ig_{zy})\beta_e H_z + \tfrac{1}{2}(g_{yx} + ig_{yy})\beta_e H_y + \tfrac{1}{2}(g_{xx} + ig_{xy})\beta_e H_x$$

$$\langle - |\mathcal{H}_z| - \rangle = -\tfrac{1}{2} g_{zz}\beta_e H_z - \tfrac{1}{2} g_{yz}\beta_e H_y - \tfrac{1}{2} g_{xz}\beta_e H_x \qquad \text{A8}$$

The matrix elements are exactly the same as those which would be obtained by defining a fictitious spin operator S which would act on the states $|+\rangle$ and $|-\rangle$ in the same way as the true spin operator acts on the α and β states, and by using a Hamiltonian of the form

$$\mathcal{H} = \beta_e \underline{H} \cdot g \cdot \underline{S} \qquad \text{A9}$$

where g is a second rank tensor.

Thus it is possible to obtain expressions for the Zeeman energy of the system by considering the starting states to be pure spin states and by using a Hamiltonian containing only spin operators, hence the spin Hamiltonian.

By comparing the elements of the spin Hamiltonian with those of the true Hamiltonian, it can be shown that in general

$$g_{ij} = g_e \delta_{ij} - 2\xi \sum_n \frac{\langle \phi_o | L_i | \phi_n \rangle \langle \phi_n | L_j | \phi_o \rangle}{E_n - E_o} \qquad \text{A10}$$

It follows from the Hermitean properties of the angular momentum operator that $g_{ij} = g_{ji}$ ie the g-tensor is symmetric.

(b) The Magnetic Hyperfine Interaction[2]

As noted earlier, there are three contributions to this interaction.

1. The contact interaction of the form

$$\mathcal{H}_c = \frac{8\pi}{3} g_e g_N \beta_e \beta_N \delta(r)\, \underline{I} \cdot \underline{S} \qquad \text{A11}$$

where $\delta(r)$ is the Dirac delta function which, integrated over the electronic wave function, gives the square of the value of the wave-function at the nucleus.

2. The spin-dipolar interaction between the nuclear magnetic moment and the spin magnetic moment of the electron

$$\mathcal{H}_{SI} = - g_e g_N \beta_e \beta_N \; (r^2\, \underline{S}.\underline{I} - 3(\underline{S}.\underline{r})(\underline{r}.\underline{I})\;)\; r^{-5} \qquad \text{A12}$$

where $\underline{r}$ is the radius vector between the electron and the nucleus. This can be expanded to give

$$\begin{aligned}\mathcal{H}_{SI} = r^{-3} P' \; (&S_z I_z(3\cos^2\theta - 1) + S_x I_x(3\sin^2\theta\cos^2\phi - 1) + S_y I_y(3\sin^2\theta\sin^2\phi - 1) \\ &+ 3S_x I_y \sin^2\theta \sin\phi\cos\phi + 3I_z S_x \cos\theta \sin\theta\cos\phi + 3S_y I_x \sin^2\theta \sin\phi\cos\phi \\ &+ 3S_z I_x \sin\theta\cos\theta\cos\phi + 3S_y I_z \sin\theta\cos\theta\sin\phi + 3S_z I_y \sin\theta\cos\theta\sin\phi)\end{aligned} \qquad \text{A13}$$

where $P' = g_e g_N \beta_e \beta_N$

3. The orbital-dipolar interaction between the nuclear magnetic moment and the electron's orbital moment

$$\mathcal{H}_{LI} = 2 g_N \beta_e \beta_N r^{-3}\, \underline{L} \cdot \underline{I} \qquad \text{A14}$$

These contributions can be combined to produce an expression for the total hyperfine energy of the form

$$\mathcal{H} = A_x I_x + A_y I_y + A_z I_z \qquad \text{A15}$$

where

$$A_x = r^{-3} P' \left(\frac{8\pi}{3} \delta(r) r^3 S_x + (3\cos^2\phi \sin^2\theta - 1) S_x + 3 \sin^2\theta \sin\phi \cos\phi S_y \right.$$
$$\left. + 3 \sin\theta \cos\theta \cos\phi S_z + L_x \right)$$

$$A_y = r^{-3} P' \left(\frac{8\pi}{3} \delta(r) r^3 S_y + (3\cos^2\theta \sin^2\phi - 1) S_y + 3 \sin^2\theta \sin\phi \cos\phi S_x \right.$$
$$\left. + 3 \sin\theta \cos\theta \sin\phi S_z + L_y \right)$$

$$A_z = r^{-3} P' \left(\frac{8\pi}{3} \delta(r) r^3 S_z + (3\cos^2\theta - 1) S_z + 3 \cos\theta \sin\theta \cos\phi S_x \right.$$
$$\left. + 3 \sin\theta \cos\theta \sin\phi S_y + L_z \right)$$

Note the similarity between the Hamiltonians in equations A15 and A3. The matrix elements of the hyperfine Hamiltonian can now be written down. Since the Hamiltonian now contains nuclear spin operators, the basis orbitals are now of the form $|+, m_I\rangle$ and $|-, m_I\rangle$. The matrix elements thus have the form

$$\langle +,m_I|\mathcal{H}|+,m_I'\rangle = \langle +,m_I|A_xI_x|+,m_I'\rangle + \langle +,m_I|A_yI_y|+,m_I'\rangle + \langle +,m_I|A_zI_z|+,m_I'\rangle$$

$$\langle +,m_I|\mathcal{H}|-,m_I'\rangle = \langle +,m_I|A_xI_x|-,m_I'\rangle + \langle +,m_I|A_yI_y|-,m_I'\rangle + \langle +,m_I|A_zI_z|-,m_I'\rangle$$

$$\langle -,m_I|\mathcal{H}|+,m_I'\rangle = \langle -,m_I|A_xI_x|+,m_I'\rangle + \langle -,m_I|A_yI_y|+,m_I'\rangle + \langle -,m_I|A_zI_z|+,m_I'\rangle$$

$$\langle -,m_I|\mathcal{H}|-,m_I'\rangle = \langle -,m_I|A_xI_x|-,m_I'\rangle + \langle -,m_I|A_yI_y|-,m_I'\rangle + \langle -,m_I|A_zI_z|-,m_I'\rangle$$

A17

The following substitutions can now be made, similar to those in equation A7.

$$\langle +,m_I|A_jI_j|+,m_I'\rangle = -\langle -,m_I|A_jI_j|-,m_I'\rangle = \tfrac{1}{2} A_{jz} \langle m_I|I_j|m_I'\rangle$$

$$\langle -,m_I|A_jI_j|+,m_I'\rangle = \langle +,m_I|A_jI_j|-,m_I'\rangle^* = \tfrac{1}{2}(A_{jx} + i A_{jy}) \langle m_I|I_j|m_I'\rangle \quad \text{A18}$$

The matrix elements thus become

$$\langle +,m_I|\mathcal{H}|+,m_I'\rangle = \tfrac{1}{2} A_{xz} \langle m_I|I_x|m_I'\rangle + \tfrac{1}{2} A_{yz} \langle m_I|I_y|m_I'\rangle + \tfrac{1}{2} A_{zz} \langle m_I|I_z|m_I'\rangle$$

$$\langle +,m_I|\mathcal{H}|-,m_I'\rangle = \tfrac{1}{2}(A_{xx} - iA_{xy})\langle m_I|I_x|m_I'\rangle + \tfrac{1}{2}(A_{yx} - iA_{yy})\langle m_I|I_y|m_I'\rangle + \tfrac{1}{2}(A_{zx} - iA_{zy})\langle m_I|I_z|m_I'\rangle$$

$$\langle -,m_I|\mathcal{H}|+,m_I'\rangle = \tfrac{1}{2}(A_{xx} + iA_{xy})\langle m_I|I_x|m_I'\rangle + \tfrac{1}{2}(A_{yx} + iA_{yy})\langle m_I|I_y|m_I'\rangle + \tfrac{1}{2}(A_{zx} + iA_{zy})\langle m_I|I_z|m_I'\rangle$$

$$\langle -,m_I|\mathcal{H}|-,m_I'\rangle = -\tfrac{1}{2}A_{xz}\langle m_I|I_x|m_I'\rangle - \tfrac{1}{2}A_{yz}\langle m_I|I_y|m_I'\rangle - \tfrac{1}{2}A_{zz}\langle m_I|I_z|m_I'\rangle \qquad \text{A19}$$

These matrix elements are the same as those which would have been obtained by using the fictitious spin operator S, as before, and a spin Hamiltonian of the form

$$\mathcal{H} = \underline{S}.A.\underline{I} \qquad \text{A20}$$

where A is a second rank tensor.

Thus the energy of the system, including Zeeman and hyperfine interactions can be expressed in terms of a spin Hamiltonian of the form

$$\mathcal{H} = \beta_e \underline{H}.g.\underline{S} + \underline{S}.A.\underline{I} \qquad \text{A21}$$

(c) <u>The Quadrupolar Interaction</u>[5]

The energy of interaction between a nucleus and the electrostatic field due to the surrounding electrical charges is given by

$$E = \int \rho(\tau)\, V(\tau)\, d\tau \qquad \text{A22}$$

where $\rho(\tau)\, d\tau$ is the increment of nuclear charge in the volume element $d\tau$, and the integration is over the volume of the nucleus. The potential $V(\tau)$ can be expanded, using McLaurin's theorem as

$$V(\tau) = V(0) + \sum_i iV_i + \tfrac{1}{2}\sum_{i,j} i\,j\,V_{ij} + - - - - \qquad \text{A23}$$

where $i, j = x, y$ or z, and $V_{ij} = \left[\dfrac{\partial^2 V}{\partial i \partial j}\right]_{r=0}$

Thus

$$E = V(0)\int \rho(\tau)\, d\tau + \sum_i V_i \int i\rho(\tau)\, d\tau + \tfrac{1}{2}\sum_{i,j} V_{ij} \int ij\, \rho(\tau)\, d\tau + - - - - \qquad A24$$

The contributions to the above energy can be seen to arise from the interaction of the various electric moments of the nucleus with the surrounding electric potential and its derivatives. The quadrupolar contribution is given by

$$E_Q = \tfrac{1}{2} \sum_{i,j} V_{ij} \int ij\, \rho(\tau)\, d\tau \qquad A25$$

The quadrupole interacts with the negative first derivative of the electric field. The function Q_{ij} can now be defined as

$$Q_{ij} = \int (3\, ij - \delta_{ij}\, r^2)\, \rho(\tau)\, d\tau \qquad A26$$

Equation A25 now becomes

$$E_Q = \frac{1}{6} \sum_{i,j} V_{ij}\, Q_{ij} + \frac{1}{6}\, \delta_{ij} \sum_{i,j} V_{ij} \int r^2 \rho(\tau)\, d\tau \qquad A27$$

Poisson's equation states that $\nabla^2 V$ = constant, so

$$E_Q = \frac{1}{6} \sum_{i,j} V_{ij}\, Q_{ij} + \text{constant} \qquad A28$$

Since the constant term leads to a constant contribution to all the energy levels of the system it does not contribute to the transition energies and can be ignored in this case.

The matrix elements of the Q functions can be calculated by using the Wigner-Eckart theorem, which states that the matrix elements of these functions are proportional to those of the equivalent nuclear angular momentum operators, ie

$$\langle m_I | e \sum (3\, ij - \delta_{ij}\, r^2) | m_I' \rangle = c \langle m_I | 3I_i\, I_j - \delta_{ij}\, I^2 | m_I' \rangle \qquad A29$$

In the above equation the integral has been replaced by a sum which is over all the protons in the nucleus. The constant c can be obtained by evaluating any of the components of E_Q, but in fact it is usually expressed in terms of Q_{zz}, evaluated for $m_I = m_I' = I$, which leads to

$$c = \frac{\langle m_I = I | e\sum (3z^2 - r^2) | m_I = I \rangle}{I(2I - 1)}$$

$$= \frac{eQ}{I(2I - 1)} \qquad \text{A30}$$

where Q is called the quadrupole moment of the nucleus. Thus the quadrupolar Hamiltonian can be written as

$$\mathcal{H}_Q = \frac{eQ}{6I(2I - 1)} \sum_{i,j} V_{ij} (3I_i I_j - \delta_{ij} I^2) \qquad \text{A31}$$

Since $\sum_{i,j} V_{ij} = 0$, this reduces to

$$\mathcal{H}_Q = \frac{eQ}{6I(2I - 1)} \sum_{i,j} 3 V_{ij} I_i I_j$$

$$= \underline{I} \cdot P \cdot \underline{I} \qquad \text{A31}$$

where P is the quadrupole coupling tensor, whose components are of the form

$$P_{ij} = \frac{eQ V_{ij}}{2I(2I - 1)} \qquad \text{A33}$$

P is a symmetric tensor, and $\sum_i P_{ii} = 0$. If $\mathcal{H}_Q$ is written in its diagonal form, and the following substitutions are made

$$V_{zz} = q \qquad V_{xx} = -\tfrac{1}{2} q (1 - \eta)$$

$$\eta = \frac{V_{xx} - V_{yy}}{q} \qquad V_{yy} = -\tfrac{1}{2} q (1 + \eta) \qquad \text{A34}$$

the Hamiltonian becomes

$$\mathcal{H}_Q = \frac{eQq}{4I(2I-1)} \left(3I_z^2 - \underline{I}^2 + \eta(I_x^2 - I_y^2) \right) \qquad A35$$

sometimes written as

$$\mathcal{H}_Q = \frac{eQq}{4I(2I-1)} \left(3I_z^2 - I(I+1) + \eta(I_x^2 - I_z^2) \right) \qquad A36$$

where I is the nuclear spin quantum number.

In systems with axial symmetry, η is equal to zero, and equation A36 is sometimes written as

$$\mathcal{H}_Q = Q' \left(I_z^2 - \tfrac{1}{3}I(I+1)\right) \qquad A37$$

where $Q' = \dfrac{3\,eQq}{4I(2I-1)}$

The total spin Hamiltonian can thus be most generally written as

$$\mathcal{H} = \beta_e \underline{H} \cdot g \cdot \underline{S} + \underline{S} \cdot A \cdot \underline{I} + \underline{I} \cdot P \cdot \underline{I} \qquad A38$$

In systems where rotation of the molecule is able to average out the anisotropic contributions to the various tensors, equation A38 can be written as

$$\mathcal{H} = g_o \beta_e \underline{H} \cdot \underline{S} + A_o \underline{S} \cdot \underline{I} \qquad A39$$

APPENDIX B

SOLUTION OF THE SPIN HAMILTONIAN[1-3]

Consider the general case where a molecule lies in an applied magnetic field H, which has direction cosines l, m and n with respect to the principal tensor axes X, Y and Z, of the molecule and assume that the same set of axes diagonalises all the tensors. The spin Hamiltonian is thus of the form

$$\mathcal{H} = \beta_e (g_{xx}\, l\, S_x + g_{yy}\, m\, S_y + g_{zz}\, n\, S_z)H + \sum_i (A_{ii}\, S_i\, I_i + P_{ii}\, I_i^2) \qquad B1$$

where i = X, Y, Z. The problem can be solved by considering first the Zeeman interaction alone, and by considering the hyperfine and quadrupolar terms as successive perturbations. The basis states for the problem are of the form $|\alpha, m_I\rangle$ and $|\beta, m_I\rangle$. The energy matrix can be diagonalised with respect to the Zeeman term by carrying out the transformation

$$\begin{aligned} S_x &= a_{11}\, S_x' + a_{12}\, S_y' + a_{13}\, S_z' \\ S_y &= a_{21}\, S_x' + a_{22}\, S_y' + a_{23}\, S_z' \\ S_z &= a_{31}\, S_x' + a_{32}\, S_y' + a_{33}\, S_z' \end{aligned} \qquad B2$$

If the direction cosines of Z' with respect to the X, Y and Z axes are defined to be $g_{xx}\, l\, g^{-1}$, $g_{yy}\, m\, g^{-1}$ and $g_{zz}\, n\, g^{-1}$ the Zeeman term becomes $\mathcal{H}_Z = g\beta_e H S_z'$.

If the Z' axis is chosen as the axis of quantisation for the electron spin functions α and β, these states are eigenfunctions of the transformed Zeeman term, with energies of $\pm \frac{1}{2} g \beta_e H$. From the properties of the direction cosines

$$g^2 = g_{xx}^2\, l^2 + g_{yy}^2\, m^2 + g_{zz}^2\, n^2 \qquad B3$$

The transformed hyperfine term in the Hamiltonian now becomes

$$= S_x'(a_{11}A_{xx}I_x + a_{21}A_{yy}I_y + a_{31}A_{zz}I_z) + S_y'(a_{12}A_{xx}I_x + a_{22}A_{yy}I_y + a_{32}A_{zz}I_z)$$

$$+ S_z'(a_{13}A_{xx}I_x + a_{23}A_{yy}I_y + a_{33}A_{zz}I_z) \qquad B4$$

The hyperfine term can now be treated using non-degenerate perturbation theory, providing it has no off-diagonal matrix elements between states which are degenerate in zero order. This can be achieved by a second transformation of the form

$$I_x = b_{11}\,I_x'' + b_{12}\,I_y'' + b_{13}\,I_z''$$

$$I_y = b_{21}\,I_x'' + b_{22}\,I_y'' + b_{23}\,I_z''$$

$$I_z = b_{31}\,I_x'' + b_{32}\,I_y'' + b_{33}\,I_z'' \qquad B5$$

If the coefficients in B5 are so defined that Z'' has direction cosines with respect to the X, Y and Z axes of $a_{13}\,A_{xx}\,A^{-1}$, $a_{23}\,A_{yy}\,A^{-1}$ and $a_{33}\,A_{zz}\,A^{-1}$, the term in S_z' in the transformed Hamiltonian has the form $AS_z'\,I_z''$. If Z'' is now chosen as the axis of quantisation of the nuclear spin states, the term $AS_z'\,I_z''$ has only diagonal matrix elements, and yields a first order contribution to the perturbation energy of $A\,m_S\,m_I$.

Again, from the properties of direction cosines

$$A^2 = (g_{xx}^2\,l^2\,A_{xx}^2 + g_{yy}^2\,m^2\,A_{yy}^2 + g_{zz}\,n^2\,A_{zz}^2)\,g^{-2} \qquad B6$$

The remaining hyperfine terms in the Hamiltonian can now be treated using second order perturbation theory. The quadrupolar terms can subsequently be treated in a straightforward way by applying second order perturbation theory to the eigenfunctions of the Zeeman plus hyperfine interaction Hamiltonian, and expressions can be derived for the energies of the $|\alpha, m_I\rangle$ and $|\beta, m_I\rangle$ states and for the energies of the allowed $\Delta m_S = +1$, $\Delta m_I = 0$ transitions.

These energies are given by

$$\Delta E = g\beta_e H + Am_I + \frac{1}{4g\beta_e H}\left(A_1(m_I^2 - I(I+1)) + 2A_2 m_I^2\right)$$

$$+\frac{1}{2A}\left(P_1(18I(I+1) - 34m_I^2 - 5) + P_2(2I(I+1) - 2m_I^2 - 1)\right.$$

$$\left. - P_3(20I(I+1) - 36m_I^2 - 6)\right) \qquad \text{B7}$$

where g and A are defined above, and

$$A_2A^2g^2 = (A_{xx}^2 - A_{yy}^2)^2 g_{xx}^2 g_{yy}^2 l^2m^2 + (A_{yy}^2 - A_{zz}^2)^2 g_{yy}^2 g_{zz}^2 m^2n^2$$

$$+ (A_{xx}^2 - A_{zz}^2)^2 g_{xx}^2 g_{zz}^2 l^2n^2$$

$$A_1A^2g^4 = (A_{xx}^2 A_{yy}^2 g_{zz}^2 n^2 + A_{yy}^2 A_{zz}^2 g_{xx}^2 l^2 + A_{xx}^2 A_{zz}^2 g_{yy}^2 m^2)$$

$$- g^2 (A_{xx}^2 A_{yy}^2 + A_{xx}^2 A_{zz}^2 + A_{yy}^2 A_{zz}^2)$$

$$P_1A^4g^4 = (A_{xx}^2 P_{xx} g_{xx}^2 l^2 + A_{yy}^2 P_{yy} g_{yy}^2 m^2 + A_{zz}^2 P_{zz} g_{zz}^2 n^2)$$

$$P_2 = (P_{xx}^2 + P_{yy}^2 + P_{zz}^2) - 2 (P_{xx}^2 P_{yy}^2 A_{zz}^2 g_{zz}^2 n^2 + P_{yy}^2 P_{zz}^2 A_{xx}^2 g_{xx}^2 l^2$$

$$+ P_{zz}^2 P_{xx}^2 A_{yy}^2 g_{yy}^2 m^2) A^{-2} g^{-2}$$

$$P_3 A^2 g^2 = (P_{xx}^2 A_{xx}^2 g_{xx}^2 l^2 + P_{yy}^2 A_{yy}^2 g_{yy}^2 m^2 + P_{zz}^2 A_{zz}^2 g_{zz}^2 n^2) \qquad \text{B8}$$

For the case where the field lies along a principal axis direction, the expression reduces to

$$\Delta E = g_{ii}\beta_e H + A_{ii} m_I + \frac{(A_{jj}^2 + A_{kk}^2)}{4g_{ii}\beta_e H}\left(I(I+1) - m_I^2\right)$$

$$+ m_I \frac{(P_{kk} - P_{jj})^2}{2A_{ii}} (2I(I+1) - 2m_I^2 - 1) m_I \qquad \text{B9}$$

or, in terms of the usual experimental arrangement, the resonant fields are given by

$$H_i = H_o - a_{ii} m_I - \frac{(a_{jj}^2 + a_{kk}^2)}{4H_i} \left(I(I+1) - m_I^2\right)$$

$$- \frac{(p_{jj} - p_{kk})^2}{2a_{ii}} \left(2I(I+1) - 2m_I^2 - 1\right) m_I \qquad \text{B10}$$

where the various parameters are now in gauss. This equation reduces to that of Bleaney[2] in the case where the tensors are axially symmetric.

APPENDIX C

DERIVATION OF MOLECULAR ORBITAL COEFFICIENTS FROM SPIN HAMILTONIAN PARAMETERS

The equations relating the molecular orbital coefficients in the complexes studied in this work to their spin Hamiltonian parameters can be derived[1] using the equations given in Appendix A. In deriving these equations, the wavefunctions which should be used for the complexes should be antisymmetrised functions of the Slater determinantal type formed from linear combinations of the products of the one-electron molecular orbitals for the complex. These may be written as $\psi(\phi_1, \phi_2, \ldots\ldots \phi_n)$ where the Slater determinantal function ψ is formed from the molecular orbitals $\phi_1 \ldots\ldots \phi_n$, the order of the molecular orbital functions in the brackets reflecting the row which the functions occupy in the Slater determinant.

In practice, however, it is possible to discuss the problem in terms of one-electron wavefunctions, if use is made of the following theorem.[2]

Consider two Slater functions $\psi(\phi_1 \ldots \phi_i \ldots \phi_n)$ and $\psi'(\phi_1 \ldots \phi_i' \ldots \phi_n)$, which differ only due to ϕ_i in ψ being replaced by ϕ_i' in ψ'. If these are connected by a one-electron operator

$$A = \sum_n a(n) \qquad C1$$

then it can be shown that

$$\langle \psi | A | \psi' \rangle = \langle \phi_i | a(i) | \phi_i \rangle \qquad C2$$

This is only true if the molecular orbitals in ψ are written in the same order as those in ψ', with ϕ_i' occupying the position in ψ' previously held by ϕ_i in ψ. If the order is changed, the sign of the relationship C2 is changed according to the rules governing the sign of the wavefunctions of Slater determinants.

The derivation of the equations for the spin Hamiltonian parameters involves the evaluation of matrix elements between states differing only in the form of the molecular orbital for the unpaired electron, so that it is possible to work with one-electron molecular orbital basis functions, instead of the full Slater functions.

Henceforth, therefore, the wavefunctions for the various states involved in the equations will be labelled in terms of the symmetry and spin of the molecular orbital containing the unpaired electron. Thus in an $A_1\alpha$ state the unpaired electron occupies a molecular orbital of A_1 symmetry and has α spin.

(a) Vanadyl Chelates

In the absence of spin-orbit coupling, the ground state wavefunctions for a vanadyl chelate with C_{2v} symmetry are $A_1^*\alpha$ and $A_1^*\beta$, where

$$A_1^* = \alpha_1^* (a d_{x^2-y^2} + b d_{z^2} + c s) + \alpha_1^{*I}\phi_{L1} \qquad C3$$

The axis system, and the exact form of ϕ_{L1} are given in part II.

Spin-orbit coupling mixes into the ground state contributions from all possible excited states of the correct symmetry, but in general it is necessary to consider only those states which are closest to the ground state in energy. In this case these are states which are produced by promotion of the unpaired electron into an antibonding molecular orbital of mainly 3d character. The next lowest states in vanadyl chelates are those states produced by promoting an electron from a bonding orbital into A_1^*, but since these are at twice the energy of the previous states, and since the bonding orbitals in this case are mainly ligand in character, they have practically no effect on the spin Hamiltonian parameters.

The molecular orbitals which are found to contribute to the ground state have the form

$$A_2^* = \alpha_2^* d_{xy} + \alpha_2^{*I} \phi_{L2}$$

$$B_1^* = \beta_1^* d_{xz} + \beta_1^{*I} \phi_{L3} + \beta_1^{*II} \phi_{L4}$$

$$B_2^* = \beta_2^* d_{yz} + \beta_2^{*I} \phi_{L5} + \beta_2^{*II} \phi_{L6} \qquad C4$$

The ligand group orbitals again have the form given in part II. All these functions are spin doublets. The spin-orbit coupling Hamiltonian is of the form

$$\mathcal{H}_{LS} = \xi_v \, \underline{L}.\underline{S} \qquad C5$$

Spin-orbit coupling on the ligands can be ignored, because the orbitals involved are mainly metal ion in character and also because the oxygen spin-orbit coupling constant is much less than that of vanadium.

The form of the ground state functions $|+\rangle$ and $|-\rangle$ after spin-orbit coupling is included can now be obtained using equations A2 to give

$$|+\rangle = A_1^*\alpha - \frac{ia\alpha_2^*\alpha_1^*\xi_v A_2^*\alpha}{\Delta E(A_2^*)} - \frac{\beta_1^*\alpha_1^*\xi_v (a - b\sqrt{3}) B_1^*\beta}{2\Delta E(B_1^*)} + \frac{i\beta_2^*\alpha_1^*\xi_v (a + b\sqrt{3}) B_2^*\beta}{2\Delta E(B_2^*)}$$

$$|-\rangle = A_1^*\beta + \frac{ia\alpha_2^*\alpha_1^*\xi_v A_2^*\beta}{\Delta E(A_2^*)} + \frac{\beta_1^*\alpha_1^*\xi_v (a - b\sqrt{3}) B_1^*\alpha}{2\Delta E(B_1^*)} + \frac{i\beta_2^*\alpha_1^*\xi_v (a + b\sqrt{3}) B_2^*\alpha}{2\Delta E(B_2^*)} \qquad C6$$

In evaluating the various matrix elements, terms of the form

$$\langle d|\mathcal{H}_{LS}|\phi_L\rangle \quad \text{and} \quad \langle \phi_L|\mathcal{H}_{LS}|\phi_{L'}\rangle \qquad C7$$

are ignored, due to the r^{-3} dependence of the vanadium spin-orbit coupling constant. Expressions for the g-tensor components can now be derived by comparing the matrix elements of equations A4 and A8.

These yield the following expressions for the g-tensor components.

$$g_{xx} = 2.0023 - \frac{2(a + b/\sqrt{3})^2 \xi_v \alpha_1^{*2} \, Pmd(B_2^*)}{\Delta E(B_2^*)}$$

$$g_{yy} = 2.0023 - \frac{2(a - b/\sqrt{3})^2 \xi_v \alpha_1^{*2} \, Pmd(B_1^*)}{\Delta E(B_1^*)}$$

$$g_{zz} = 2.0023 - \frac{8a^2 \alpha_1^{*2} \xi_v \, Pmd(A_2^*)}{\Delta E(A_2^*)} \qquad C8$$

where $Pmd(A_2^*)$ is the metal orbital population in the A_2^* molecular orbital etc. In obtaining these expressions, use is made of the Hermitean property of the angular momentum operators such that

$$\langle d|L_i|\phi_L\rangle = \langle \phi_L|L_i|d\rangle^* \qquad C9$$

Contributions from terms involving $\alpha_1^{*I}\phi_{L1}$ are ignored, because it is known that in these chelates the unpaired electron is located almost exclusively on the metal in A_1^*, so that α_1^{*I} is small. Terms of the order $(\xi_v/\Delta E)^2$ are also ignored.

It is possible to derive expressions for the principal values of the hyperfine coupling tensor in a similar way, by comparing the matrix elements of A17 and A19. This yields the following expressions for the hyperfine coupling constants.

$$A_{xx} = P(-K + \frac{2}{7}(a^2-b^2)\alpha_1^{*2} + \frac{4\sqrt{3}}{7}ab\alpha_1^{*2} - \Delta g_{xx} + \frac{(3a+b\sqrt{3})}{14(a-b\sqrt{3})}\Delta g_{yy} + \frac{b}{7a}\Delta g_{zz})$$

$$A_{yy} = P(-K + \frac{2}{7}(a^2-b^2)\alpha_1^{*2} - \frac{4\sqrt{3}}{7}ab\alpha_1^{*2} - \Delta g_{yy} + \frac{(3a-b\sqrt{3})}{14(a+b\sqrt{3})}\Delta g_{xx} - \frac{b}{7a}\Delta g_{zz})$$

$$A_{zz} = P(-K - \frac{4}{7}(a^2-b^2)\alpha_1^{*2} - \frac{(3a+b\sqrt{3})}{14(a-b\sqrt{3})}\Delta g_{yy} - \frac{(3a-b\sqrt{3})}{14(a+b\sqrt{3})}\Delta g_{xx} - \Delta g_{zz}) \quad C10$$

where $\Delta g_{ii} = 2.0023 - g_{ii}$ and $P = \langle d | g_e g_N \beta_e \beta_N r^{-3} | d \rangle$

In deriving these equations, terms of the form $\langle d | \mathcal{H} | \phi_L \rangle$ and $\langle \phi_L | \mathcal{H} | \phi_L \rangle$ are ignored because of the r^{-3} term in equations A16. The term -PK represents the Fermi contact interaction contribution to the hyperfine coupling. In many transition metal complexes the ground state does not contain any s-orbital character, but the -PK term is still finite, the contact interaction arising from the polarisation of inner filled s electron shells by the unpaired electron. This interaction results in a negative value for the hyperfine coupling constant since the polarisation results in the unpaired spin density at the nucleus having the opposite orientation from that of the unpaired electron.[3]

In the case of vanadyl chelates, there is a contribution to -PK from spin polarisation, and also a direct contribution from the presence of some 4s character in the ground state molecular orbital. The latter gives a positive contribution to the hyperfine coupling constant, and so -PK is smaller in those cases where the 4s contribution to the ground state is significant.

(b) Bis-(π-cyclopentadienyl) Pseudohalides

The equations which relate the spin Hamiltonian parameters to the molecular orbital coefficients in these complexes are similar in form to those for the vanadyl chelates.

In the absence of spin-orbit coupling, the ground state wavefunctions for the complexes, which are assumed to have C_{2v} symmetry, are again $A_1^*\alpha$ and $A_1^*\beta$, where

$$A_1^* = \alpha_1^* (a d_{x^2-y^2} + b d_{z^2}) + \alpha_1^{*I} \phi_{L1} \qquad C11$$

where the axis system, and the form of ϕ_{L1} are those given in part III. The metal 4s and 4p orbitals, and three of the other ligand group orbitals, also have A_1 symmetry, but from the molecular orbital calculation on these complexes it is known that these contribute very little to A_1^* in this case.

The spin-orbit interaction in these complexes results in appreciable contributions to the ground state wavefunctions from two types of state.

1. The states closest to the ground state in energy are those produced by promotion of the unpaired electron into an antibonding molecular orbital which has a large amount of metal 3d character. The orbitals of this type which are found to contribute to the ground state have the form

$$A_2^* = \alpha_2^* d_{xy} + \alpha_2^{*I} \phi_{L2} + \alpha_2^{*II} \phi_{L3} + \alpha_2^{*III} \phi_{L4}$$

$$B_1^* = \beta_1^* d_{xz} + \beta_1^{*I} \phi_{L5} + \beta_1^{*II} \phi_{L6} + \beta_1^{*III} \phi_{L7} + \beta_1^{*IV} \phi_{L8}$$

$$B_2^* = \beta_2^* d_{yz} + \beta_2^{*I} \phi_{L9} + \beta_2^{*II} \phi_{L10} + \beta_2^{*III} \phi_{L11} \qquad C12$$

All the above states are spin doublets, and the forms of the ligand group orbitals $\phi_2 - \phi_{11}$ are given in chapter 3. Contributions to B_1^* and B_2^* from the metal $4p_x$ and $4p_y$ orbitals respectively, although significant, have been ignored, since they contribute nothing to the final equations, due to the absence of $4p_z$ character in A_1^*.

2. The second set of states which are important are those produced by promoting an electron into A_1^* from one of the bonding molecular orbitals derived mainly from the cyclopentadienide ring orbitals, which lie close to A_1^* in energy.

These charge transfer states are of importance in these complexes whereas they were not in the vanadyl chelates, because they lie closer to the ground state in energy and also because the bonding in these complexes is much more covalent than that in the vanadyl chelates, so that the bonding molecular orbitals have appreciable metal ion orbital character. Thus, the orbitals of this type which contribute to the ground state have the form

$$A_2 = \alpha_2 d_{xy} + \alpha_2^{I}\phi_{L2} + \alpha_2^{II}\phi_{L3} + \alpha_2^{III}\phi_{L4}$$

$$B_1 = \beta_1 d_{xz} + \beta_1^{I}\phi_{L5} + \beta_1^{II}\phi_{L6} + \beta_1^{III}\phi_{L7} + \beta_1^{IV}\phi_{L8}$$

$$B_2 = \beta_2 d_{yz} + \beta_2^{I}\phi_{L9} + \beta_2^{II}\phi_{L10} + \beta_2^{III}\phi_{L11} \qquad C13$$

Again all these states are spin doublets, and the $4p_x$ and $4p_y$ contributions to B_1 and B_2 are ignored.

The form of the ground state functions $|+\rangle$ and $|-\rangle$ can now be obtained, using the spin-orbit Hamiltonian of the form

$$\mathcal{H}_{LS} = \zeta_M \underline{L}.\underline{S} + \zeta_{x1} \underline{L}.\underline{S} + \zeta_{x2} \underline{L}.\underline{S}$$

where ζ_M is the metal ion spin-orbit coupling parameter, and ζ_x is the spin-orbit coupling parameter for the ligand atom of the pseudohalide bound to the metal.

The new ground state wavefunctions have the form

$$|+\rangle = A_1^*\alpha - \frac{\alpha_1^*\beta_1^*(a-b\sqrt{3})\xi_M}{2\Delta E(B_1^*)}\left[1 + \frac{\alpha_1^{*I}\beta_1^{*III}\xi_x}{\alpha_1^*\beta_1^*(a-b\sqrt{3})\xi_M}\right]B_1^*\beta$$

$$- \frac{\alpha_1^*\beta_1(a-b\sqrt{3})\xi_M}{2\Delta E(B_1)}\left[1 + \frac{\alpha_1^{*I}\beta_1^{III}\xi_x}{\alpha_1^*\beta_1(a-b\sqrt{3})\xi_M}\right]B_1\beta + \frac{i(a+b\sqrt{3})\alpha_1^*\beta_2^*\xi_M}{2\Delta E(B_2^*)}B_2^*\beta$$

$$+ \frac{i(a+b\sqrt{3})\alpha_1^*\beta_2\xi_M}{2\Delta E(B_2)}B_2\beta - \frac{ia\alpha_1^*\alpha_2^*\xi_M}{\Delta E(A_2^*)}\left[1 + \frac{\alpha_1^{*I}\alpha_2^{*III}\xi_x}{2a\alpha_1^*\alpha_2^*\xi_M}\right]A_2^*\alpha$$

$$- \frac{ia\alpha_1^*\alpha_2\xi_M}{\Delta E(A_2)}\left[1 + \frac{\alpha_1^{*I}\alpha_2^{III}\xi_x}{2a\alpha_1^*\alpha_2\xi_M}\right]A_2\alpha$$

$$|-\rangle = A_1^*\beta + \frac{\alpha_1^*\beta_1^*(a-b\sqrt{3})\xi_M}{2\Delta E(B_1^*)}\left[1 + \frac{\alpha_1^{*I}\beta_1^{*III}\xi_x}{\alpha_1^*\beta_1^*(a-b\sqrt{3})\xi_M}\right]B_1^*\alpha$$

$$- \frac{\alpha_1^*\beta_1(a-b\sqrt{3})\xi_M}{2\Delta E(B_1)}\left[1 + \frac{\alpha_1^{*I}\beta_1^{III}\xi_x}{\alpha_1^*\beta_1(a-b\sqrt{3})\xi_M}\right]B_1\alpha + \frac{i(a+b\sqrt{3})\alpha_1^*\beta_2^*\xi_M}{2\Delta E(B_2^*)}B_2^*\alpha$$

$$+ \frac{i(a+b\sqrt{3})\alpha_1^*\beta_2\xi_M}{2\Delta E(B_2)}B_2\alpha + \frac{ia\alpha_1^*\alpha_2^*\xi_M}{\Delta E(A_2^*)}\left[1 + \frac{\alpha_1^{*I}\alpha_2^{*III}\xi_x}{2a\alpha_1^*\alpha_2^*\xi_M}\right]A_2^*\beta$$

$$+ \frac{ia\alpha_1^*\alpha_2\xi_M}{\Delta E(A_2)}\left[1 + \frac{\alpha_1^{*I}\alpha_2^{III}\xi_x}{2a\alpha_1^*\alpha_2\xi_M}\right]A_2\beta \qquad \text{C14}$$

The expressions for the g-tensor components can now be derived by comparing the matrix elements of A4 and A8 to give

$$g_{xx} = 2.0023 - 2(a+b\sqrt{3})^2\alpha_1^{*2}\xi_M\left[\frac{Pmd(B_2^*)}{\Delta E(B_2^*)} - \frac{Pmd(B_2)}{\Delta E(B_2)}\right]$$

$$g_{yy} = 2.0023 - 2(a-b\sqrt{3})^2\alpha_1^{*2}\xi_M\left[1 + \frac{\alpha_1^{*I}\beta_1^{*III}\xi_x}{\alpha_1^*\beta_1^*(a-b\sqrt{3})\xi_M}\right]\frac{Pmd(B_1^*)}{\Delta E(B_1^*)}$$

$$+ 2(a-b\sqrt{3})^2\alpha_1^{*2}\xi_M\left[1 + \frac{\alpha_1^{*I}\beta_1^{III}\xi_x}{\alpha_1^*\beta_1(a-b\sqrt{3})\xi_M}\right]\frac{Pmd(B_1)}{\Delta E(B_1)}$$

$$g_{zz} = 2.0023 - 8a^2 \alpha_1^{*2} \xi_M \left[1 + \frac{\alpha_1^{*I} \alpha_2^{*III} \xi_x}{2\alpha_1^* \alpha_2^* a \xi_M} \right] \frac{Pmd(A_2^*)}{\Delta E(A_2^*)}$$

$$+ 8a^2 \alpha_1^{*2} \xi_M \left[1 + \frac{\alpha_1^{*I} \alpha_2^{*III} \xi_x}{2\alpha_1^* \alpha_2 a \xi_M} \right] \frac{Pmd(A_2)}{\Delta E(A_2)} \qquad C15$$

In evaluating these expressions, terms involving $\alpha_1^{*I} \phi_{L1}$ are ignored because of the small value of α_1^{*I}, and terms of the order $\left(\frac{\xi}{\Delta E}\right)^2$ are ignored. It is important to note that the form of ϕ_{L1} is such that there is no contribution to the mixing of B_2 states into the ground state due to spin-orbit coupling on the ligands, and as a result the value of g_{xx} is independent of the ligand spin-orbit coupling constant.

Expressions for the principal values of the metal ion hyperfine coupling tensor can now be derived by comparing the matrix elements of A17 and A19. In fact since the only terms which contribute to these expressions are of the form

$$\langle d|\mathcal{H}|d\rangle,$$

the expressions depend only on the form of the metal orbital contribution to the molecular orbital containing the unpaired electron in the ground state, and the result is that the expressions in this case are exactly the same as those of equations C10. In this case the metal s orbital is not expected to contribute significantly to the value of -PK.

APPENDIX D

E.P.R. LINESHAPES IN MAGNETICALLY DILUTE POLYCRYSTALLINE OR FROZEN SOLUTION SPECTRA

Glassy and polycrystalline spectra are similar in that absorption occurs over a wide range of field values. In both cases the samples contain a large number of individual molecules held rigidly in the solid in random orientations with respect to the applied magnetic field. In general molecules lying at different orientations to the applied field have different g-factors and different effective hyperfine coupling constants, so that the spectrum observed arises from the superposition of the spectra from all these different molecules, each contribution being weighted with respect to the probability of a molecule lying at a particular orientation to the applied field.

It is possible to distinguish three separate cases

(a) Molecules with Spherical Symmetry ($g_{11} = g_{22} = g_{33}$)

In this case the g-factor is isotropic and for a molecule with $S = \frac{1}{2}$, $I = 0$, absorption would occur at one field only.

(b) Molecules with Axial Symmetry ($g_{11} = g_{22} \neq g_{33}$)

This case has been treated by Sands[1] for molecules with $S = \frac{1}{2}$, $I = 0$. In this case the resonant field depends only on the angle θ between the applied magnetic field and the symmetry axis of the molecule.

For a random orientation, the fraction of the molecules, dN, lying at an angle between θ and $\theta + d\theta$ is given by

$$dN = \tfrac{1}{2} \sin\theta \, d\theta \qquad \text{D1}$$

If the molecules in the interval $d\theta$ have resonant fields in the interval dH, then the amplitude of absorption g(H) is given by

$$g(H) = \frac{dN}{dH} = \frac{dN}{d\theta} \frac{d\theta}{dH} \qquad \text{D2}$$

$$= \frac{1}{2} \sin\theta \frac{d\theta}{dH} \qquad D3$$

But it is known that

$$g^2 = (g_{33}^2 \cos^2\theta + g_{22}^2 \sin^2\theta) \qquad D4$$

Thus, if the expression for $\frac{d\theta}{dH}$ is evaluated and substituted into D3, g(H) becomes

$$g(H) = \frac{h\nu_o}{2\beta_e H^3} \left[\frac{1}{H_{33}^2} - \frac{1}{H_{22}^2}\right]^{-\frac{1}{2}} \left[\frac{1}{H^2} - \frac{1}{H_{22}^2}\right]^{-\frac{1}{2}} \qquad D5$$

where $H_{33} = \frac{h\nu_o}{g_{33}\beta_e}$ etc.

So far it has been assumed that the e.p.r. transitions are infinitely sharp. In fact, line broadening does occur, and if the lines are assumed to be Gaussian in shape[2,3], the broadened line shape has the form $g(H')$.

$$g(H') = \int_{H = H_{22}}^{H = H_{33}} g(H)\, Y(H - H')\, dH \qquad D6$$

where $Y(H - H')$, the Gaussian lineshape function, is given by

$$Y(H - H') = \frac{1}{2\pi^{\frac{1}{2}}\beta} \exp\left(-(H - H')^2 (2\beta)^{-2}\right) \qquad D7$$

where the width of the line is controlled by the broadening parameter β.

Thus, absorption occurs between $H = H_{33}$ and $H = H_{11} = H_{22}$, and the lineshape function D5 exhibits a discontinuity at H_{33} and becomes infinite at $H = H_{11} = H_{22}$, since at that point $\frac{dH}{d\theta}$ goes to zero.

The functions $g(H)$ and $g(H')$ are plotted in figure 1 below, and the first derivative of $g(H')$ is plotted in figure 2.

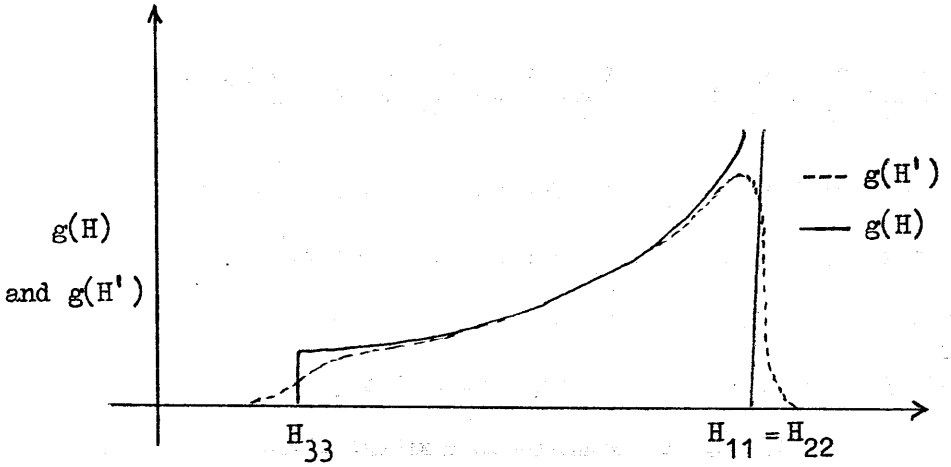

Figure 1

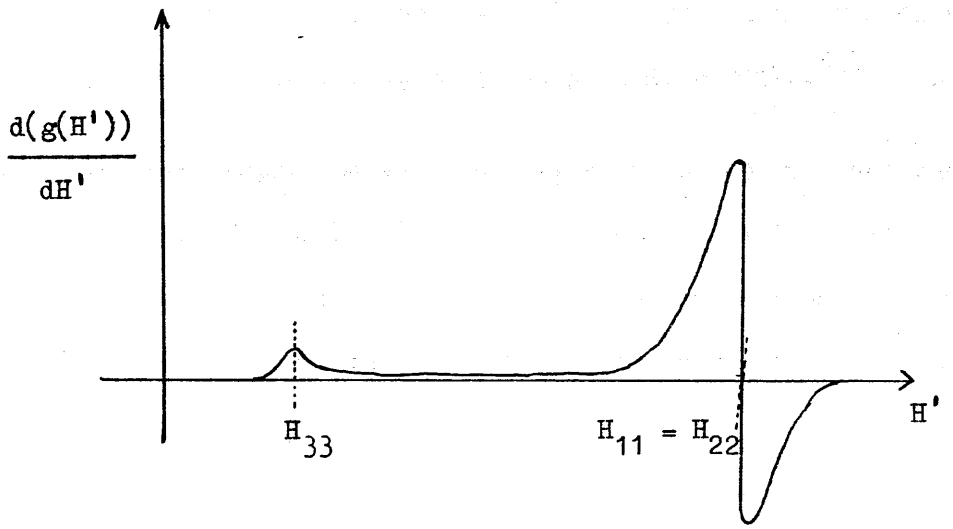

Figure 2

Thus it is possible from such spectra to obtain values for the absorption fields corresponding to the cases where the field lies along the principal axis directions of the molecule, and hence to obtain values for the principal g-tensor values.

As noted above, the function $g(H)$ becomes infinite when $\frac{dH}{d\theta}$ becomes zero, which it always does when $\theta = 90^{\circ}$. For the case of a molecule with $S = \frac{1}{2}$, $I = I$, the expression for $\frac{dH}{d\theta}$ becomes

$$\frac{dH}{d\theta} = \frac{\sin\theta \cos\theta \; h^2 \nu_o^2}{g^3 \beta_e^3} \left\{ h\nu_o \left[\frac{1}{H_{33}^2} - \frac{1}{H_{22}^2} \right] - m_I \left[2K \left[\frac{1}{H_{33}^2} - \frac{1}{H_{22}^2} \right] - K^{-1} \left[\frac{A_{33}^2}{H_{33}^2} + \frac{A_{22}^2}{H_{22}^2} \right] \right] \right\}$$

where

$$K^2 g^2 = (A_{22}^2 g_{22}^2 \cos^2\theta + A_{33}^2 g_{33}^2 \sin^2\theta) \qquad D9$$

This function again goes to zero for $\theta = 90^\circ$, but in addition certain combinations of g-factors and hyperfine coupling constants can also cause the function to go to zero when $0^\circ < \theta < 90^\circ$. In these cases the resonant field is not a monotonic function of θ, and the resonant field passes through a maximum or minimum for $0^\circ < \theta < 90^\circ$, giving rise to a peak in the polycrystalline spectrum which does not correspond to a case with the applied field along a principal axis direction. Such peaks are referred to as polycrystalline peaks.[4,5]

In most cases, however, such peaks do not occur, and the observed spectrum for an $S = \frac{1}{2}$, $I = I$ species can be interpreted in terms of a superposition of $2I + 1$ curves of the type shown in figure 2. As an example, the broadened first derivative curve for an $S = \frac{1}{2}$, $I = \frac{1}{2}$ molecule is shown below

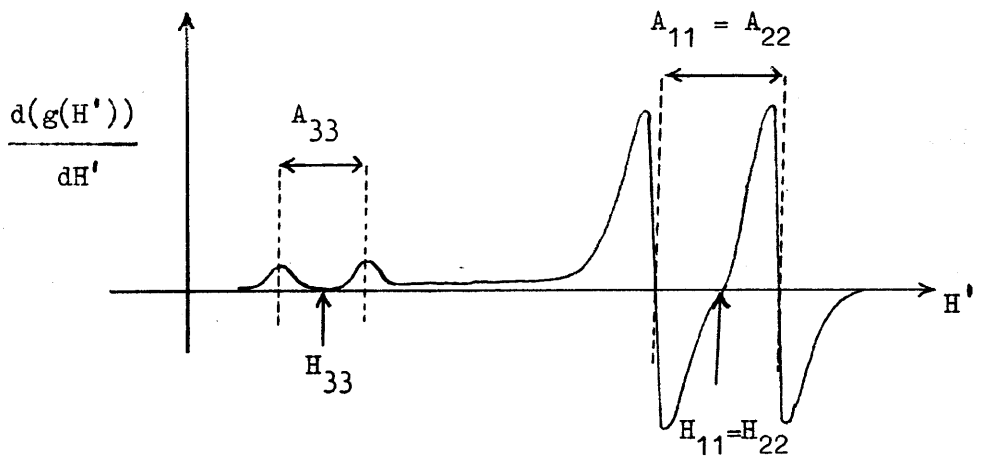

Figure 3

Thus from the above spectra it is possible to obtain values for the resonant fields for the applied field lying along the principal axis directions and the values of the principal g and hyperfine tensor components can then be calculated using equations B10 of appendix B.

(c) Molecules with Rhombic Symmetry ($g_{11} \neq g_{22} \neq g_{33}$)

The derivation of the lineshape function is more complicated in this case because the resonant field depends on two orientation angles, instead of one as in the case of axially symmetric molecules. As a result, there is a range of combinations of the two orientation angles which lead to resonance at a particular field, and consequently the amplitude of absorption depends on the probability of the molecule having any one of a combination of orientation angles which lead to resonance at a particular field.

The case of a molecule with $S = \frac{1}{2}$, $I = 0$ has been treated by Kneubuhl[6], and the lineshape function has the form below for $H_{33} < H_{22} < H_{11}$

1. In the interval $H_{11} \geqslant H \geqslant H_{22}$

$$g(H) = \frac{2 H_{11} H_{22} H_{33}}{\pi H^2 (H_{11}^2 - H_{22}^2)^{\frac{1}{2}} (H^2 - H_{33}^2)^{\frac{1}{2}}} \quad K(l')$$

2. In the interval $H_{22} \geqslant H \geqslant H_{33}$

$$g(H) = \frac{2 H_{11} H_{22} H_{33}}{\pi H^2 (H_{22}^2 - H_{33}^2)^{\frac{1}{2}} (H_{11}^2 - H^2)^{\frac{1}{2}}} \quad K(l) \qquad \text{D10}$$

where $K(l)$ is the standard elliptic integral

$$K(l) = \int_0^{\frac{\pi}{2}} \frac{dx}{(1 - l^2 \sin^2 x)^{\frac{1}{2}}}$$

$$= \frac{\pi}{2}\left[1 + \left(\frac{1}{2}\right)^2 l^2 + \left(\frac{1.3}{2.4}\right) l^4 + \cdots\right] \qquad \text{D11}$$

and $$(l')^2 = \frac{1}{l^2} = \frac{(H_{11}^2 - H_{22}^2)(H^2 - H_{33}^2)}{(H_{11}^2 - H^2)(H_{22}^2 - H_{33}^2)} \qquad \text{D12}$$

Thus absorption occurs between H_{11} and H_{33}. The function $g(H)$ has discontinuities at $H = H_{11}$ and at $H = H_{33}$. The function becomes infinite at $H = H_{22}$, where 1 and $1'$ both equal one, and the elliptic integrals expand to infinity.

Again $g(H)$ gives the form of the unbroadened lineshape. The broadened form of $g(H)$ and its first derivative are plotted in figures 4 and 5 respectively.

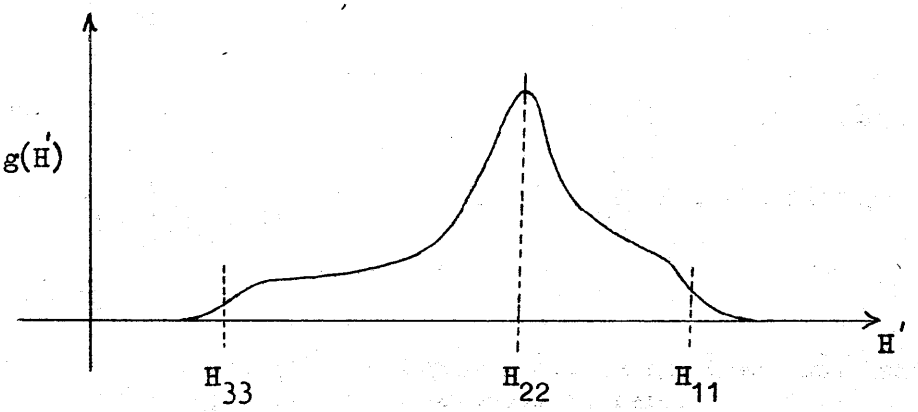

Figure 4

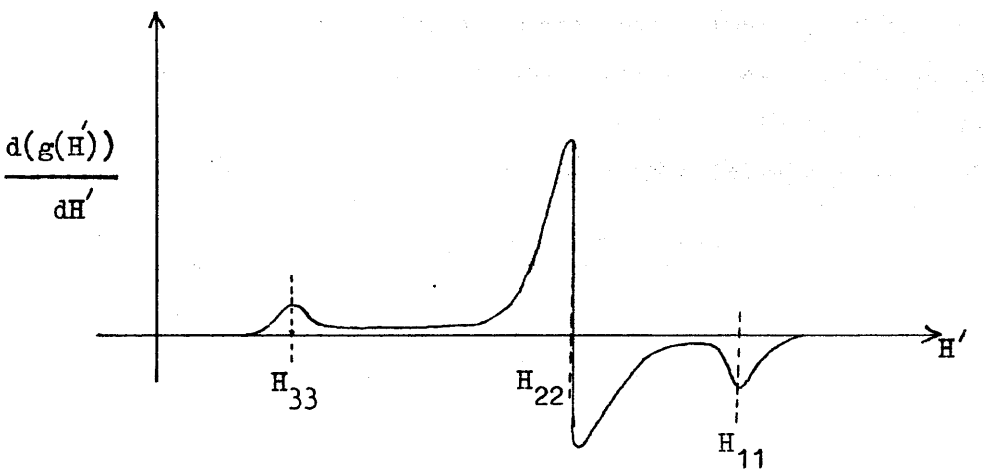

Figure 5

In most cases the spectra of species with $S = \frac{1}{2}$, $I = I$ can be interpreted in terms of a superposition of $2I + 1$ curves of the type shown in figure 5, and in favourable cases it is again possible to extract values for all of the principal tensor components of the molecule from such spectra, in the same way as for systems with axial symmetry.

REFERENCES

Part I

The discussion presented in part I, together with much of the basic theory used in the subsequent parts of the thesis, was based on the following sources.

1. B R McGarvey, 'Transition Metal Chemistry', R L Carlin ed., Edward Arnold, London, 1966, Vol. 3, p. 90.
2. A Carrington and A D McLachlan, 'Introduction to Magnetic Resonance', Harper and Row, New York, 1967.
3. C P Slichter, 'Magnetic Resonance', Harper and Row, New York, 1963.
4. A Abragam and B Bleaney, 'Electron Paramagnetic Resonance in Transition Ions', Clarendon Press, Oxford, 1970.
5. J A S Smith, J Chem. Ed., 1971, 48, 39, A77, A147 and A243.
6. C J Ballhausen and H B Gray, 'Molecular Orbital Theory', W A Benjamin and Co., New York, 1965.
7. P B Ayscough, 'Electron Spin Resonance in Chemistry', Methuen, London, 1967.

Part II

1. B A Goodman and J B Raynor, Adv. Inorg. Chem. and Radiochem., 1970, 13, 135, and references therein.
2. J Selbin, Chem. Rev., 1965, 65, 153.
3. J Selbin, Co-ordination Chem. Rev., 1966, 1, 293.
4. C J Ballhausen and H B Gray, Inorg. Chem., 1962, 1, 111.
5. D Kivelson and S K Lee, J Chem. Phys., 1964, 41, 1896.
6. L J Boucher, E C Tynan and T F Yen, 'Electron Spin Resonance of Metal Complexes', T F Yen Ed., Adam Hilger, London, 1969, p.175.
7. T R Ortolano, J Selbin and S P McGlynn, J Chem. Phys., 1964, 41, 262.
8. R M Golding, Mol. Phys., 1962, 5, 369.
9. I Bernal and P H Rieger, Inorg. Chem., 1963, 2, 256.
10. R Wilson and D Kivelson, J Chem. Phys., 1966, 44, 154.
11. M A Hitchmann and R L Belford, Inorg. Chem., 1969, 8, 958.
12. J Selbin, R H Holmes and S P McGlynn, J Inorg. Nuc. Chem., 1965, 25, 1359.
13. J Selbin, H R Manning and G Cussac, J Inorg. Nuc. Chem., 1963, 25, 1253.
14. A Abragam and M H L Pryce, Proc. Roy. Soc. (A), 1951, 205, 135.
15. F K Kneubuhl, J Chem. Phys., 1960, 33, 1074.
16. B Bleaney, Phil. Mag., 1951, 42, 441.

17. R M Golding, 'Applied Wave Mechanics', Van Nostrand, New York, 1969, p.452.

18. L Petrarkis, J Chem. Ed., 1967, 44, 432.

19. C P Poole Jun., 'E.S.R.', Interscience, New York, 1967, p.775.

20. R L Dutta and S Lahiry, J Ind. Chem. Soc., 1964, 41, 546.

21. B R McGarvey, 'Transition Metal Chemistry', R Carlin ed., Edward Arnold, London, 1966, vol. 3, p.90.

22. E C Tynan and T F Yen, Inorg. Chem., 1968, 7, 731.

23. M A Hitchmann, C D Olson and R L Belford, J Chem. Phys., 1969, 50, 1195.

24. T M Dunn, Trans. Far. Soc., 1961, 57, 1441.

25. A J Freeman and R E Watson, 'Magnetism', eds., G T Rado and H Suhl, Academic Press, New York, 1965, Vol IIA, p.167.

26. S Antosik, N M D Brown, A A McConnell and A L Porte, J Chem. Soc A, 1969, 545.

27. R P Dodge, D H Templeton and A Balkin, J Chem. Phys., 1961, 35, 55.

28. P K Hon, R L Belford and C E Pfluger, J Chem. Phys., 1965, 43, 1323, 3111.

29. B R McGarvey, J Phys. Chem., 1967, 71, 51.

30. E Clementi, 'Tables of Atomic Functions', I.B.M. Corporation Development Lab Reports, 1965; I.B.M. J Res. Dev., 1965, 9, 2.

Part III

1. D W Pratt, Nuclear Science Abstracts, 1967, 21, 34254.

2. G F Kokoszka, H C Allen jun., and G Gordon, Inorg. Chem., 1966, 5, 91.

3. D C Bradley, R H Moss, and K D Sales, Chem. Commun., 1969, 1255.

4. E C Alyea and D C Bradley, J Chem. Soc. (A), 1969, 2330.

5. C E Holloway, F E Mabbs and W R Smail, J Chem. Soc. (A), 1968, 2980.

6. R S Title and M W Shafer, Phys. Rev. Letters, 1972, 28, 808.

7. D C Bradley and M H Chisholm, J Chem. Soc. (A), 1971, 1511.

8. J C W Chien, J Phys. Chem., 1963, 67, 2477.

9. C J Ballhausen and J P Dahl, Acta Chem. Scand., 1961, 15, 1333.

10. G Doyle, and R S Tobias, Inorg. Chem., 1968, 7, 2479.

11. G Wilkinson and J M Birmingham, J Am. Chem. Soc., 1954, 76, 4281.

12. E O Fischer and A Treiber, Chem. Ber., 1961, 94, 2193.

13. F W Siegert and H J De Liefde Meijer, J Organometallic Chem., 1970, 23, 177.

14. F W Siegert and H J De Liefde Meijer, Rec. Trav. Chim, 1969, 88, 1445.

15. S Ya Skachilova, A V Skavitskii and R Ya Vlaskina, Zhurnal Obschei Khimii, 36, 6, 1059.

16. A Abragam and M H L Pryce, Proc. Roy. Soc. (A), 1951, 205, 135.

17. R M Golding, 'Applied Wave Mechanics', Van Nostrand, New York, 1969, p.452.

18. J C Barnes and P Day, J Chem. Soc., 1964, 3886.

19. J L Burmeister, E A Deardorff, A Jensen and V H Christiansen, Inorg. Chem., 1970, 9, 58.

20. C J Ballhausen and H B Gray, 'Molecular Orbital Theory', W A Benjamin and Co., New York, 1965.

21. D A Brown, 'Transition Metal Chemistry', R L Carlin ed., Edward Arnold, London, 1966, Vol.3, p.2.

22. W N Lipscomb, and A G Whittaker, J Am. Chem. Soc., 1945, 67, 2019.

23. G Engebretson and R E Rundle, J Am. Chem. Soc., 1963, 85, 481.

24. Y Morino and H Uehara, J Chem. Phys., 1966, 45, 4543.

25. M A Bush and G A Sim, J Chem. Soc. (A), 1971, 2225.

26. W Moffit, J Am. Chem. Soc., 1954, 76, 3386.

27. L C Cusachs, B L Trus, D G Carroll and S P McGlynn, Internat. J Quantum Chemistry, 1967, 1, 423.

28. L C Cusachs, and J H Corrington, 'Sigma Molecular Orbital Theory', O Sinanoglu and K W Wiberg, Yale University Press, 1970, p.256.

29. E Clementi, 'Tables of Atomic Functions', I.B.M. Corporation Development Lab Reports, 1965; I.B.M. J Res. Dev., 1965, 9, 2.

30. V I Vedeneyev, L V Gurvich, N N Kondrat' yev and Ye L Frankevich, 'Bond Energies, Ionisation Potentials and Electron Affinities', Edward Arnold, London, 1966.

31. M Wolfsberg, and L Helmholtz, J Chem. Phys., 1952, 20, 837.

32. T M Dunn, Trans. Farad. Soc., 1961, 57, 1441.

33. B A Goodman and J B Raynor, Adv. Inorg. Chem. and Radiochem., Academic Press, London, 1970, 13, 135.

34. B R McGarvey, 'Transition Metal Chemistry', R L Carlin ed., Edward Arnold, London, 1966, Vol.3, p.90.

35. L D Rollmann and S I Chan, 'Electron Spin Resonance of Metal Complexes', T F Yen ed., Adam Hilger, London, 1969, p.175.

36. A Hudson and G R Luckhurst, Chem. Rev., 1969, 69, p.213.

Part IV

1. H M McConnell, J Chem. Phys., 1956, 25, 709.

2. D Kivelson, J Chem. Phys., 1960, 33, 1094.

3. R Wilson and D Kivelson, J Chem. Phys., 1966, 44, 154.

4. P W Atkins and D Kivelson, J Chem. Phys., 1966, 44, 169.

5. C P Slichter, 'Principles of Magnetic Resonance', Harper and Row, New York, 1963, p.127.

6. A G Redfield, I.B.M. J Res. Dev., 1957, 1, 19.

7. A Hudson and G R Luckhurst, Chem. Rev., 1969, 69, 191.

8. P Debye, 'Polar Molecules', Dover Publications Inc., New York, 1945, Chapter 5.

9. A Carrington and A D McLachlan, 'Introduction to Magnetic Resonance', Harper and Row, New York, 1967, p.187.

10. G Wilkinson and J M Birmingham, J Am. Chem. Soc., 1954, 76, 4281.

11. F W Siegert and H J De Liefde Meijer, J Organometallic Chem., 1970, 23, 177.

12. F W Siegert and H J De Liefde Meijer, Rec. Trav. Chim., 1969, 88, 1445.

13. S McLean, C J Webster and R J D Rutherford, Can. J Chem., 1969, 47, 1555.

14. 'International Critical Tables', McGraw-Hill, New York, 1930, Vol.7.

15. G F Kokoszka, H C Allen and G Gordon, J Chem. Phys., 1967, 46, 3013, 3020.

16. H Kon and N E Sharpless, J Chem. Phys., 1965, 42, 906.

17. H Kon and N E Sharpless, J Chem. Phys., 1965, 43, 1081.

18. J Sierro, Phys. Chem. Solids, 1967, 28, 417.

19. J H Thornley, B W Magnum, J H E Phillips and J Owen, J Proc. Phys. Soc. (London), 1961, 78, 1263.

20. A Carrington and A D McLachlan, 'Introduction to Magnetic Resonance', Harper and Row, New York, 1967, pp. 205-208.

21. J Gendel, J H Freed and G K Fraenkel, J Chem. Phys., 1962, 37, 2832.

Part V

1. E Schempp and P J Bray, 'Physical Chemistry', H Eyring, D Henderson and W Jost eds., Academic Press Inc., New York, 1970, Vol.IV, Chapter 11.

2. E A C Lucken, 'Nuclear Quadrupole Coupling Constants', Academic Press Inc., New York, 1969.

3. A H Reddoch, J Chem. Phys., 1961, 35, 1085.

4. A Zalkin and D E Sands, Acta. Cryst., 1958, 11, 615.

5. E Schempp and G E Peterson, J Chem. Phys., 1970, 53, 306.

6. R R Hewitt, Phys. Rev., 1961, 121, 45.

7. J Fuggle, Ph.D. Thesis, University of Glasgow, 1970.

8. A J Edwards, J Chem. Soc., 1964, 3714.

9. D C Bradley, B N Chakravarti and W Wardlaw, J Chem. Soc., 1956, 2381.

10. D C Bradley, B N Chakravarti, A K Chatterjee and A Whittley, J Chem. Soc., 1953, 99.

11. H Funk, and W Baumann, Z Anorg. Allgem. Chemie, 1937, 231, 264.

12. P N Kapoor, and R C Merotra, J Less-Common Metals, 1965, 8, 339.

13. C P Slichter, 'Magnetic Resonance', Harper and Row, New York, 1963, p.160.

14. M H Cohen, Phys. Rev., 1954, 96, 1278.

15. M Chihara, N Nakamura, H Okuma and S Seki, J Phys. Soc. Japan, 1968, 24, 306.

Appendix A

1. A Abragam and M H L Pryce, Proc. Roy. Soc. (A), 1951, 205, 135.

2. B R McGarvey, 'Transition Metal Chemistry', R L Carlin ed., Edward Arnold, London, 1966, 3, 97.

3. A Carrington and A D McLachlan, 'Introduction to Magnetic Resonance', Harper and Row, 1967, Chapter 9.

4. H A Kramers, Proc. Acad. Sci. Amsterdam, 1930, 33, 953.

5. C P Slichter, 'Magnetic Resonance', Harper and Row, New York, 1963, p.160.

Appendix B

1. R M Golding, 'Applied Wave Mechanics', Van Nostrand, New York, 1969, p.452.

2. B Bleaney, Phil. Mag., 1951, 42, 441.

3. A Abragam and B Bleaney, 'Electron Paramagnetic Resonance in Transition Ions', Clarendon Press, Oxford, 1970, Chapter 3.

Appendix C

1. B R McGarvey, 'Transition Metal Chemistry', R L Carlin ed., Edward Arnold, London, 1966, 3, 141.

2. A Abragam and B Bleaney, 'Electron Paramagnetic Resonance in Transition Ions', Clarendon Press, Oxford, 1970, p.593.

3. A J Freeman and R E Watson, 'Magnetism', G T Rado and H Suhl eds., Academic Press, New York, 1965, Vol. IIA, p.167.

Appendix D

1. R H Sands, Phys. Rev., 1955, 99, 1222.

2. L Petrarkis, J Chem. Ed., 1967, 44, 432.

3. C P Poole jun., 'E.S.R.', Interscience, New York, 1967, p.775.

4. R Nieman and D Kivelson, J Chem. Phys., 1961, 35, 156.

5. H R Gersmann and J D Swalen, J Chem. Phys., 1964, 36, 3221.

6. F K Kneubuhl, J Chem. Phys., 1960, 33, 1074.